A Preliminary Investigation Using Unnatural Amino Acids to Stabilise Peptide Radiotracers

By: Andrew T. King

A Thesis Submitted for the Fulfilment of the Degree of Master of Research

Department of Molecular Sciences,
Macquarie University

Supervisor:
Associate Professor Joanne Jamie

November 2018

Certificate of Authorship and Originality

I certify that the work in this thesis has not previously been submitted for a degree nor has it been submitted as part of the requirements for a degree except as fully acknowledged within the text.

I also certify that the thesis has been written by me. Any help that I have received in my research work and the preparation of the thesis itself has been acknowledged. In addition, I certify that all the information sources and literature used are indicated in the thesis.

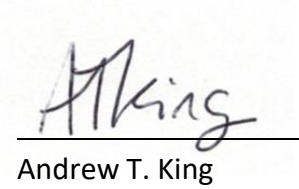

Andrew T. King
(BForSc, BSc(Hon))
2nd November, 2018

Acknowledgements

I would like to give my sincere thanks and acknowledgements to my supervisor, Associate Professor Joanne Jamie from Macquarie University, Department of Molecular Sciences, and co-supervisors Associate Professor Andrew Katsifis from the Department of PET & Nuclear Medicine, Royal Prince Alfred Hospital and Dr Lidia Matesic from the Australian Nuclear Science and Technology Organisation. Without all of their hard work, endless support, assistance and guidance during this project none of the results would have been produced.

Furthermore, I would like to acknowledge the Australian Commonwealth Government for providing me with a Research Training Program (RTP) scholarship that allowed me to complete this research and further my studies.

I would also like to thank the Department of Molecular Sciences, Macquarie University, for providing funding, equipment and chemicals and enabling me to undertake this research. Thanks are also given to Mr Anthony Gurlica and Dr Nicole Cordina for training and use of the NMR and variable temperature NMR experiments, Dr Sophie Goodchild for training and use of the UV-Vis equipment, Mr Mark Tran for training and use of the FTIR and melting point equipment and Dr Kavita Ragini for training and use of the LRESI-MS equipment. Furthermore, thanks are given to Dr Ian Jamie, Dr Fei Liu, Professor Peter Karuso and Professor Alison Rodger, for either use of equipment and/or supply of chemicals. I would also like to thank Leanne who helped me with editing my thesis.

Finally, I would like to give special thanks to my friends, family and everyone in the research laboratory who has supported me during this year, with a special mention to my parents Noel and Denise King and girlfriend Renee Ashton.

Table of Contents

Abstract

Peptide-based radiotracers are a valuable tool for diagnostic and therapeutic applications in nuclear medicine. However, some peptide-based radiotracers exhibit low metabolic stability and are rapidly degraded by proteolytic enzymes *in vivo.* This rapid degradation contributes to insufficient accumulation and high background radioactivity, ultimately leading to poor diagnostic and therapeutic capabilities.

Previous work has shown that peptide-based radiotracers with unnatural amino acids linking the radioisotope and the peptide can improve the metabolic stability of the peptide. A promising unnatural amino acid linker that has demonstrated improvement in metabolic stability of peptides, but is still relatively underexplored, is the β-amino acid.

A series of aliphatic and aromatic β-amino acids and their isostere conjugates, linked *via* their carboxyl groups to the amine group of glycine ethyl ester, were synthesised to assess their comparative metabolic stability. A range of synthetic strategies were performed to obtain the conjugates, which were fully characterised by nuclear magnetic resonance spectroscopy and mass spectrometry. Preliminary *in vitro* incubation studies with porcine liver esterase (as a model of human esterase) provided some evidence for the aromatic β-amino acid-glycine ethyl ester conjugate being more stable than its α-amino acid analogue, but further studies are needed for more conclusive results.

Chapter 1: Introduction

Nuclear medicine is a powerful diagnostic and therapeutic tool that is currently used in a range of cardiology, neurology and oncology based diseases.[1-2] Nuclear medicine relies on the use of radioactive molecules, often referred to as radiotracers, that have a high degree of specificity and selectivity to a range of biological targets.[3] These targets include, protein and peptide receptors, cell transporters and other metabolic processes.[3] While a range of specific radiolabelled peptides that target peptide receptors have evolved, including the recently developed SARTATE™,[4] many are hampered due to their intrinsic property of poor metabolic stability.[5-6]

Along with exhibiting specific target interaction and high radioisotope stability for clinical use, peptide-based radiotracers should be sufficiently stable against proteolytic degradation *in vivo*, to enable high target accumulation.[7] Insufficient accumulation at the target site, due to rapid degradation of the radiotracer *in vivo,* can therefore contribute to poor diagnostic imaging capability and poor therapeutic effect.[7]

In this work, a novel method of increasing metabolic stability of peptide-based radiotracers, using beta (β) amino acid peptide linkages, has been investigated and compared against other peptide linkages. To provide context to this work, the introductory chapter gives an overview of nuclear medicine, methods of radiolabelling peptides and current methods employed to improve their metabolic stability. The aims and objectives of this work are also outlined.

1.1 Nuclear Medicine Imaging Strategies

Current clinical imaging strategies include magnetic resonance imaging (MRI) and computed tomography (CT), which provide anatomical information, and the nuclear medicine techniques of positron emission tomography (PET) and single photon emission computed tomography (SPECT), which provide metabolic functional information.[1] PET and SPECT are known as molecular imaging techniques due to their ability to provide whole-body profiles of metabolic processes being studied.[1]

Nuclear medicine currently uses PET and SPECT scans for diagnostic procedures to analyse, stage and evaluate potential treatment options for a variety of conditions including cardiology, neurology and oncology based diseases.[1-2] PET relies on the decay *via* a positron (β^+) emission pathway of the

radioactive nuclei of a radiotracer, and its subsequent collision with an electron a short distance away.[1-2] This collision, also known as annihilation, produces two gamma (γ) photons that are 180° from each other.[1-2] The 511 keV photons travel through the body before being detected externally and are reconstructed into a 3D image of the radiotracer's location in the body **(Figure 1.1)**.[2] SPECT requires radioisotopes that decay *via* direct production of a γ photon, which then travels through the body to where it is detected externally *via* a SPECT scanner **(Figure 1.1)**.[8-9]

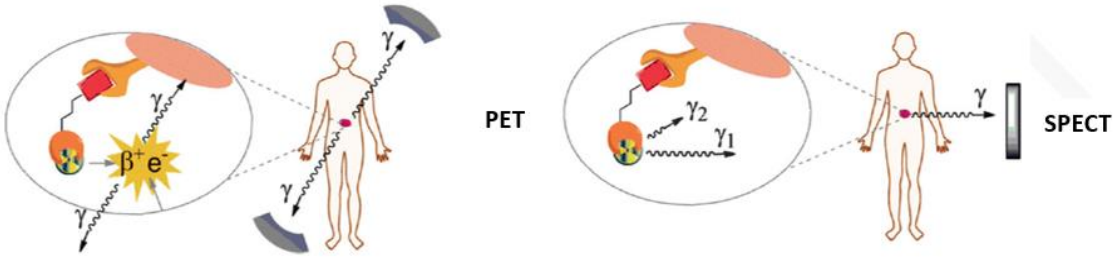

Figure 1.1 Nuclear medicine scanning techniques PET and SPECT[8]
Reprinted from Ramogida *et al.,* Tumour targeting with radiometals for diagnosis and therapy, *Chemical Communications*, **2013**, *49* (42), 4720-4739, with permission from Royal Society of Chemistry

SPECT scans have wider use in the clinic compared to PET scans because of their extensive availability and lower associated cost.[10] However, PET scans have greater superiority in relation to sensitivity and spatial resolution compared to SPECT scans.[2] Furthermore, the minimal physiological effect from the PET tracer, the ease of accurate quantification, and it being a non-invasive technique,[1-2] also contributes to the advantages of PET over other imaging modalities *i.e.* CT and MRI.

1.2 Radiotracers and Radioisotopes

Nuclear medicine, regardless of whether it is used for diagnostic or therapeutic purposes, requires the use of a radiotracer as an *in vivo* molecular probe.[3] The overall structure of protein and peptide-based radiotracers **(Figure 1.2)** is typically made up of three parts; a targeting moiety, a linker, which can be modified, and a radioactive nucleus.[3] Several different factors must be considered when selecting the most appropriate radioisotope for use.[2] An overarching factor is the half-life of the radioisotope **(Table 1.1)**, which must be considered in a multi-step synthesis of the radiotracer. Also to be considered is the time needed for transport to and administration to the patient.[2] This decision, of which radioisotope, is also dependent on its availability and production, radioactive decay properties, image quality, patient safety and cost.[2]

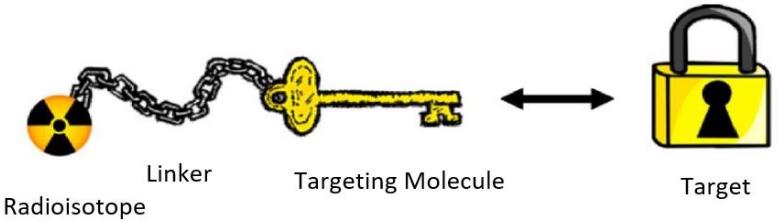

Figure 1.2 General structure of a protein and peptide-based radiotracer[3]

Table 1.1 PET Isotope Half-Lives

PET Isotopes (β^+ Decay)			
Radioisotope	**Half-life**	**Radioisotope**	**Half-life**
^{11}C	20.3 min	^{64}Cu	12.8 h
^{13}N	9.97 min	^{68}Ga	67.6 min
^{15}O	2.1 min	^{86}Y	14.7 h
^{18}F	110 min	^{89}Zr	78.4 h

Although positron emitting isotopes of carbon, nitrogen and oxygen exist, their clinical use is limited due to their short half-lives, and the required infrastructure needed to produce and handle them.[3] An ideal radioisotope for a PET radiotracer is [^{18}F]fluorine because of its reasonably long half-life, 110 minutes (min), which enables sufficient time for multi-step radiosynthesis and subsequent imaging.[1] Additionally, [^{18}F]fluorine has high spatial resolution in PET scans due in part to its low β^+ energy.[1] Likewise, the similar size and *Van der Waals* radii, between the fluorine and hydrogen atoms, makes the carbon-fluorine bond analogous to the carbon-hydrogen bond enabling it to be well tolerated by the body.[11]

Currently, the most widely used PET radiotracer in the clinic is [^{18}F]fluorodeoxyglucose ([^{18}F]FDG), due to its ability to be taken up by cells, particularly tumour and inflammatory cells, with high glucose metabolism.[1, 12] Although, [^{18}F]FDG is effectively taken up into tumour cells by glucose transporters and phosphorylated by hexokinase, it is not metabolised further and is thus trapped in the cell, enabling PET imaging. However, [^{18}F]FDG is not a specific radiotracer as it cannot differentiate between neoplastic cells or with those that have a high glucose metabolic rate from other etiologies.[1, 13-14] Additionally, some tumour cell types do not exhibit a high metabolic rate,

further contributing to its lack of specificity.[14] Therefore, much research and development has been focused on PET radiotracers that can target specific biomarkers.[8, 15-16]

Even though [^{18}F]fluorine is recognised as the standard PET isotope, significant research has been undertaken into radiometal PET isotopes.[14] This is attributed to the use of radiometals circumnavigating some of the synthetic limitations of [^{18}F]fluorine incorporation to peptides, such as harsh and time consuming labeling procedures.[8, 14] Additionally, the longer half-lives of radiometals, such as [^{64}Cu]copper and [^{89}Zr]zirconium, at 12.8 hours (h) and 78.4 h, respectively, allow for imaging of biological targets that have slow pharmacokinetics and long biological half-lives.[12]

1.3 Targeted Radiotracers

Over the last decade an increase in research has been directed towards the development of radiotracers that target specific diseases through interactions with specific targeting vectors.[1, 8, 15-16] These targeting vectors can comprise of proteins, antibodies or peptides.[17-18] Early efforts were directed towards radiolabelling antibodies,[19] however, the use of peptides is now regarded as more beneficial due to issues with slow pharmacokinetics limiting the use of antibodies.[19]

Peptides offer several advantages over small molecule radiotracers or the larger radiolabelled proteins and antibody analogues.[20] These advantages include facile synthesis performed by automated processes;[20] a decreased chance of generating an immunogenic response from the body;[20] and the smaller size of peptides compared to proteins and antibodies, enabling more rapid clearance from the blood and non-target organs.[17] Peptides also typically have improved tissue penetration and higher tumour uptake, leading to improved tumour to background ratio and producing favourable image quality.[17-18, 20] However, peptide-based radiotracers still present challenges with their radiolabelling strategies and metabolic stability.[5, 17]

1.3.1 Strategies to Radiolabel Peptides

Ideally, when radiolabelling a peptide, the radioisotope should be incorporated in a manner that does not alter the natural biological behaviour of the peptide.[5] Many peptides have been radiolabelled using radiometals and a bifunctional chelator (BFC) for attachment of the peptide and radioisotope.[5, 8, 14] However, continued development of methodologies have seen both the

introduction of a radiolabelled prosthetic group or direct radiolabelling approaches increasingly applied to radiolabelling peptides, especially with [^{18}F]fluorine.[5, 14, 17, 21]

1.3.1.1 Bifunctional Chelator (BFC) Radiolabelling

A range of BFCs have been developed to complex the radiometals [^{64}Cu]copper, [^{89}Zr]zirconium, [^{68}Ga]gallium and [^{177}Lu]lutetium and form a covalent bond with a peptide **(Figure 1.3)**.[14] There are two main styles of bifunctional chelators, *i.e.* macrocyclic chelators **(1-3)** and acyclic chelators **(4)** that can be used in radiolabelling procedures **(Figure 1.4)**. The two most widely used macrocyclic chelators are the 2,2',2'',2'''-(1,4,7,10-tetraazacyclododecane-1,4,7,10-tetrayl)tetraacetic acid (DOTA) **(1)** and the smaller 1,4,7-triazacyclononane-1,4,7-triacetic acid (NOTA) **(2)** based systems. The newer sarcophagine based systems, such as diamsar **(3)**, are particularly useful for copper radioisotopes.[22]

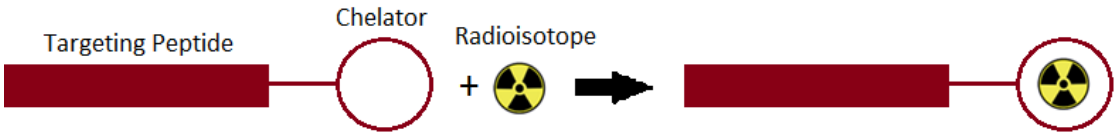

Figure 1.3 Radiolabelling a peptide *via* a bifunctional chelator[5]

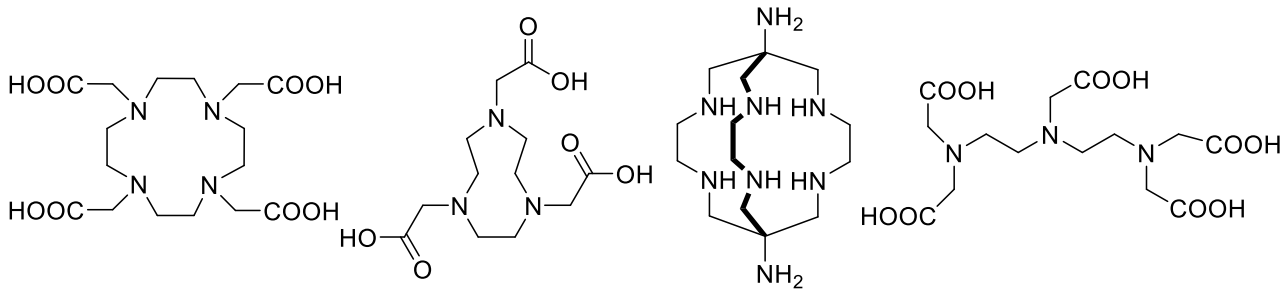

Figure 1.4 Examples of bifunctional chelators

Bifunctional chelators are an attractive method of radiolabelling, as the time-consuming synthetic manipulation steps to attach the peptide are performed before the radioisotope is introduced, saving many half-lives of radioactivity.[8] Similarly, the incorporation of the radiometal is viewed as easier to perform compared to non-metal radiolabelling reactions.[23] However, some BFCs, for example DOTA **(1)** with the radiometals of [^{68}Ga]gallium and [^{177}Lu]lutetium, still require heating to incorporate the radiometal into the chelator in an efficient manner and timeframe.[21-22] The large

size of the chelator can also have adverse effects on peptide radiotracer pharmacokinetics and pharmacodynamics properties, *i.e.* affecting the targeting and the *in vivo* stability.[8, 24]

1.3.1.2 Prosthetic Radiolabelling

An alternative method of introducing a radioisotope into a peptide is through the prosthetic radiolabelling methodology **(Figure 1.5)**, whereby a small molecule is first radiolabelled and then coupled to the peptide of interest.[14, 21] Generally, these prosthetic methods are restricted to radioisotopes such as [^{18}F]fluorine and [^{11}C]carbon. The main advantage of using prosthetic radiolabelling methodologies is that the harsh radiolabelling conditions are performed on the small molecule before the conjugation step to the peptide.[25] The traditional method of nucleophilic displacement, using [^{18}F]fluoride to incorporate an [^{18}F]fluorine atom into a peptide structure, typically requires harsh reactions conditions that are strongly basic, and therefore, are not suitable for peptides.[17, 26-27]

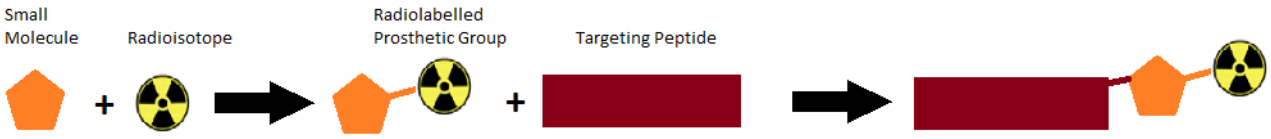

Figure 1.5 Radiolabelling a peptide *via* a prosthetic group[5]

Currently, the conjugation of the peptide can be achieved through nucleophilic procedures[25] with a range of reactive groups **(Figure 1.6)**. They predominantly feature activated esters **(5)** or acids **(6)** that can react with the *N*-terminus of a peptide or free amine groups.[17, 21, 27] Strategies involving thiols or cysteine residues can also be conducted using maleimide **(7)** reactive groups. [17, 21, 27] There is also strong development towards the use of click chemistry approaches using azido **(8)** and click **(9)** reactive agents.[21, 27-28] However, each of these strategies often suffer from requiring a multi-step syntheses, and thus produce products in low radiochemical yield.[29-31]

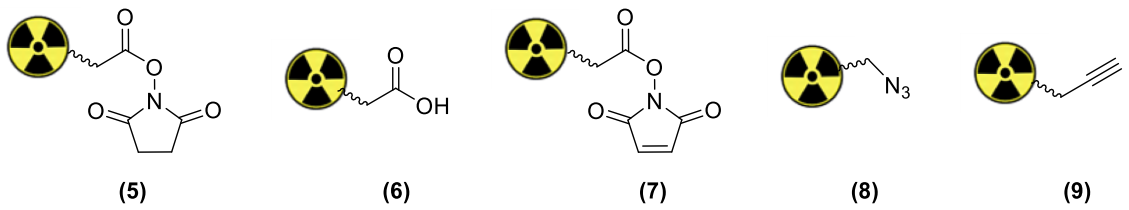

Figure 1.6 Reactive conjugation groups for prosthetic radiolabelling

1.3.1.3 Direct Radiolabelling

The least common method to introduce [^{18}F]fluorine into a peptide is *via* a direct labeling strategy where the radioisotope replaces an activated leaving group **(Figure 1.7)**. The implementation of this method in peptides had been difficult due to incompatibility with amino acid side chain functional groups, the harsh basic conditions and high temperatures needed.[32] Renewed interest in this method has been observed because of the higher radiochemical yields that can be obtained, compared to using prosthetic methods, and this has led to development of new strategies that can be applied to biologically relevant peptides.[14]

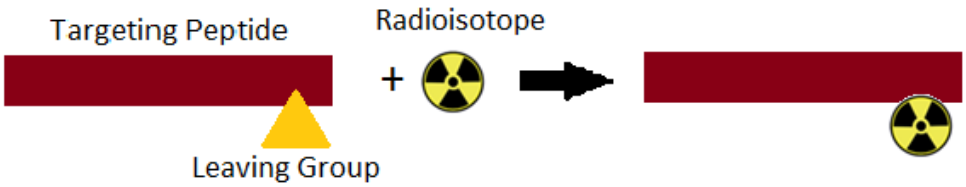

Figure 1.7 Radiolabelling a peptide *via* a direct labelling strategy[5]

The development of direct radiolabelling methods was inspired by the prosthetic group family of fluorobenzoic acids **(10)**; however, the harsh reaction conditions limited their use.[32] Further development with other aromatic systems has demonstrated that the presence of an electron withdrawing group (EWG), for example CF_3 or CN in the *meta* position, increased the reactivity of trimethylammonium or nitro leaving groups.[33-34] This reduced the temperature for the nucleophilic reaction to occur, hence making it suitable for direct peptide radiolabelling procedures.[33] Alternative methods using heteroatoms of silicon **(11)** and boron **(12)** have also been explored because of their ability to form strong bonds with fluorine and their avoidance of harsh reaction conditions **(Figure 1.8)**.[14, 21, 25] However, these approaches have presented new challenges due to radiolabelling methods producing radiotracers with lower molar (radio)activity and intolerance *in vivo*. [14, 21, 35] Studies have also exploited the strong bond (high bond enthalpy) exhibited between aluminium and fluoride through a NOTA **(2)** aluminium – [^{18}F]fluoride ([^{18}F]AlF) complex.[36-37] The approach has been hampered by the high temperature (>100°C) reaction conditions required for complexation with the NOTA **(2)** chelator,[37-38] however, recent investigations with alternative acyclic chelators **(13)**, have enabled complexation at room temperature, allowing for continued development of these [^{18}F]AlF methods **(Figure 1.8)**.[38]

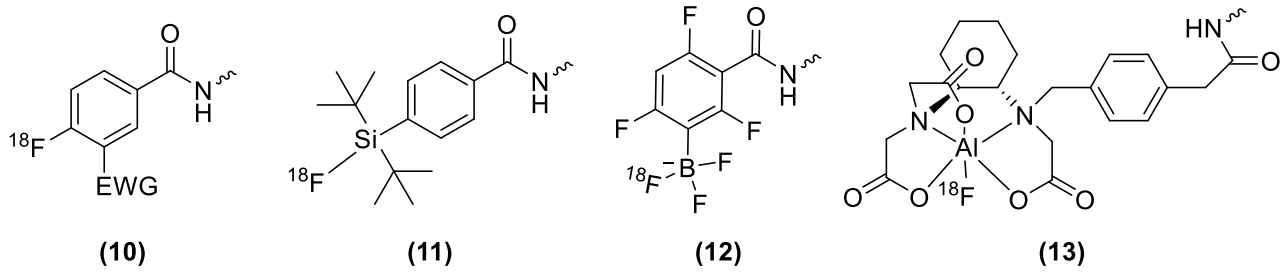

Figure 1.8 Direct peptide-radiolabelling groups[38]

1.3.2 Strategies to Improve Metabolic Stability of Peptide-Based Radiotracers

The advantages of peptide-based radiotracers and the development of methods for radiolabelling them, have led to significant investigation of them in the nuclear medicine industry.[5, 14, 39] Nonetheless, many of these have poor pharmacological properties, including poor metabolic stability.[5, 7, 16, 40-41] This instability is attributed to proteolytic degradation by a range of endopeptidase and exopeptidase enzymes that break down the peptide radiotracer during circulation.[5, 7, 40-41] This in turn affects the targeting efficiency and binding capability of the peptide radiotracer, which ultimately leads to poor diagnostic and therapeutic effects, and may increase the radiation dose to healthy organs.[7, 41]

Efforts have been recently concentrated towards improving the metabolic stability of peptide-based radiotracers.[5-7, 42] This includes modifications to the linker, which are discussed in the following sections 1.3.2.1 and 1.3.2.2.[7, 42-46] Methods of cyclisation[47-49] as well as enzyme inhibitors alongside the peptide-based radiotracers have also been explored,[40] but are not further discussed in the thesis.

1.3.2.1 Chemical Modifications to Improve Metabolic Stability

Various chemical modifications of the linker between the radioisotope and the peptide backbone **(Figure 1.2)** have been investigated to enhance metabolic stability, and other pharmacological properties, of peptide-based radiotracers. Common modifications featured in the literature **(Figure 1.9)** are use of linear **(14)** or cyclic **(15)** carbon chains, or use of polyethylene glycol **(16)** linkers.[7]

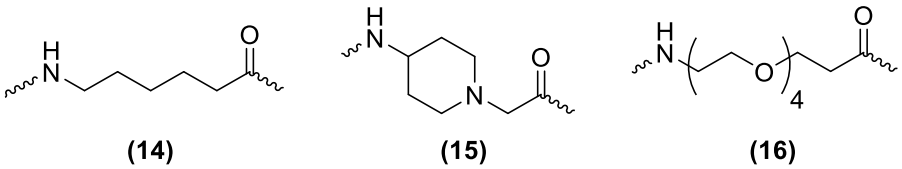

(14) **(15)** **(16)**

Figure 1.9 Examples of linkers **(14-16)** from the literature[7,43,51]

PEGylation involves the use of repeating monomer units of polyethylene glycol (PEG), which is known to shield peptides from proteolytic degradation, increasing their metabolic stability and half-life in the blood.[50] PEGylation has been used as a chemical modification to improve the metabolic stability of the bombesin peptide radiotracers, which are known to undergo rapid proteolytic degradation.[7, 43, 50-51]

Studies conducted by Maecke and co-workers[51] indicated that the addition of a PEG_4 chain **(17)** as a linker improved the metabolic stability of their bombesin peptide radiotracer **(Figure 1.10)**.[51] Results from their subsequent study[43] indicated that the length of the PEG chain is crucial to achieving an increase in metabolic stability. Likewise, they demonstrated that the PEG_6 **(19)** chain had the highest stability in human serum with >90% of **(19)** still intact after 96 h. Whereas the shorter PEG_2 chain **(18)** displayed the lowest stability in human serum with <80% intact at the same time period.[43] Dapp and co-workers showed that a large 5 KDa PEG group, as a linker in the bombesin peptide radiotracers, increased the amount of the radiotracer present in human serum, from 14% (unmodified) to 52% (stabilised), over a 5-day incubation period.[50, 52]

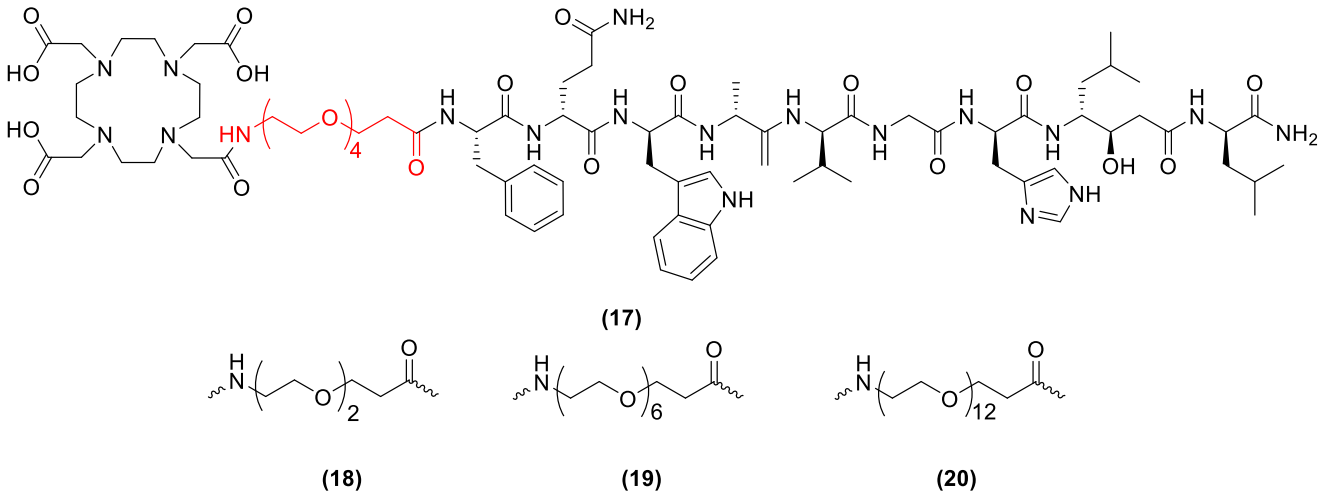

(17)

(18) **(19)** **(20)**

Figure 1.10 Bombesin peptide radiotracer **(17)** investigated by Maecke and co-workers and alternative lengths of PEG chains **(18**, **19** and **20)** investigated.[43,51]

During studies conducted by Bacher *et al.*,[7] evaluations were made on a series of linear and cyclic carbon chains to ascertain if an increase in metabolic stability could be observed on a bombesin

radiotracer **(Figure 1.11)**.[7] Initially, at 30 min, the linear carbon chain **(21)** increased the percentage of peptide radiotracer intact in the human serum, indicating an increase in metabolic stability.[7] However, further analysis at the longer (> 60 min) time points displayed a lower percentage of intact compound compared to the unmodified form.[7] Likewise, the cyclic carbon chain **(22)** displayed a lower percentage of peptide radiotracer intact after incubation for 90 min in human serum, indicating lower metabolic stability.[7] Bacher and co-workers also investigated a PEG_3 chain to increase the metabolic stability, with the results demonstrating that this method increased the stability, over a 90 min timeframe, compared to the unmodified form.[7]

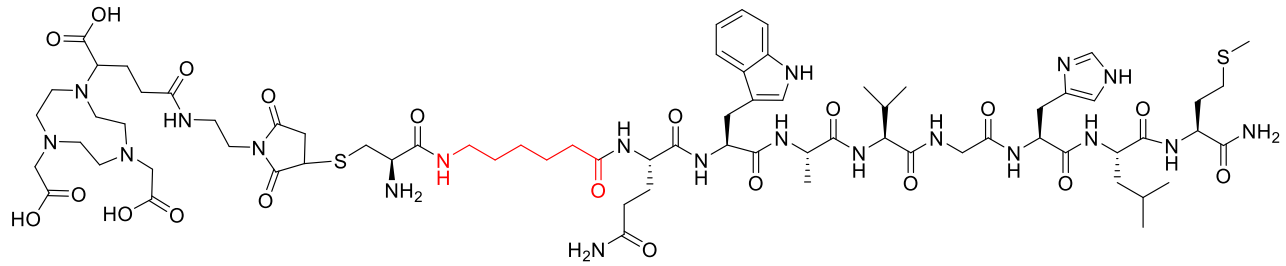

(21)

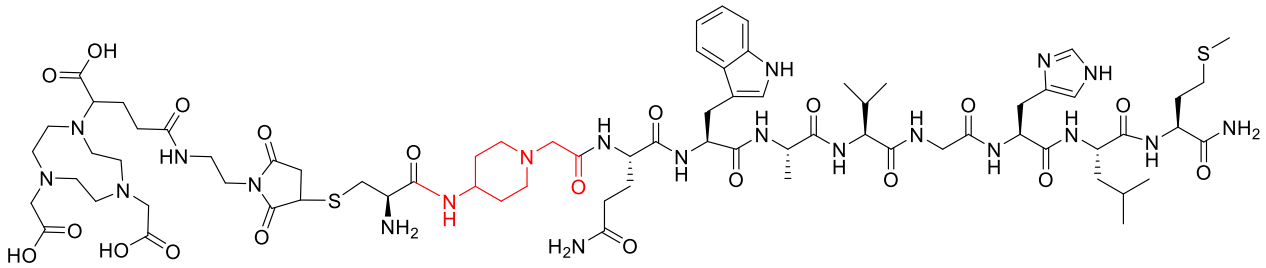

(22)

Figure 1.11 Bombesin peptide radiotracers **(21** and **22)**, with chemical modifications highlighted in red, investigated by Bacher *et al.*[7]

1.3.2.2 Unnatural Amino Acid Incorporation to Improve Metabolic Stability

The incorporation of unnatural amino acids has been used as a chemical modification to increase the *in vivo* stability of peptide-based radiotracers.[53-54] The rationale is that these unnatural amino acids make the peptide-based radiotracer less recognisable to the natural peptidases, decreasing proteolytic degradation.[5] This method of increasing metabolic stability is featured heavily in the literature.[5] Many of the examples have the modification within the backbone of the peptide rather than at the end where the radioisotope is attached.[55-56] However, this can lead to significant modification of the peptide and decrease its target specificity, which must be avoided.[57] Limited, but promising, studies have been on the inclusion of unnatural amino acids at the radioisotope

connection point to the peptide, *i.e.* at the *N*- and *C*-terminus. Examples of these are discussed below.

The inclusion of D-amino acids directly linked to the peptide has been used in a range of peptide-based radiotracers, including those containing octreotide, mingiastrin and bombesin.[53-54, 58] The unnatural D-amino acid linkage results in a structural change at the connection point to the peptide, making the peptide less recognisable to proteolytic enzymes,[5] and as the peptide binding site is unmodified, targeting capability is maintained. Somatostatin is a cyclic peptide that contains 14 amino acids and binds with high affinity to somatostatin receptors. However, it has an extremely short plasma half-life of 1-2 min and is rapidly degraded by proteolytic enzymes.[58] Shortening of the peptide, and including a D-amino acid at the *N*-terminus, resulted in the octreotide peptide **(23)**, exhibiting a plasma half-life of 1.5-2 h, and an improved binding affinity to somatostatin receptors.[46, 58-60] This improved half-life has allowed the peptide octreotide **(23**, **Figure 1.12)** and subsequent derivatives, to be radiolabelled using a radiometal chelator system and be extensively used for imaging procedures.

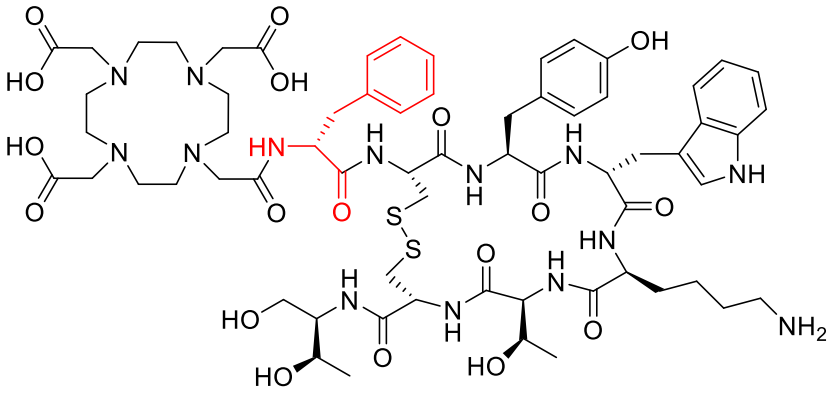

(23)

Figure 1.12 Octreotide with a DOTA chelator attached with D-amino acid in red **(23)**

Mingiastrin peptide radiotracers target the overexpression of the cholecystokinin subtype 2 receptors found on a range of thyroid, lung and ovarian cancers.[61] Initially, mingiastrin radiotracers displayed high kidney retention,[53] however, this was counteracted by reducing the amount of glutamic acid residues which decreased the negative charge in the structure.[53] While these truncated mingiastrin radiotracers displayed lower kidney retention, they also exhibited lower metabolic stability in human serum.[53] Kolenic-Petial *et al*. found that the use of non-ionic D-amino acids **(24-27)** as linkers improved the half-life in human serum over alternative chemical modifications, *i.e.* PEG linkers.[53] Furthermore, they also demonstrated that metabolic stability of

the peptide radiotracer increased with the length of the linker.[53] It was determined that six D-glutamine amino acids **(27**, **Figure 1.13)** provided the optimal length to increase the metabolic stability of the radiotracer in human serum.[53]

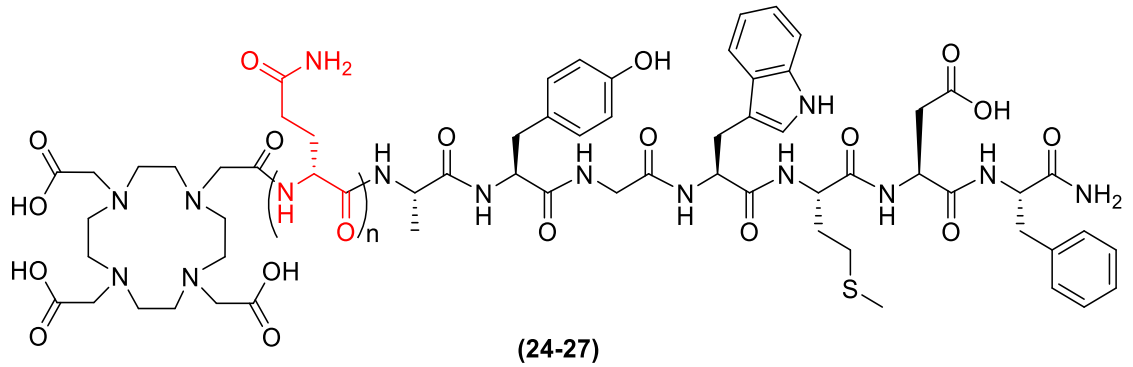

(24-27)
24, n=2; **25**, n=3; **26**, n=4; **27**, n=6

Figure 1.13 Mingiastrin peptide radiotracers **(24-27)** with D-amino acid substitution highlighted in red[53]

Recent work conducted by Valverde and co-workers[54] indicated that the inclusion of a PEG_4-D-amino acid linker increased the metabolic stability of their bombesin peptide radiotracers.[54] They investigated the effect of D-phenylalanine **(28)**, D-tyrosine **(29)** and D-alanine **(30)** attached to the PEG_4 linker to evaluate which, if any, offered an increase in metabolic stability.[54] Results from their studies showed that each of the D-amino acids in compounds **(28-30)** increased the biological half-life of the peptide in human plasma studies, with the aliphatic amino acid linker of D-alanine **(30)** and PEG_4 having the largest increase in stability **(Figure 1.14)**.[54]

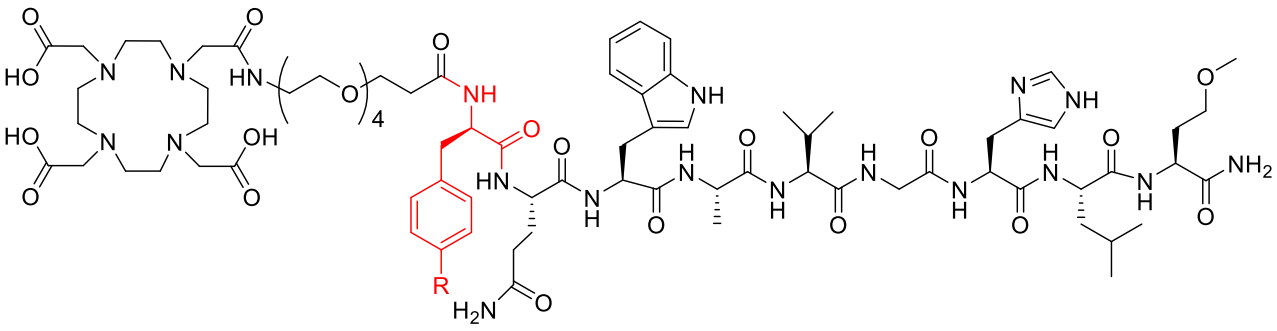

(28) R = H, **(29)** R = OH

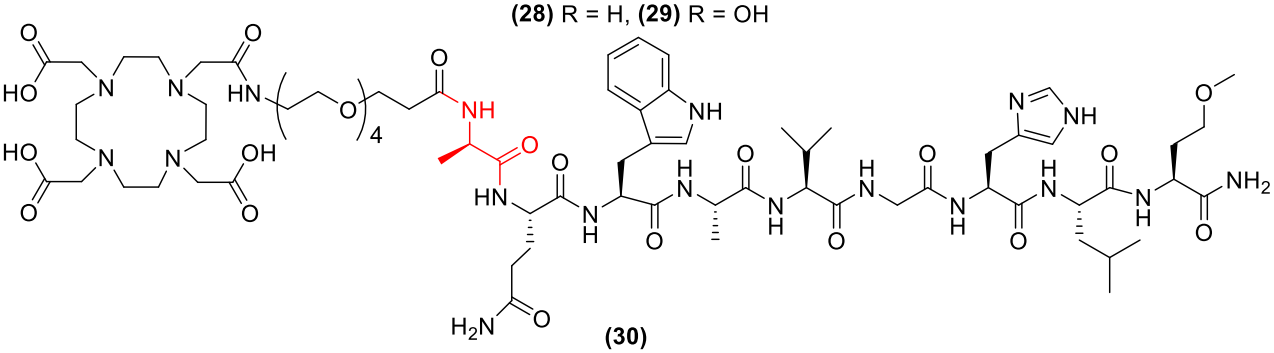

(30)

Figure 1.14 Bombesin peptide radiotracers **(28-30)** with D-amino acid substitution highlighted in red[54]

1.3.2.2.1 Unnatural β-amino acids

Unnatural β-amino acids and β-amino acid scaffolds have been used increasingly in the pharmaceutical field. This is due to a wide variety of desirable pharmacological properties reported, including an increase in *in vivo* metabolic stability[62-66] and potency.[62, 67] The inclusion of a $\beta^{2,2}$-amino acid, highlighted in red **(Figure 1.15)**, by Torfoss *et al.,* increased the metabolic stability of the heptapeptide **(31)**.[66] Studies conducted using α-chymotrypsin showed that 92% of the peptide **(31)** was intact after a 4-day incubation period.[66] Likewise, it was found that the inclusion of the single $\beta^{2,2}$-amino acid, highlighted in red **(Figure 1.15)**, protected the two adjacent residues from being readily hydrolysed *via* proteolytic enzymes.[66] Further work by Hansen *et al*.[65] showed that the $\beta^{2,2}$-amino acid scaffold, with a β-free amino group, increased the metabolic stability of their small (M_w <500) antimicrobial peptides and prevented hydrolysis by proteases.[65] Similarly, the *N*-alkyl modification of the β-amino acid side chain of the anti-cancer drug Paclitaxel has also been shown to increase *in vivo* potency of the second generation drug, Docetaxel.[62, 67]

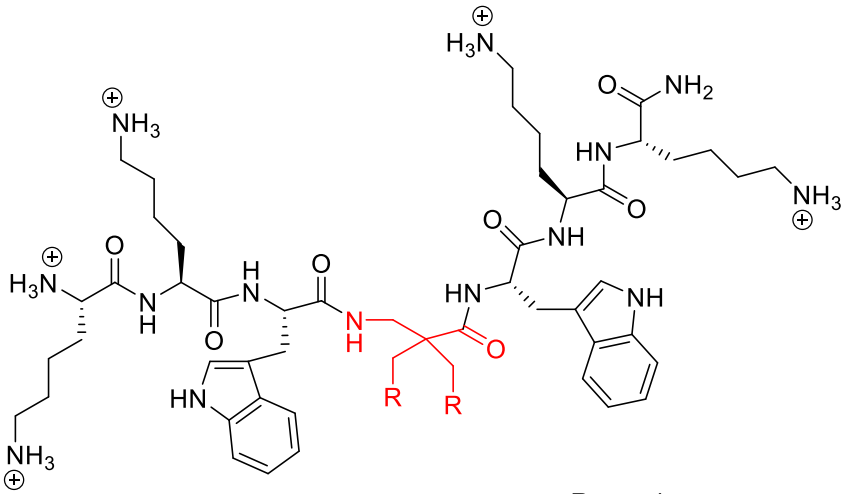

(31)

Figure 1.15 The $\beta^{2,2}$-amino acid, in red, investigated by Torfoss *et al.* to increase metabolic stability of **(31)**[66]

The inclusion of a β-alanine-β-alanine **(32, Figure 1.16)** linker in bombesin peptide radiotracers by Garayoa *et al*.[68] led to a 2-fold increase in stability towards proteolytic degradation, compared to the unmodified structure (without the linker) in studies conducted in tumour cells.[68] However, studies conducted using plasma showed a decrease towards *in vivo* metabolic stability of the modified compound.[68] Garayoa *et al*.[69] also investigated alternative β-amino acids **(33-35)** linked to bombesin, including those that could hold a charge when incorporated into the final overall peptide

radiotracer.[69] They found these modifications did not influence the metabolic stability compared to the already stabilised peptide radiotracer **(32)**.[69]

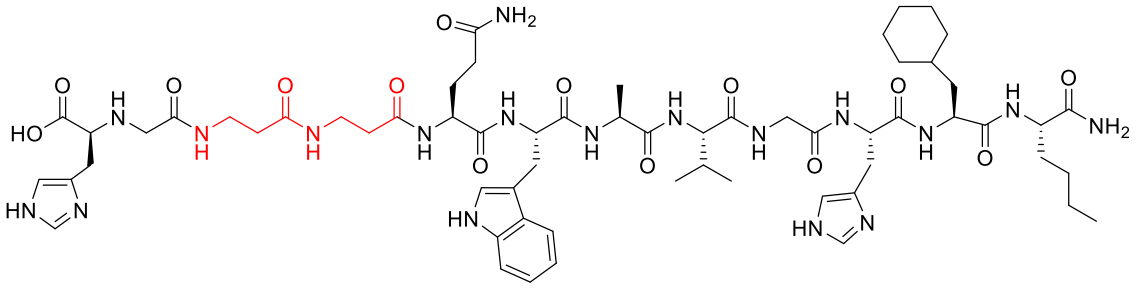

(32)

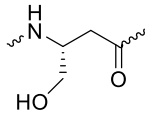

(33)

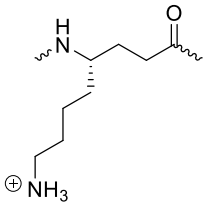

(34)

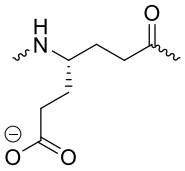

(35)

Figure 1.16 Bombesin peptide radiotracer **(32)** using β-amino acid scaffolds, highlighted in red, to increase the metabolic stability and alternative β-amino acids linkers **(33-35)**[68,69]

Similar studies, using only a single β-alanine linker **(Figure 1.17)**, were carried out by Maecke and co-workers[45] on their GRP peptide-based radiotracer.[45] The final structure of the β-alanine linker **(36)** included the nitrogen group alkylated with a methyl group.[45] Results by Macke and co-workers showed that a slight increase in *in vivo* metabolic stability was observed compared to the unmodified form.[45]

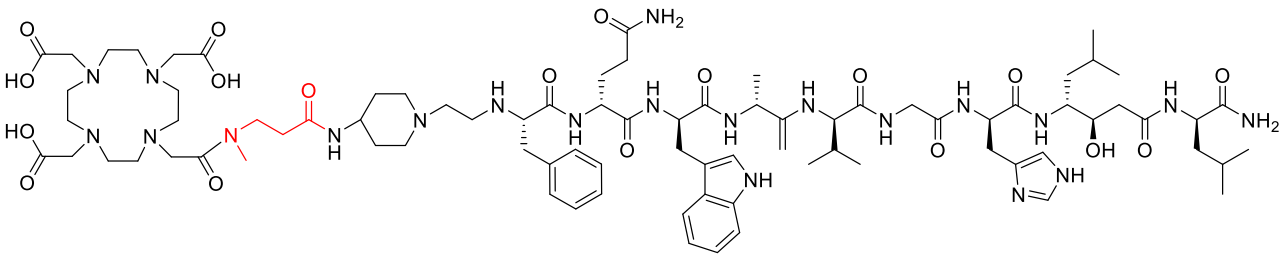

(36)

Figure 1.17 Bombesin peptide radiotracer **(36)** using a β-amino acid scaffold highlighted in red, to increase the metabolic stability[45]

Although Maecke *et al.*[45] and Garayoa *et al*. [68-69] displayed the use of β-amino acids improve the *in vivo* stability metallic radiolabelled peptide radiotracers, the use of β-amino acids to stabilise ^{18}F-fluorine radiolabelled peptide radiotracers has not been reported. Recently, Schjoeth-Eskensen *et al.*[70] described radiolabelling of the β-amino acid **(37, Figure 1.18)** with [^{18}F]fluorine at the α-

carbon.[70] While this was performed successfully, to date, no peptide conjugation data or *in vivo* stability studies could be located.[70]

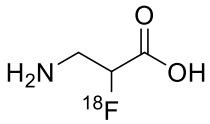

(37)

Figure 1.18 ^{18}F-Fluorinated β-amino acid investigated by Schjoeth-Eskensen *et al.*[70]

1.4 Research Objectives/Aims

Inspired by the work of Maecke *et al.*[45], Garayoa *et al.*[68-69] and Schjoeth-Eskensen *et al.*,[70] the aim of this research was to increase the limited understanding and knowledge about β-amino acids and their scaffolds with regards improvements in metabolic stability of ^{18}F-fluorinated peptide-radiotracers. Resulting from constraints of time and resources, this project focused on developing model compounds for stability studies.

The specific aims of this project were as follows:

- To synthesise a range of aryl and aliphatic β-amino acids, α-amino acids and non-amino acid isosteres conjugated to glycine ethyl ester as simple models of peptides conjugated to linkers.
- Investigate and evaluate the stability of these compounds using porcine liver esterase, which has amidase and esterase activity, to increase the knowledge and understanding about β-amino acids and their scaffolds with regards to metabolic stability.

The conjugates to be synthesised are to be linked *via* their carboxyl groups to the amine group of glycine ethyl ester. The aryl and aliphatic β-amino acids, α-amino acids derived conjugates, will continue to possess a free amine group. This will enable greater control of the solubility of the conjugates in aqueous mediums for stability studies. Likewise, it also provides a handle for future modifications *i.e.* enhanced membrane permeability if required in future studies.

Chapter 2: Results and Discussion - Synthesis

2.1 Target Compounds and Initial Synthetic Strategies

The objective of this project was to investigate if the incorporation of a β-amino acid moiety can confer metabolic stability when used for peptide-linked radiotracers. Research has shown that β-amino acids linked through both their *N*- and *C*-terminus provide stability for some specific peptide-linked systems.[45, 68-69] The specific aims of the project were to synthesise a series of glycine ethyl ester conjugates **(38-43)** and examine the enzymatic stability of their amide bonds against porcine liver esterase **(Figure 2.1)**.

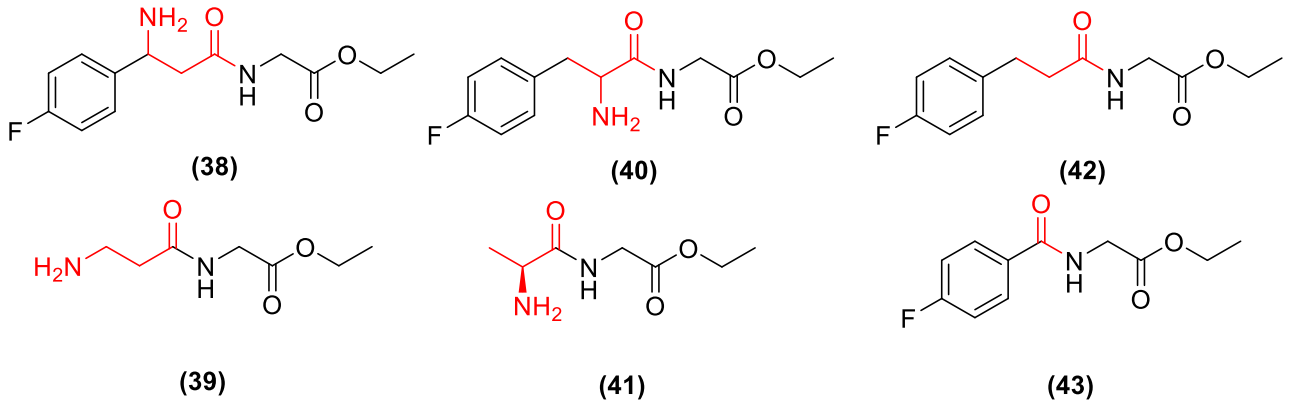

Figure 2.1 Target compounds for metabolic stability **(38-43)**

The target compounds **38**, **40**, **42** and **43** feature a *para*-fluoro substituted aromatic ring to enable translation of results to future studies involving ^{18}F-fluorinated radiolabelled peptides. Compound **43** was designed as a scaffold illustrative of current methods to radiolabel peptides with [^{18}F]fluorine. The aliphatic compounds **(39** and **41)** were considered following the recent report by Schjoeth-Eskensen *et al.* to synthesise the β-amino acid **(37)**.[70] Due to time constraints of the project, the aliphatic compounds omitted the fluorine atom as it was understood that this inclusion would not greatly affect the metabolic stability studies. Conjugation to glycine ethyl ester was chosen to provide a simple model 'peptide' system, and also offered the ability to serve as an internal standard (due to the ethyl ester) during metabolic studies carried out with porcine liver esterase.

The proposed synthetic procedures for compounds **38**-**43** are shown in Schemes 2.1-2.6. For synthesis of target compounds **38**-**41** the reactions involved *tert*-butyloxycarbonyl (*t*-Boc) protection of the free amines of compounds **44**, **47**, **50** and **55**, conjugation of the intermediate compounds **45**, **48**, **51** and **56** to glycine ethyl ester, followed by a deprotection to obtain the final target compounds **(38**-**41)**. The intermediate compound **55** was proposed to occur *via* a modified Knoevenagel condensation, and **59** *via* a Knoevenagel condensation followed by reduction. Synthesis of the scaffold **(43)** was proposed *via* a simple conjugation reaction of 4-fluorobenzoic acid **(60)** and glycine ethyl ester.

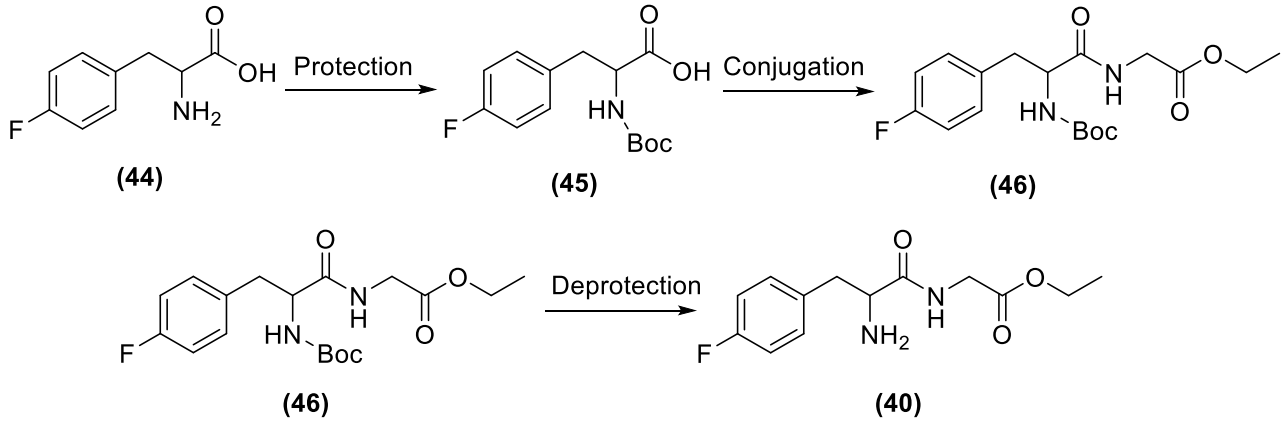

Scheme 2.1 Synthetic strategy to form compound **(40)**

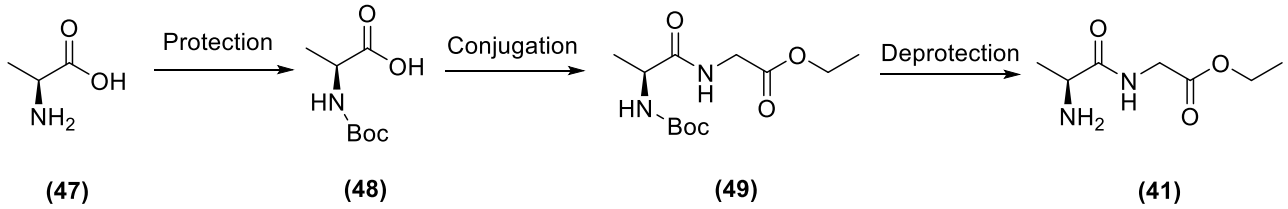

Scheme 2.2 Synthetic strategy to form compound **(41)**

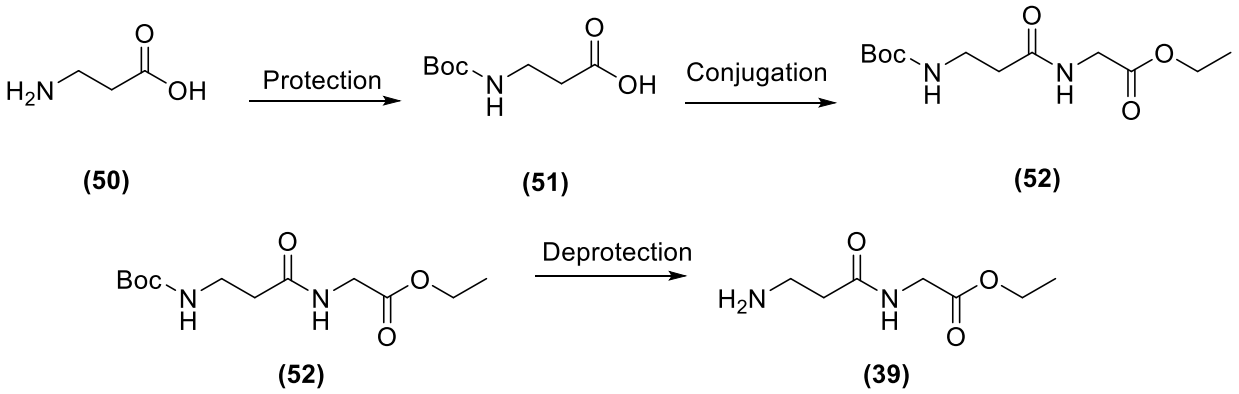

Scheme 2.3 Synthetic strategy to form compound **(39)**

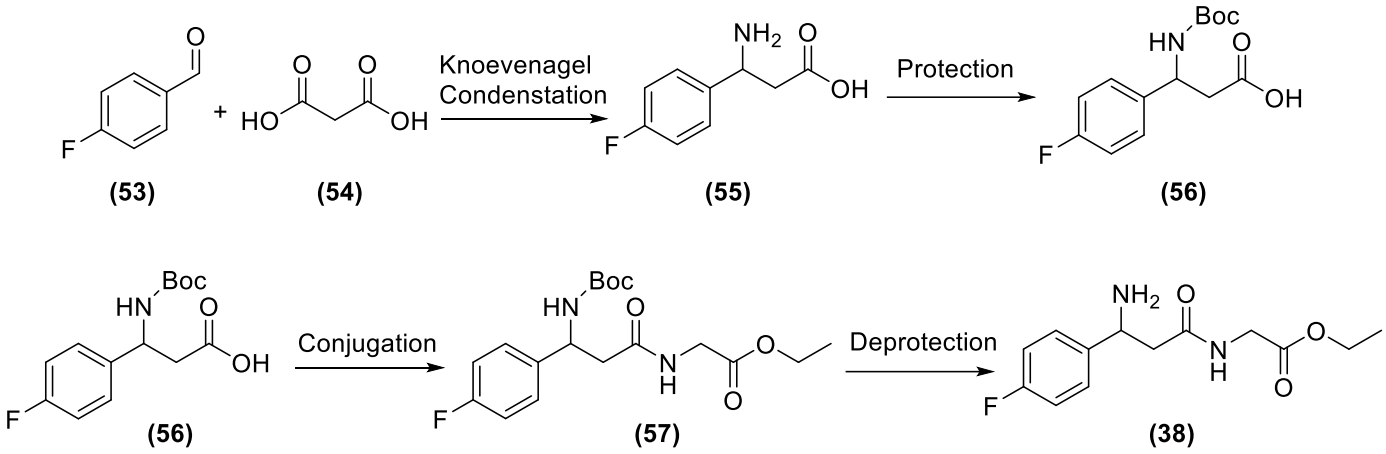

Scheme 2.4 Synthetic strategy to form compound **(38)**

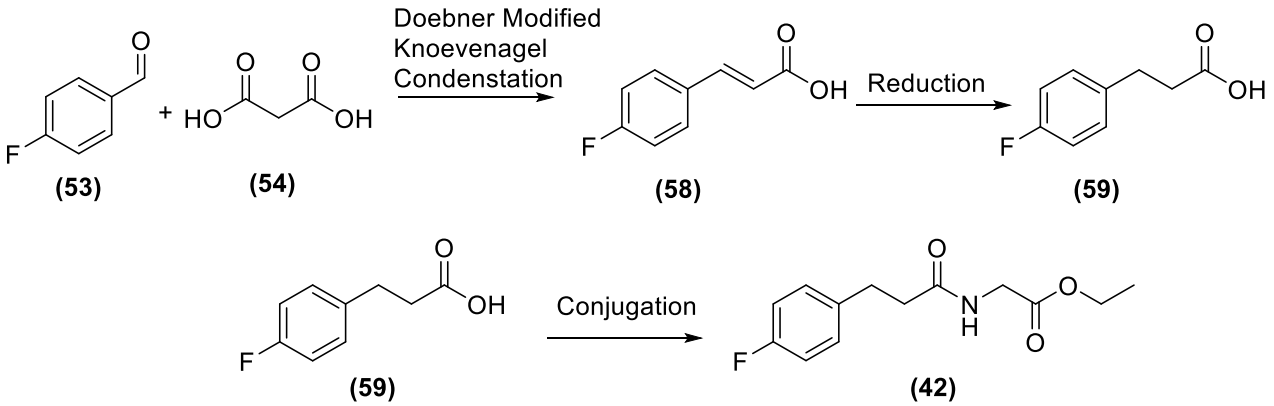

Scheme 2.5 Synthetic strategy to form compound **(42)**

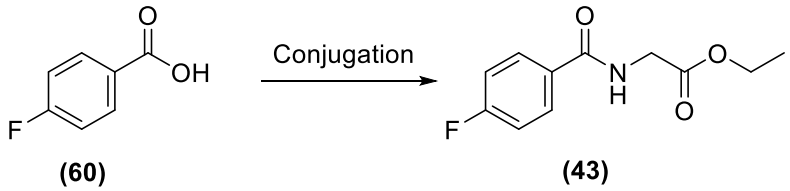

Scheme 2.6 Synthetic Strategy to form control scaffold **(43)**

2.2 Coupling Reactions

2.2.1 Synthesis of 3-Amino-3-(4-fluorophenyl)propanoic Acid (55)

3-Amino-3-(4-fluorophenyl)propanoic acid **(55)** was successfully synthesised in 39% yield according to the method of Martin *et al*.[71] *via* a modified Knoevenagel condensation reaction **(Scheme 2.7)**. No major modifications were made to the experimental method. Full characterisation of the product was obtained and data were in agreement with literature values.[63, 71] The ^{1}H and ^{13}C nuclear magnetic resonance (NMR) and low resolution electrospray ionisation-mass spectrometry (LRESI-

MS) spectra confirmed that the product obtained was pure. Characteristic chemical shifts and *J* coupling constants of the methine (CH) (dd, *J* 7.6, 7.6 Hz) and the methylene (CH_2) protons, as two sets of doublet of doublets (*J* 14.4 and 7.6 Hz), further confirmed the formation of the product.

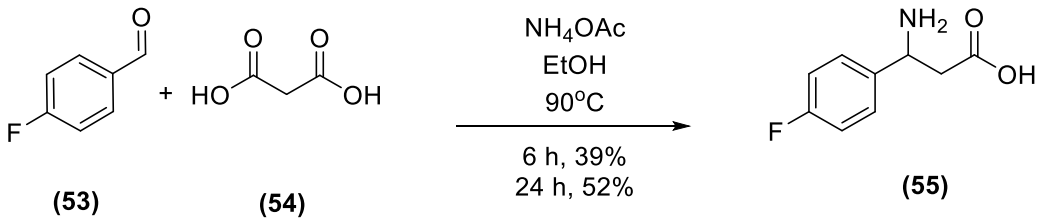

Scheme 2.7 Reaction Conditions for synthesis of 3-amino-3-(4-fluorophenyl)propanoic acid **(55)**

Modification of the standard Knoevenagel condensation reaction conditions were required as the standard method forms an α,β-unsaturated compound.[72] To form the β-amino acid **55**, the inclusion of ammonium acetate was required as a source to generate the primary amine. Scheme 2.8 shows a plausible reaction mechanism[63, 73] for the formation of β-amino acid **55**, which is hypothesised to proceed *via* the imine formation **(53d)** and its subsequent condensation with the enol intermediate of malonic acid **(54')**. This is followed by decarboxylation of the intermediate dicarboxylic acid **(53e)** and tautomerisation **(53f)** to form the final desired β-amino acid **(55)**.

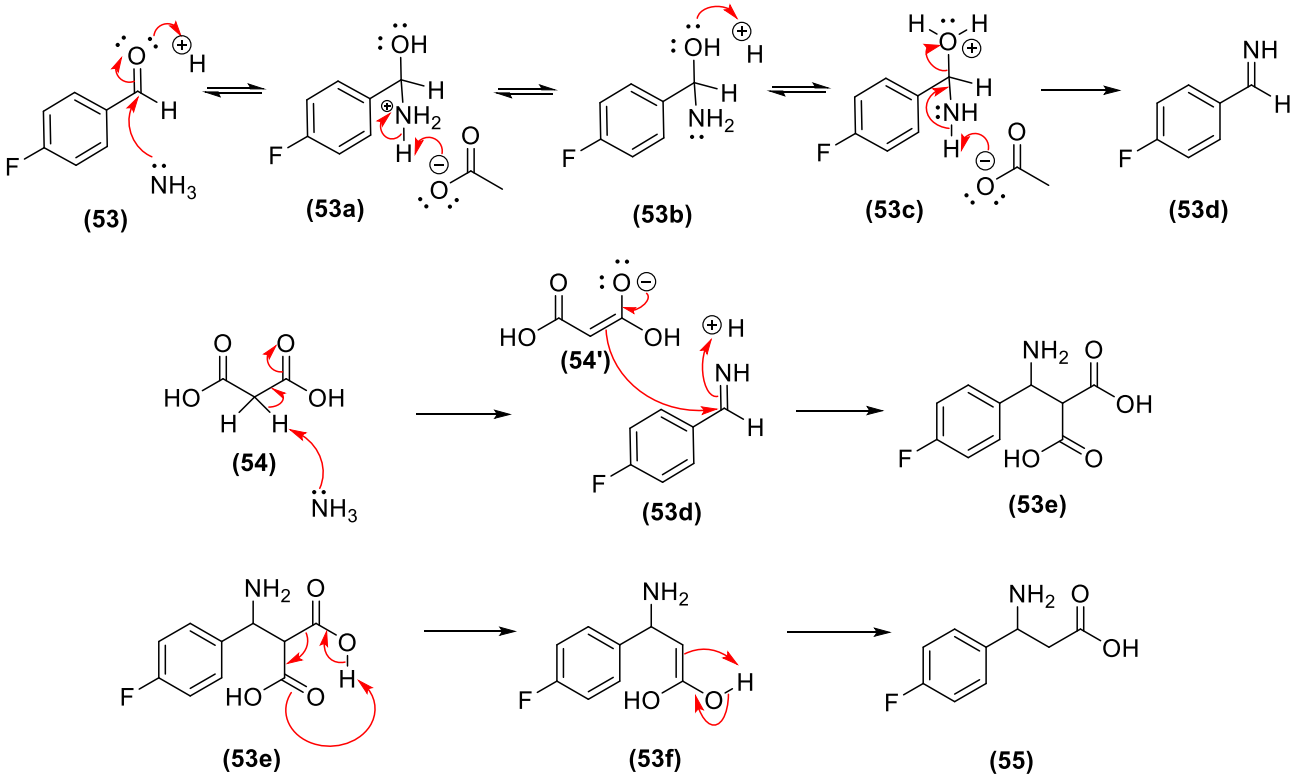

Scheme 2.8 Proposed mechanism for the formation of 3-amino-3-(4-fluorophenyl)propanoic acid **(55)**

Martin *et al*. reported a purified yield of 73% for this reaction **(Scheme 2.7)**, when conducted over 6 h.[71] To improve on the 39% yield obtained, the reaction was repeated with monitoring *via* thin layer chromatography (TLC) for disappearance of the starting aldehyde **(53)** and production of the final product **(55)**. Normal phase and cellulose plates were used, along with a ninhydrin stain, to monitor the presence of the primary amine group (*via* a colour change to purple spot on the TLC plate upon heating). Aliquots taken at 4 and 6 h displayed starting material of 4-fluorobenzaldehyde **(53)** still present in the reaction mixture. At 24 h, TLC indicated that the aldehyde **(53)** had been consumed and the product **(55)** had formed. The reaction was therefore worked up to give a crude product of 66% yield. While the ^{1}H NMR, in D_2O, indicated that the desired aryl β-amino acid **(55)** had formed, the sample also had a singlet at δ 3.1 ppm. This singlet was hypothesised to be a di-ammonium adduct formed from excess ammonium acetate and malonic acid in the reaction. This was removed from the sample by triturating the crude reaction mixture with a 1:1 mixture of ethanol and water. This afforded the pure aryl β-amino acid **(55)** in 52% yield. Although increasing of the reaction time improved the yield, it was still lower than that reported by Martin *et al.*[71]

2.2.2 Synthesis of *(E)*-3-(4-Fluorophenyl)acrylic Acid (58)

(E)-3-(4-Fluorophenyl)acrylic acid **(58)** was synthesised using the method of Li e*t al.*[74] *via* a Doebner modified Knoevenagel condensation reaction **(Scheme 2.9)**. Using the reactions conditions in Scheme 2.9, the crude acrylic acid **(58)** was obtained as a pale yellow solid. Inspection of the ^{1}H NMR spectrum showed that the desired product had been formed, with *J* coupling analysis of the vinylic protons ($^{3}J_{trans}$ - 16 Hz) confirming the *E* isomer was present. Small amounts of trace impurities were visible in the δ 1-3 ppm region of the ^{1}H NMR spectrum, and were removed by recrystallisation using a 1:1 mixture of ethanol and water. Recrystallisation afforded a pure white solid of the acrylic acid **(58)** in 64% yield. The ^{1}H and ^{13}C NMR and LRESI-MS data were in agreement with the literature.[75]

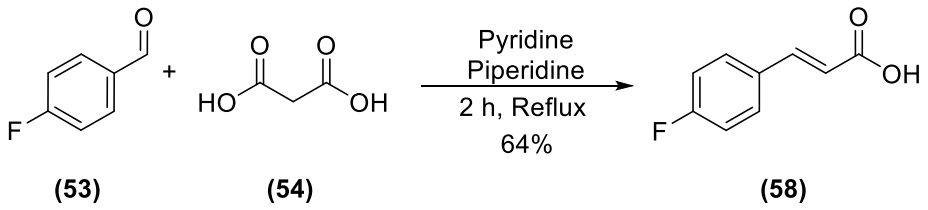

(53) **(54)** **(58)**

Scheme 2.9 Reaction conditions for synthesis of *(E)*-3-(4-fluorophenyl)acrylic acid **(58)**

The proposed reaction mechanism **(Scheme 2.10)** for the formation of **58** is attack of the electrophilic carbonyl centre of 4-fluorobenzaldehyde **(53)** by the nucleophilic enol intermediate **(54')**, followed by base induced decarboxylation of the aldol intermediate **(62a)** to produce the desired product **58**.[72]

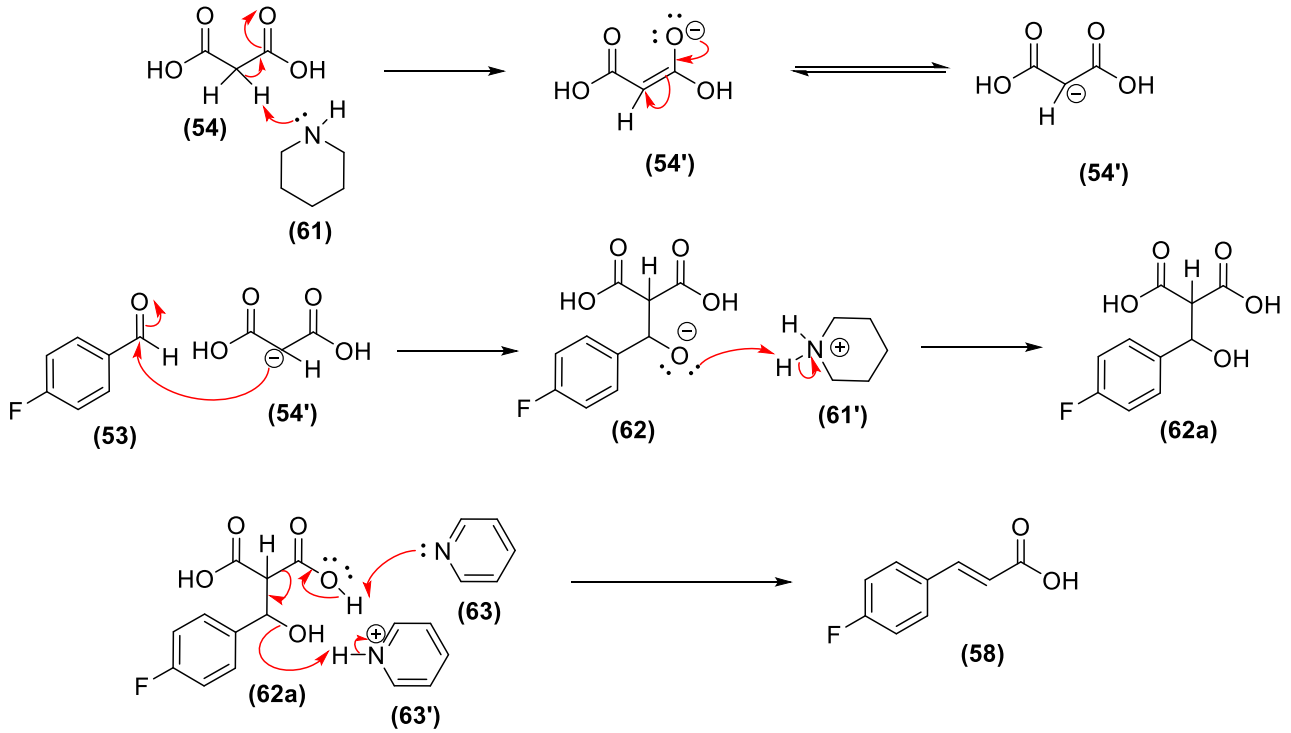

Scheme 2.10 Mechanism to form *(E)*-3-(4-fluorophenyl)acrylic acid **(58)** *via* a Doebner modified Knoevenagel condensation pathway

2.3 Protection Group Reactions

The next stage for the synthesis of the target compounds **(38**-**41)** was the *t*-Boc protection of the primary amine in the intermediate compounds **(44**, **47**, **50** and **55)**. The commonly employed *t*-Boc protection group was investigated as it offered a selective method to protect the free amines, using a carbamate, while also the ability to remain stable during the conjugation step and be deprotected using relatively mild conditions.[72]

2.3.1 3-((*tert*-Butoxycarbonyl)amino)-3-(4-fluorophenyl)propanoic Acid (56)

3-((*tert*-Butoxycarbonyl)amino)-3-(4-fluorophenyl)propanoic acid **(56)** was successfully synthesised in 54% yield according to the method of Axten *et al*.[76] **(Scheme 2.11)**, with the small modification of using 2 M HCl (due to it being readily available) in the work up instead of citric acid. TLC showed that the product was no longer ninhydrin positive, consistent with the protection having been successful. Characterisation using LRESI-MS confirmed the negative molecular ion ([M-H]$^-$) of *m/z*

282.1 for $[C_{14}H_{17}FNO_2]^-$. The ^1H NMR spectrum, run in DMSO-d_6, displayed the relevant resonances attributed to the compound. However, a shoulder peak on the *tert*-butyl resonance (δ 1.23 ppm) and two amide resonances at δ 4.75 and 7.44 ppm, respectively, were also observed.

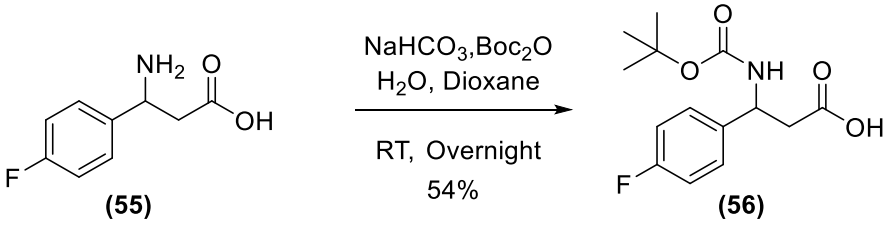

Scheme 2.11 Conditions to form 3-((*tert*-butoxycarbonyl)amino)-3-(4-fluorophenyl)propanoic acid **(56)**

Initial thoughts were that the sample was impure, however, further investigations of the literature revealed that similar α-*N*-*t*-Boc-amino acids can exist as conformational isomers (rotamers).[77] The conformational isomerism of carbamates is due to the ability for the carbamate to have a pseudo double bond *via* resonance stabilisation.[78] This pseudo π-double bond restricts the free rotation around the formal single σ-bond, creating the potential for two conformational isomers that coexist in solution. This is shown in Figure 2.2 A and B for the carbamate **56**, with the resonance structures **(56** and **56a)** and the *syn* **(56)** and *anti* **(56')** conformational isomers.

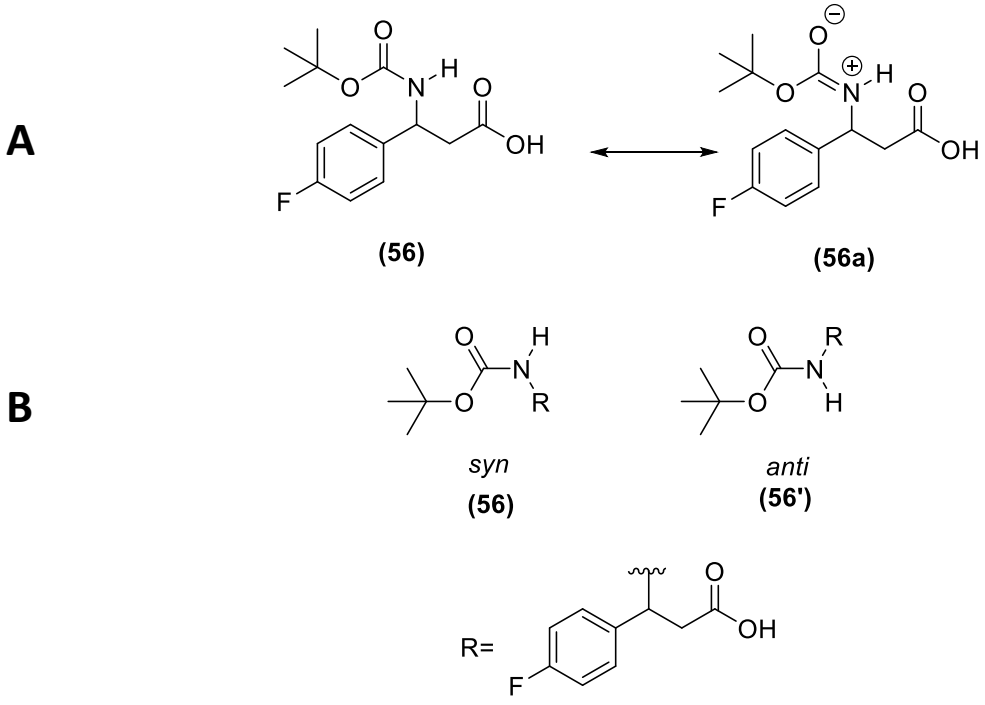

Figure 2.2 A Resonance stabilised structures of **(56)**; **B** *syn* **(56)** and *anti* **(56')** conformational isomers of **(56)**[78]

To determine if conformational isomerism was occurring for **56**, a series of variable temperature ^{1}H NMR experiments were carried out **(Figure 2.3)**. The resonance attributed to the *tert*-butyl protons sharpened to δ 1.34 ppm as the temperature was increased from 298 K to 318 K. Likewise, the resonance at δ 4.75 ppm, which was attributed to the NH protons of one of the isomers, was shown to disappear and a concomitant increase in integration at δ 7.43 ppm for the other NH was seen. Furthermore, the analysis showed the isomer signals that had disappeared at higher temperature had returned when the temperature was reduced again. Additionally, it was identified that at room temperature the compound is in a consistent ratio of 0.85:0.15 between the two isomers.

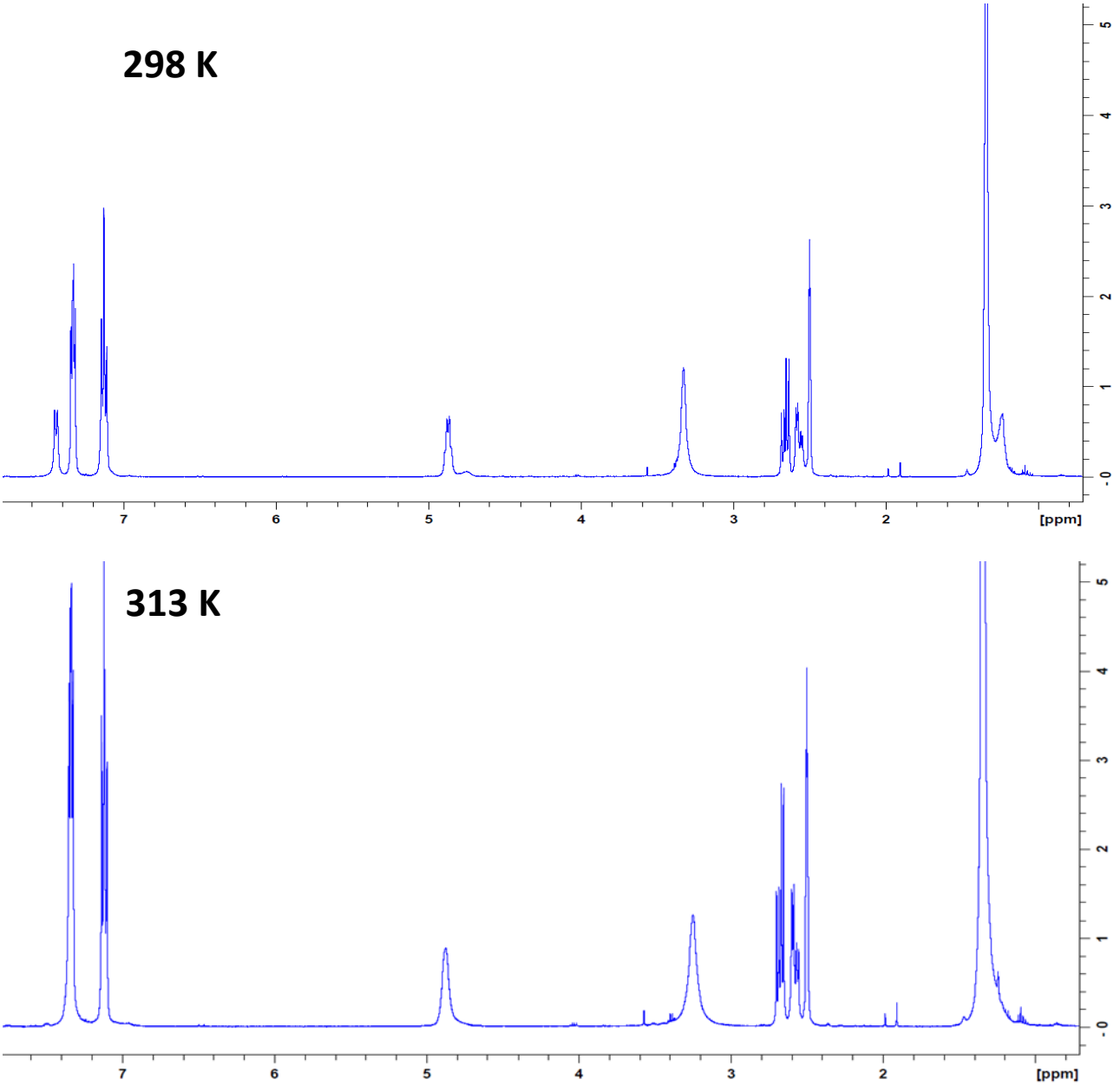

Figure 2.3 Variable temperature ^{1}H NMR of **(56)** at 298 K and 313 K

2.3.2 2-((*tert*-Butoxycarbonyl)amino)-3-(4-fluorophenyl)propanoic Acid (45)

Following the successful synthesis of **56** using the modified method of Axten *et al*.,[76] the same method was applied to synthesise 2-((*tert*-butoxycarbonyl)amino)-3-(4-fluorophenyl)propanoic acid **(45)**. Using the reaction conditions in Scheme 2.12 it was ascertained that the formation of α-*N*-*t*-Boc-amino acid **(45)** as a white solid occurred in 54% yield. TLC showed that the product was no longer ninhydrin positive, consistent with the protection having been successful. Full spectral characterisation of the product *via* ^{1}H and ^{13}C NMR and LRESI-MS indicated a pure product had formed. The presence of the additional nine methyl protons at δ 1.31 ppm in the ^{1}H NMR and the carbonyl and quaternary carbon resonances from the carbamate moiety at δ 155.4 and 74.1 ppm, respectively, in the ^{13}C NMR, further confirmed the synthesis of the product **(45)**.

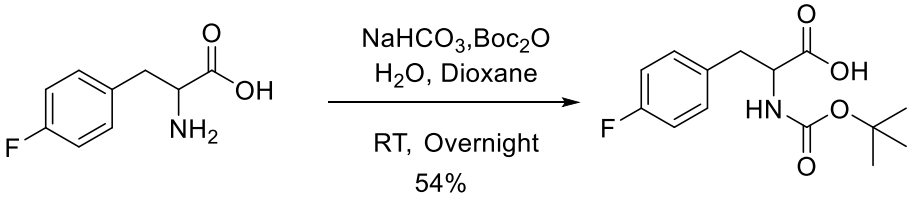

(44) **(45)**

Scheme 2.12 Conditions to form 2-((*tert*-butoxycarbonyl)amino)-3-(4-fluorophenyl)propanoic acid **(45)**

As seen for the β-*N*-*t*-Boc-amino acid **(56)**, compound **45** was present as two conformational isomers (rotamers) in DMSO-d_6 in a ratio of 0.84:0.16 at room temperature. Similar to compound **56**, variable temperature ^{1}H NMR experiments showed the disappearance of the shoulder on the *tert*-butyl resonance (δ 1.31 ppm) and converting of the two amide resonances to the single resonance at δ 6.96 ppm as the temperature was raised. Likewise, when the temperature was reduced, the analysis displayed the rotamers returning, confirming that the α-*N*-*t*-Boc-amino acid **(45)** existed as a series of rotamers at room temperature.

2.3.3 Synthesis of *t*-Boc Protected Aliphatic Amino Acids (48 and 51)

Synthesis of the aliphatic *t*-Boc protected α **(48)** and β **(51)** amino acids were performed *via* the method of Zhang *et al.*[79] **(Scheme 2.13)**. Similar to the aryl **(45** and **56)** syntheses, 2 M HCl was used during the work up stage of the reaction due to being readily available. Compound **48** and **51** were synthesised in 74% and 59% yields, respectively. TLC, ^{1}H and ^{13}C NMR and LRESI-MS showed the products were pure. All relevant resonances and *J* couplings constants were observed in both of the ^{1}H and ^{13}C NMR spectra, with the LRESI-MS data coinciding with the expected values.[79] No rotamers

were seen in either of the aliphatic α **(48)** and β **(51)** compounds by ^{1}H NMR, compared to the carbamates **45** and **56**. This is likely to be because of the extra steric bulk of the phenyl groups for compounds **45** and **56** increasing the free energy difference between the two conformations.[78] *t*-Boc reactions are generally quantitative. The relatively low yields (~55%) obtained for compounds **45**, **51**, and **56** are probably due to the partial deprotection during the work up stages with the strong acid (2M HCl). Future studies are recommended to use a weaker acid, for example 0.2 M HCl, to avoid deprotection in the work up stages.

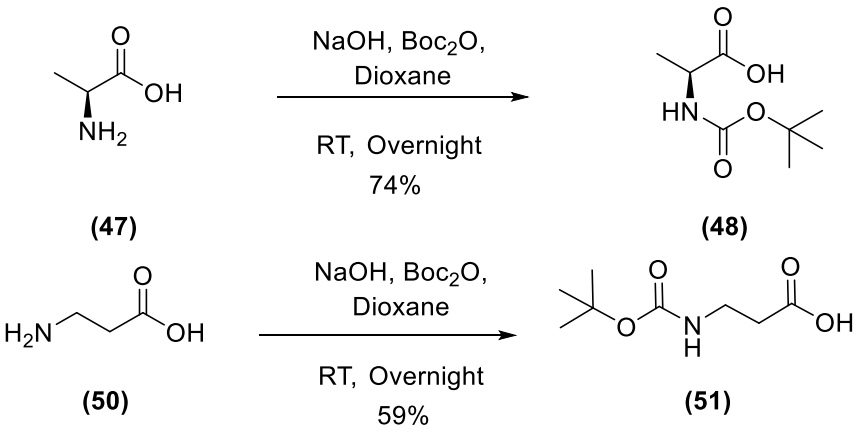

Scheme 2.13 Reaction conditions to synthesise aliphatic *t*-Boc protected α **(48)** and β **(51)** amino acids

2.4 Reduction Reactions

2.4.1 3-(4-Fluorophenyl)propanoic Acid (59) Synthesis

Following the successful synthesis of *(E)*-3-(4-fluorophenyl)acrylic acid **(58)**, its hydrogenation to the corresponding propanoic acid **(59)** was conducted in tetrahydrofuran (THF) and with Pd/C catalyst, using the method of Li *et al.*[74] Analysis of the ^{1}H NMR and GC-MS confirmed that starting material was recovered and no reduction had occurred. The use of ethers in metal catalysed reduction reactions is known to have adverse effects on the rate of the reaction.[80] This slowing or preventing of the reaction occurring is hypothesised to be due to the cyclic ether, THF, adsorbing on to the metal catalyst and blocking the sites from reaction.[80] Changing the solvent to ethanol (EtOH) **(Scheme 2.14)** afforded pure **59** in 91% yield. The disappearance of the doublet resonances at δ 7.60 and 6.52 ppm (*J* 16 Hz) in the ^{1}H NMR experiment, and the appearance of the triplet resonances at δ 2.95 and 2.68 (*J* 7.6 Hz) for the two CH_2 groups, indicated that the product had formed.

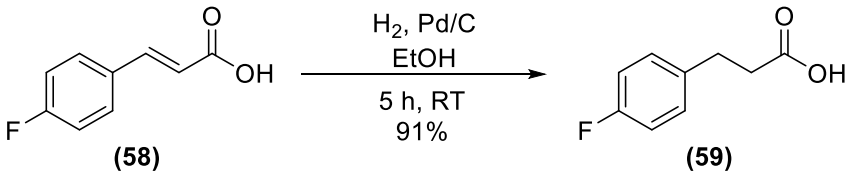

Scheme 2.14 Reaction conditions used to synthesise compound **(59)**

2.5 Conjugation Reactions

To form the glycine ethyl ester conjugates **(42, 43, 46**, **49**, **52** and **57)**, the relatively mild 1-ethyl-3-(dimethylaminopropyl)carbodiimide (EDCI) coupling method was used.[81-82] This was chosen due to its role in the facile synthesis of a wide variety of amides and ease of removal of the aqueous soluble urea side products in the work up stages.[82]

2.5.1 Synthesis of Conjugated Aliphatic Amino Acids (49 and 52)

To achieve conjugation of both the aliphatic α **(49)** and β **(52)** amino acids to glycine ethyl ester **(64)**, a similar procedure as reported by Hata *et al*.[81] was selected. During the reactions **(Scheme 2.15** and **2.16)** inconclusive results from TLC monitoring resulted in an increase of the reaction time from 24 h, as published by Hata *et al.,*[81] to 48 h. Unlike that reported by Hata *et al.,*[81] no precipitate was formed. Therefore, extractions of the products in all subsequent conjugation reactions were achieved by first acidifying to pH 2-3 using 2 M HCl and then extracting using dichloromethane (DCM).

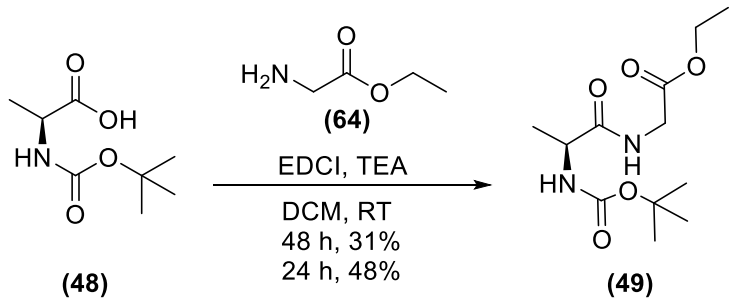

Scheme 2.15 Reaction conditions used to synthesise the aliphatic conjugated α-amino acid **(49)**

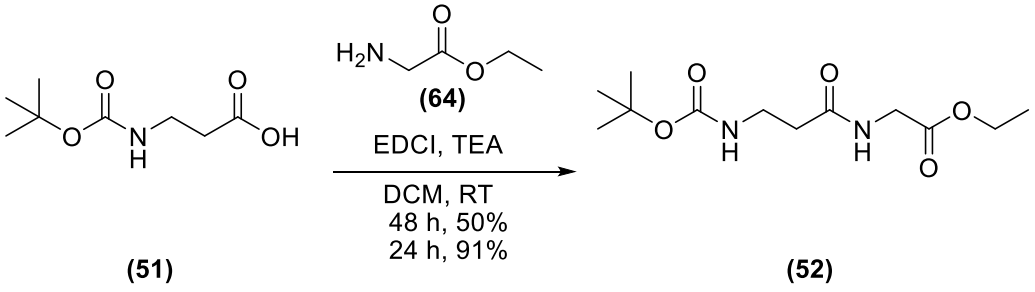

Scheme 2.16 Reaction conditions used to synthesise the aliphatic conjugated β-amino acid **(52)**

Both normal phase TLC and ^{1}H NMR showed that the desired products **(49** and **52)** had formed, but were impure. Purification of both products **(49** and **52)** *via* normal phase silica column chromatography gave the pure products, but low yields (31% for **(49)** and 50% for **(52)**) were obtained. These low yields can be possibly explained due to hydrolysis of the *O*-acylisourea intermediate occurring in the reaction because of a long reaction time and anhydrous conditions not being employed. Optimisation to increase the reaction yields were investigated by reducing the reaction time back to 24 h, as published.[81] This did lead to an increase in the yields (48% for **(49)** and 91% for **(52)**).

2.5.2 Synthesis of Conjugated Aromatic Amino Acids (46 and 57)

Considering the successful synthesis of **49** and **52**, Hata *et al*.'s method[81] was also used to conjugate the aryl *t*-Boc α **(45)** and β **(56)** amino acids to glycine ethyl ester **(64)**. Using unoptimised reaction conditions **(Scheme 2.17)**, ethyl (3-((*tert*-butoxycarbonyl)amino)-3-(4-fluorophenyl)propanoyl)glycinate **(57)** was synthesised in an impure form. Purification of the product was achieved *via* normal phase silica column chromatography to produce a pure product in 73% yield. Full spectral characterisation of the product was carried out *via* ^{1}H and ^{13}C NMR, which indicated a pure product had been isolated. The additional ^{1}H NMR resonances of an amide at δ 6.69 ppm, two CH_2 groups at δ 4.18 and 3.81 ppm, and the CH_3 group at δ 1.22 ppm, confirmed the product's **(57)** formation. Similarly, LRESI-MS analysis displayed the positive molecular ($[M+H]^+$) ion at *m/z* 369.2 for $[C_{18}H_{25}FN_2O_5]H^+$, providing further confirmation of **57** formation.

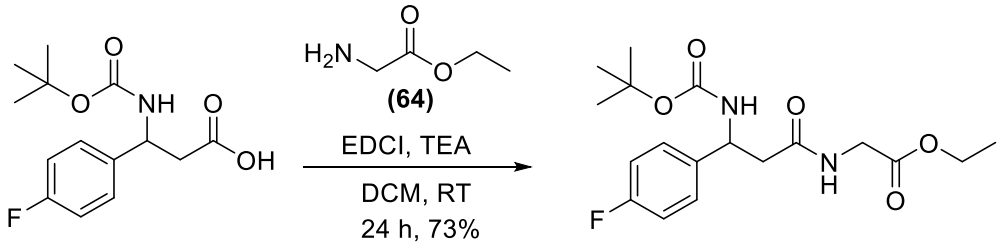

(56) **(57)**

Scheme 2.17 Reaction conditions used to synthesise the aromatic conjugated β-amino acid **(57)**

Synthesis of ethyl (2-((*tert*-butoxycarbonyl)amino)-3-(4-fluorophenyl)propanoyl)glycinate **(46)**, was performed using the reaction conditions in Scheme 2.18. Isolation of the product was performed *via* normal phase silica column chromatography to give pure **46** in 53% yield. Analysis *via* ^{1}H NMR displayed the additional resonances from the amide at δ 8.38 ppm, two CH_2 groups at δ 4.10 and 3.86 ppm, and the CH_3 group at δ 1.20 ppm, confirming the formation of **46**. The sodium adduct ion

([M+Na]$^+$) at *m/z* 391.1 and positive molecular ([M+H]$^+$) ion at *m/z* 369.2 were seen in the LRESI-MS, confirming the formation of **46**.

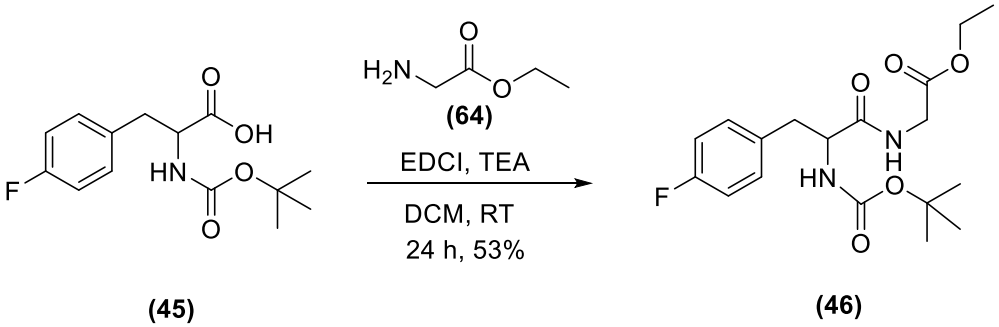

Scheme 2.18 Reaction conditions used to synthesise the aromatic conjugated α-amino acid **(46)**

2.5.3 Synthesis of Phenylethyl and Aromatic Amide Conjugates (42 and 43)

Synthesis of the glycine ethyl ester conjugates of **42** and **43** were also conducted using Hata *et al*.'s method **(Schemes 2.19** and **2.20)**.[81] For synthesis of **42 (Scheme 2.19)**, the product was obtained as a white solid, after purification *via* normal phase silica column chromatography, in 68% yield. Full spectral characterisation *via* ^{1}H, ^{13}C NMR and LRESI-MS, confirmed purity of the product. ^{1}H NMR characterisation confirmed the product *via* the new amide (NH) resonance at δ 5.88 ppm and the additional two CH_2 and CH_3 resonances at δ 4.21, 4.01 and 1.28 ppm, respectively. Further characterisation using LRESI-MS confirmed the positive molecular ([M+H]$^+$) ion of *m/z* 254.2.

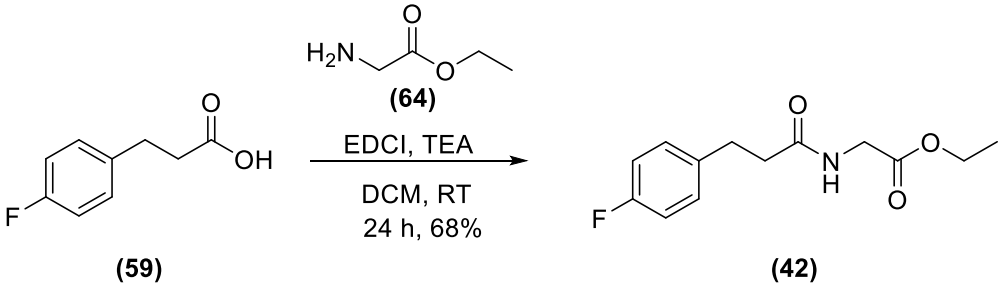

Scheme 2.19 Reaction conditions used to synthesise the phenylethyl conjugated compound **(42)**

Synthesis of the aromatic amide **(43) (Scheme 2.20)** was obtained in a 67% yield as a white solid, with no further purification required after work up. LRESI-MS (positive mode) showed the expected protonated molecular at *m/z* 226.1. Characterisation *via* ^{1}H NMR was also consistent with the product formation, with the new amide resonance being observable at δ 6.58 ppm and the additional two CH_2 and CH_3 resonances at δ 4.27, 4.23 and 1.32 ppm, respectively. ^{13}C NMR characterisation also displayed the new quaternary carbon resonance from the extra carbonyl group, at δ 166.5 ppm, further confirming the product.

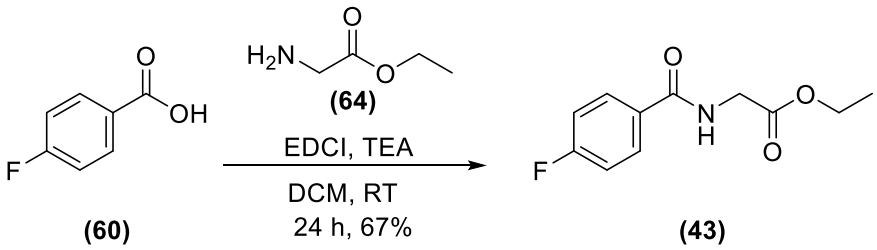

Scheme 2.20 Reaction conditions used to synthesise the conjugated control scaffold **(43)**

2.6 Deprotection of Glycine Ethyl Ester Conjugates

2.6.1 Synthesis of Aromatic α- and β-Glycine Ethyl Ester Conjugates (38 and 40)

Removal of the *t*-Boc protecting group from the *t*-Boc protected aryl α and β-glycine ethyl ester conjugates **(46** and **57)** was initially attempted using trifluoroacetic acid (TFA) *via* conditions reported for a similar compound by Duan *et al*.[83] Monitoring the reactions *via* TLC, with ninhydrin staining, showed multiple ninhydrin positive spots at various R_f values, including a spot corresponding to starting material. Subsequent investigations with varying reaction conditions *i.e.* temperature (0 °C and RT), molar equivalence of TFA (1:1 and excess), and different reaction times (40 min, 1 h, 2 h and >2h) continued to show multiple ninhydrin positive spots at various R_f values, including a spot corresponding to starting material. Further analysis of the crude products after work up by ^{1}H NMR indicated that 1:1 TFA:DCM with a reaction time of 1 h at room temperature did afford some of the desired products, as indicated by the doubling up and a slight chemical shift change of the resonances in the ^{1}H NMR from the aromatic and glycine ethyl ester parts of the molecule. However, at the longer time points (>2 h), an impure sample with the *t*-Boc still present, indicated no (or little) formation of the desired product. Attempts at variations in the work up procedure, *i.e.* trying to convert to the free base and then extracting or precipitating the hydrochloride salt out, using cold diethyl ether were also undertaken. However, ^{1}H NMR again was determined to be inconclusive for product formation.

Hata *et al.*[81] have reported that clean removal of the *t*-Boc group can be achieved using 4 M HCl in dioxane. Using conditions in Scheme 2.21, the glycine ethyl ester conjugates of **38** and **40** were obtained as the hydrochloride salts. For the synthesis of ethyl (3-amino-3-(4-fluorophenyl)propanoyl)glycinate **(38)**, the crude product was quite impure, as seen by a large amount of carbon alkyl resonances observed in the δ 1-3 ppm region of the ^{1}H NMR spectrum. To

purify the product, a reversed phase C_{18} Sep-Pak was used before the resulting solution was lyophilised to isolate the pure product in 65% yield as a white solid.

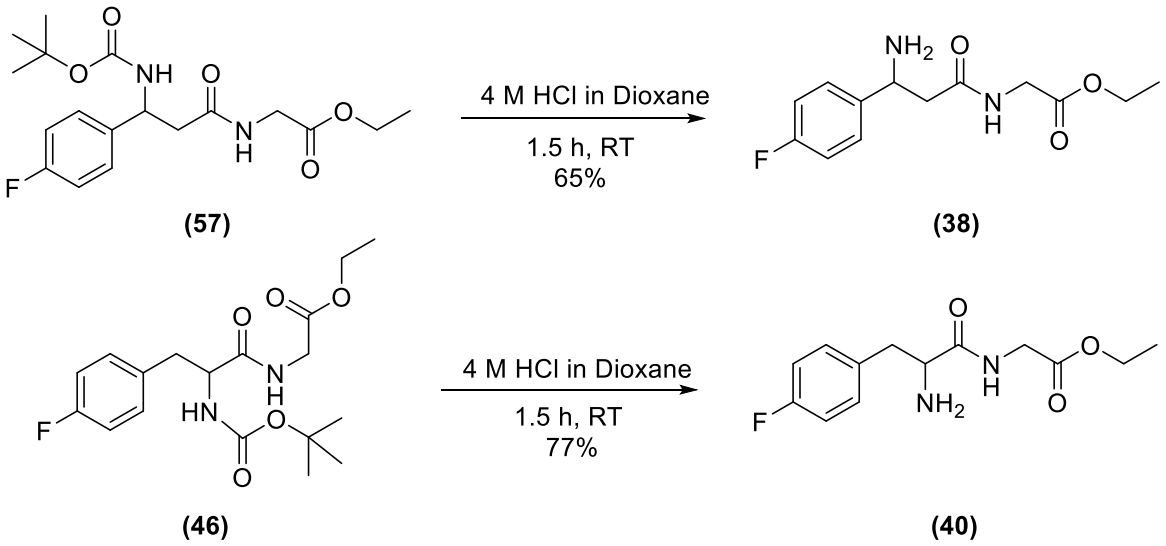

(57) **(38)** **(46)** **(40)**

Scheme 2.21 Synthesis of target aryl α-**(40)** and β-**(38)** glycine ethyl ester conjugates

Characterisation of the β-glycine ethyl ester conjugate **(38)** *via* ^{1}H and ^{13}C NMR and LRESI-MS indicated that a pure product was obtained. NMR characterisation showed the loss of the *tert*-butyl protons in the ^{1}H NMR, and the loss of carbonyl, quaternary and methyl carbon resonances from the ^{13}C NMR compared to the starting material **(57)**. The expected proton resonance from the proton on the β-carbon was not seen in the ^{1}H NMR. A 2D HSQC experiment showed a correlation between the β-carbon at δ 52.1 ppm, and a proton at δ 4.73 ppm (under the residual D_2O resonance), confirming its presence.

Due to the successful synthesis of the β-glycine ethyl ester conjugate **(38)**, 4 M HCl in dioxane was also used for the synthesis of the α-glycine ethyl ester conjugate **(40)**. Ethyl (2-amino-3-(4-fluorophenyl)propanoyl)glycinate **(40)** was synthesised in 77% yield according to the conditions in Scheme 2.21. Characterisation *via* ^{1}H and ^{13}C NMR and LRESI-MS indicated that a pure product was obtained. Confirmation of the removal of the *t*-Boc group was evident from the loss of a carbonyl, quaternary and primary carbon resonances from the ^{13}C NMR and the loss of the *tert*-butyl protons in the ^{1}H NMR compared to the starting material **(46)**. LRESI-MS (positive mode) showed a protonated molecular ion ($[M+H]^+$) being *m/z* 269.2 which is consistent with the desired compound.

2.6.2 Synthesis of Aliphatic α- and β-Glycine Ethyl Ester Conjugates (**39** and **41**)

Following the method of Hata *et al.*,[81] 4 M HCl in dioxane was also used for the *t*-Boc deprotection of **49** and **52** to give the aliphatic glycine ethyl ester conjugates of **41** and **39**, respectively **(Scheme 2.22)**. In each case, after 1h, it was determined *via* monitoring using reversed phase TLC plates that a new ninhydrin positive product had formed. The reactions were subsequently worked up and lyophilised to produce the hydrochloride salts of the aliphatic β-amino acid **(39)** as a brown waxy solid, and the aliphatic α-amino acid **(41)** as a waxy oil in 51% and 65% yields, respectively. Each reaction was characterised *via* ^{1}H and ^{13}C NMR and LRESI-MS. Confirmation of the removal of the *t*-Boc group for **39** and **41** were evident from the loss of the additional carbonyl, quaternary and primary carbon resonances in the ^{13}C NMR spectra, and the loss of the *tert*-butyl protons in the ^{1}H NMR spectra. Characterisation using LRESI-MS further confirmed the product, as both **39** and **41** displayed the expected protonated molecular ions of *m/z* 175.1 and 175.2, respectively.

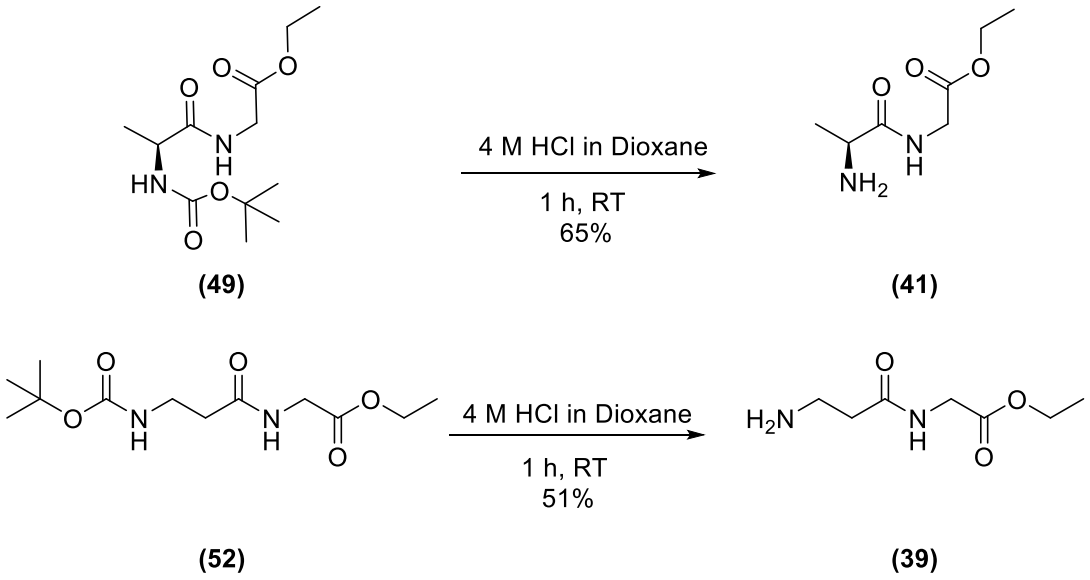

(49) **(41)** **(52)** **(39)**

Scheme 2.22 Reaction conditions used to synthesise aliphatic glycine ethyl ester conjugates **39** and **41**

Chapter 3: Results and Discussion - Enzymatic Stability

3.1 Enzyme Choice and Confirmation of Activity

Porcine liver esterase (PLE) was chosen to examine the metabolic stability of the target glycine ethyl ester conjugates **(38-43)**. In addition to being a carboxylesterase this enzyme also presents amidase activity, and has been reported to be analogous to human esterases that participate in the metabolism of many drugs.[84-86] Recent research by Loser *et al.* has also employed PLE for metabolic stability studies of their developed [^{18}F]fluorosulfonamides.[84]

The activity of the commercial PLE used was determined using a spectrophotometric assay with the substrate of *p*-nitrophenyl butyrate.[87] The initial rate of the formation of the cleavage product, *p*-nitrophenol, was determined to be linear (r^2 = 0.9914) over the first 1.5 min of the assay **(Figure 3.1A)**. Using a Michaelis-Menten plot **(Figure 3.1B)**, a Michaelis constant (K_m) of 0.11 ± 0.03 mM was found, which was consistent with the reported value of 0.14 ± 0.02 mM from Landowski *et al.*[87]

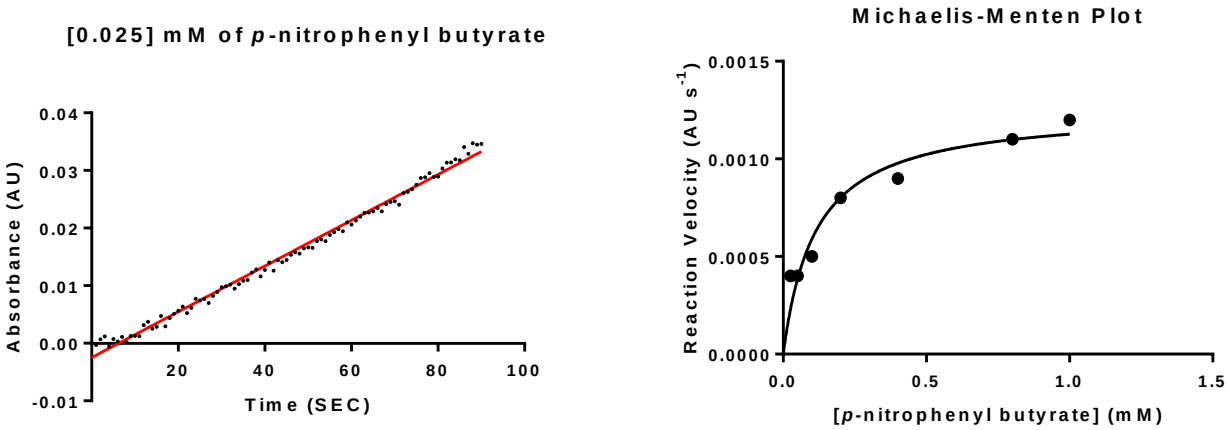

Figure 3.1 A - Example of plot used to determine initial rate of formation *p*-nitrophenol; **B** - Michaelis-Menten plot used to determine the Michaelis constant (K_m) for the enzyme assay

3.2 Metabolic Stability of Target Compounds (38-43)

The glycine ethyl ester conjugates of **38**-**43** were separately incubated with 28 µg/mL of PLE in 5% DMSO 10 mM phosphate buffer medium. Control assays of the glycine ethyl ester conjugates **(38-43)** without PLE present were also prepared in the same DMSO phosphate buffer medium and incubated in a similar manner. Predicted amide cleavage products **(Figure 3.2)**, the carboxylic acid compounds **(44**, **47**, **50**, **55**, **59** and **60)**, and glycine ethyl ester **(64)** were also incubated *via* a similar manner, without PLE, to provide reference points for analysis. Due to the potential future direction

of the work with ^{18}F-fluorinated peptide radiotracers, a 4 h incubation period was chosen as it is greater than two half-lives of [^{18}F]fluorine and enough time for PET procedures to be undertaken.

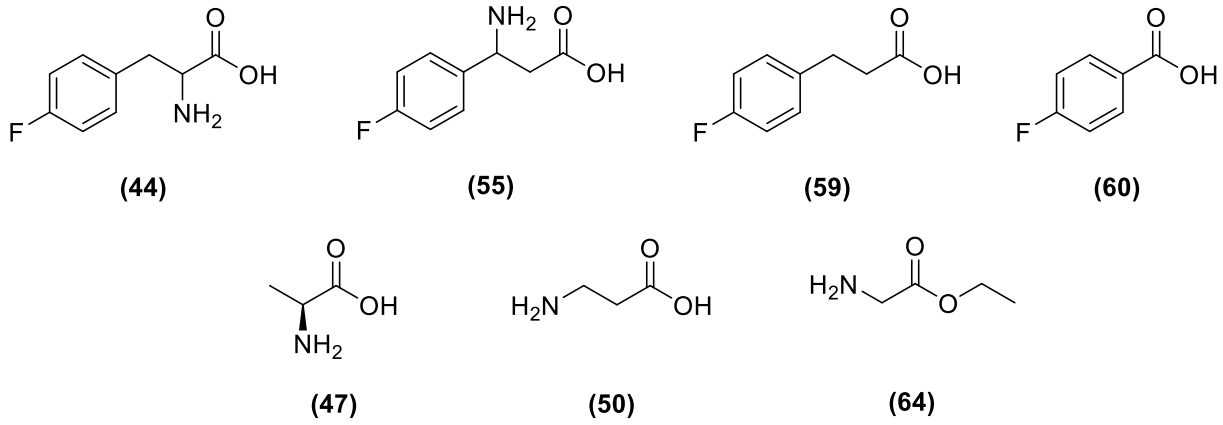

Figure 3.2 Enzyme incubation predicted amide bond cleavage products

3.2.1 Analysis *via* Reversed Phase and Cellulose TLC

To monitor the metabolic stability of glycine ethyl ester conjugates **(38**-**43)**, incubation aliquots were taken at 1 h time intervals and were quenched with a 2% *v/v* TFA in acetonitrile solution. Aliquots were analysed *via* reversed phase and cellulose TLC with visualisation of the plate performed at 254 nm for the aromatic compounds **(38**, **40**, **42** and **43)**, and with a ninhydrin stain for the aliphatic and aryl compounds **(38**-**41)**. UV-Vis analysis was not considered, despite its potential for real time analysis, due to the lack of chromophore for the aliphatic compounds **(39** and **41)** and the insufficient differentiation expected between the aromatic compounds **(38**, **40**, **42** and **43)** and their cleavage products. The control assays of the glycine ethyl ester conjugates **(38**-**43)** and the predicted amide cleavage products **(44**, **47**, **50**, **55**, **59**, **60** and **64)** were similarly quenched and examined *via* the same TLC methods. No degradation of these compounds from the control assays or the predicted amide cleavage products were observed at any of the time points.

TLC studies suggested that ester group cleavage was visible from 2 h for the aryl α **(40)** and aromatic amide **(43)** conjugates and from 1 h for the phenylethyl conjugate **(42)**. These were indicated by an additional spot to the starting materials in each of the incubation mixtures at a more polar, higher R_f (reversed phase). These did not correspond to the R_f values of glycine ethyl ester **(64)** nor the carboxylic acids of **59** and **60** expected from amide cleavage. No other new spots were seen by TLC for the remainder of the incubations. Although the additional spot seen in the assays for the aryl α **(40)** and aromatic amide **(43)** conjugates appeared to increase in intensity by TLC at 3 and 4 h, a

spot consistent with starting material was still observed at these later time points. This suggested only partial cleavage of the ester group for conjugates **40** and **43**. For the phenylethyl conjugate **(42)**, only the new compound was seen after 3 h of incubation, suggesting full cleavage of the ester group. For the aryl β-glycine ethyl ester conjugate **(38)** and the aliphatic α **(41)** and β **(39)** glycine ethyl ester conjugates, TLC indicated that the samples remained stable over the 4 h incubation period with PLE.

3.2.2 Analysis *via* Mass Spectrometry Methods

To provide more confirmation than TLC, the quenched assay samples of **(40**, **42** and **43)**, at time points where degradation was originally observed, and from the 4 h time points for the stable conjugates **(38, 39** and **41)**, were lyophilised, before being analysed *via* direct injection LRESI-MS. Control assay samples, similarly prepared, were also examined by direct injection LRESI-MS. Direct injection of the control assays (without esterase) showed the presence of the positive molecular ion ($[M+H]^+$) for each of the aryl α **(40)** and β **(38)** and the aliphatic α **(41)** and β **(39)** glycine ethyl ester conjugates, confirming their stability. Neither the positive or negative molecular ion for the phenylethyl **(42)** and aromatic **(43)** glycine ethyl ester conjugates were observed for their control assays, despite their presence indicative in the TLC analysis. This is likely a result of excess salt, from the buffers, causing ion suppression during direct injection LRESI-MS analysis.[88] LRESI-MS direct injection results of the assays (with esterase) for each of the aryl β **(38)** and aliphatic α **(41)** and β **(39)** glycine ethyl ester conjugates displayed the presence of the positive molecular ion ($[M+H]^+$), confirming their stability. No positive or negative molecular ions were observed for any of the ester or amide cleavage products, supporting their stability over the 4 h incubation period in PLE, and consistent with the TLC results.

The positive molecular ion of the aryl α **(40)** glycine ethyl ester conjugate was observed in the LRESI-MS spectrum from the assay. However, the molecular ion due to cleavage of the ethyl ester group from **40**, which was expected to be observed due to the TLC findings, was not seen in the spectra. Similar to their control assays, the positive or negative molecular ion for the phenylethyl **(42)** and aromatic **(43)** glycine ethyl ester conjugates, and the respective cleavage products, were also not observed in their respective mass spectra. The inability to see the cleavage products from the glycine ethyl ester conjugates of **40**, **42** and **43**, which were indicated to be formed *via* the TLC results, is again likely due to the ion suppression from the excess salts in the sample.[88]

To remove the salts, assay samples **(40**, **42** and **43)**, and their respective control assays, were further analysed *via* liquid chromatography-mass spectrometry (LC-MS) methods. This was performed using an analytical reversed phase C-18 column with a water to acetonitrile gradient method. Similar to the direct injection LRESI-MS result, the control assay for aryl α **(40)** glycine ethyl ester conjugate displayed a single peak in the chromatogram which corresponded to the positive molecular ion of **40**. Likewise, for the assay analysis, the positive molecular ion of the aryl α **(40)** glycine ethyl ester conjugate was observed as a single peak in the chromatogram. However, also observed in the same peak from the chromatogram and absent from the control assay, was a positive molecular ion of *m/z* 224. While this *m/z* does not correspond to the product of the ester cleavage *i.e.* the carboxylic acid, it does correspond to loss of the ethoxy (OCH_2CH_3) group. This could possibly be from formation of the acid and cleavage at the carbonyl carbon. The inability to see the positive molecular ion corresponding to the carboxylic acid is not surprising, as carboxylic acids tend to be poorly ionised, *via* ionisation sources in positive mode ESI-MS analysis.[89] The presence of the *m/z* 224 in the PLE incubated sample, but not in the control assay, suggests that the cleavage of the ester group occurred. The observation of only one peak in the LC run is likely due to the conjugate **(40)** and ester cleavage product co-eluting, as no LC method development was done due to limited time. Analysis, *via* LC-MS, of the phenylethyl **(42)** and aromatic **(43)** glycine ethyl ester conjugates displayed similar results to the direct inject methods employed. Neither the assay of the conjugates **(42** and **43),** nor their respective control assays displayed the molecular ion of the intact molecules or any of the cleavage products. This inability to see these compounds is highly likely due to the limited amount of material present in the sample and limited time for further studies.

The incubation studies suggested that none of compounds had undergone amide cleavage by the PLE. This was not unexpected as PLE has only been reported to show amidase activity towards aromatic derived amides, and not aliphatic derived amides.[84-85] However, it is interesting to note that results from both the aryl β **(38)** and aliphatic α **(41)** and β **(39)** glycine ethyl ester conjugate assays, indicated that the ester group had increased stability compared to the aryl α **(40)**, the phenylethyl **(42)** and aromatic **(43)** glycine ethyl ester conjugates. Likewise, the finding that the aryl β **(38)** was more stable than the aryl α **(40)** alludes to the fact that inclusion of a β-amino acid may also increase the stability of other functional groups in the molecule.

Chapter 4: Conclusions and Future Directions

4.1 Conclusions

The overall goal of this research was to increase the limited understanding and knowledge about β-amino acids and their scaffolds, with regards to improvements in metabolic stability of ^{18}F-fluorinated peptide radiotracers. The specific aims were to synthesise a range of aryl and aliphatic β-amino acids **(38** and **39)**, α-amino acids **(40** and **41)** and non-amino acid isosteres **(42** and **43)** conjugated to glycine ethyl ester as a simple model of a peptide conjugated system. Subsequent studies were then undertaken to compare their metabolic stability using porcine liver esterase (PLE).

All of the target compounds, six final **(38**-**43)** and eleven intermediates **(45**, **46**, **48**, **49**, **51**, **52** and **55**-**59)** were successfully synthesised and characterised *via* both NMR and MS methods. Each of the desired final and intermediate compounds were isolated pure in yields ranging from 39% to 91%. Interestingly, synthesis of the aryl *t*-Boc protected amino acids **(45** and **56)** revealed that at room temperature these compounds existed as conformational isomers (rotamers). Initial removal of the *t*-Boc group from the aryl glycine ethyl ester conjugates **(46** and **57)** with TFA and DCM had limited success. Deprotection using HCl in dioxane and purification *via* a C_{18} Sep-Pak gave the desired aryl glycine ethyl ester conjugates **(38** and **40)** as their hydrochloride salts.

TLC, LRESI-MS and LC-MS methods were used to analyse aliquots from the metabolic stability incubation studies. These results indicated that the aryl β **(38)** and the aliphatic α **(41)** and β **(39)** glycine ethyl ester conjugates were stable over the 4 h incubation period. TLC analysis suggested that the aryl α **(40)**, and the non-amino acid isostere conjugates **(42** and **43)**, cleaved the ester group. However, further analysis using LRESI-MS and LC-MS methods could not further confirm this. There was no evidence that the amide bond in any of the conjugates **(38**-**43)** had been degraded by PLE.

4.2 Future Directions

Future directions on this research involves three avenues of exploration with regards to immediate work on the current compounds, synthesis of new compounds and subsequent metabolic stability studies. Future initial work will repeat the incubations to ensure there is sufficient amounts of samples for analysis, synthesise the ester cleavage products for comparison, and focus on the

development of optimised LC-MS conditions for separation of the conjugates and their expected cleavage products, for definitive findings.

The second avenue would be to develop conjugates whereby the fluorinated moiety is connected *via* the amino group in the aryl and α- **(65)** and β- **(66)** amino acids **(Figure 4.1)**. This has greater representation of the methods currently employed to increase the metabolic stability of metallic radiolabelled peptide-based systems. Conjugation of the current investigated system, with the free amine group **(67** and **68)** will also be made to relevant biological peptides *e.g.* bombesin analogues. This will be used to provide a more realistic understanding on whether an ^{18}F-fluorinated β-amino acid or analogue improves the metabolic stability of the radiotracer. If an increase in stability is observed, investigations and experiments would then follow with ^{18}F-radiolabelled versions.

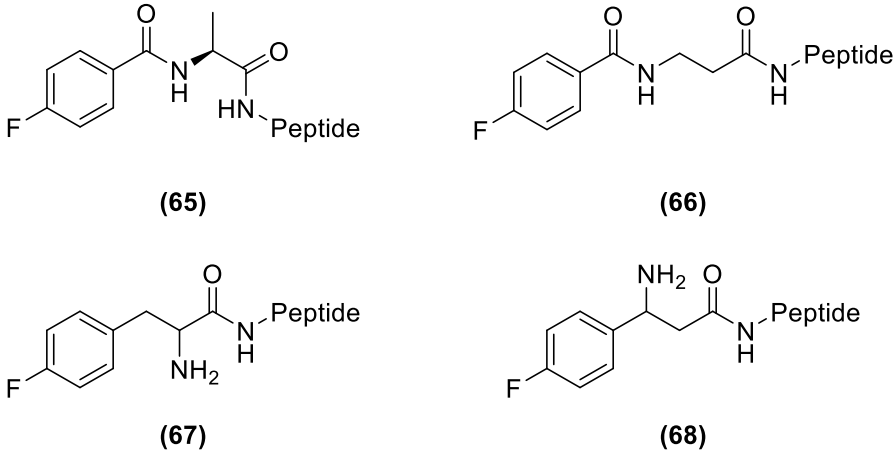

Figure 4.1 Conjugates for future investigations to examine the stability provide by a β-amino acid to a peptide radiotracer

The third avenue of exploration would be to expand the basis of enzymes used for the metabolic studies. It is known that other enzymes such as cytochrome P450s, neutral endopeptidase and other exo and endopeptidases, and amidases found in biological systems, play an important role in drug metabolism, and hence contribute to the metabolism of the radiotracer.[5, 40, 90] Similarly, other matrices containing enzymes, such as microsomes, hepatocytes and serum could also provide a better *in vitro* model to examine the metabolic stability.[90] Therefore, a future direction would be to examine these enzymes and matrices in regard to the metabolic stability of the developed peptide-based radiotracers. Additional analysis *via* HPLC, LC-MS and NMR methods, will also be investigated for their ability to characterise the work, and to provide a deeper understanding of metabolic stability of the developed peptide radiotracers.

Chapter 5: Experimental

5.1 General Experimental

All solvents and reagents were purchased from commercial suppliers with a purity of ≥ 95% and used without further purification, unless stated. All water used was purified by reverse osmosis. Solvents were removed under reduced pressure using a Heidolph rotary evaporator. Fourier transformed infrared spectra (FTIR) were obtained using a Thermo Fisher Nicolet FTIR spectrophotometer with attenuated total reflection (ATR). Melting points (M.P.) were obtained using a Stuart SMP10 melting point apparatus. Ultraviolet-visible (UV-Vis) spectra were obtained on a Jasco V-760 UV-Visible spectrophotometer.

Thin layer chromatography (TLC) was performed using normal phase silica (Merck, Silica gel 60 F_{254}), reversed phase silica (Merk, Silica gel 60 RP-18 F_{245}) and cellulose (Merck, Cellulose F) plates. Plates were visualised using both long (365 nm) and short (254 nm) UV light, and if required, they were stained with ninhydrin. Column chromatography was performed using normal phase silica (silica gel 60, 0.040-0.063 µm) and the specific mobile phases indicated as *vol/vol* ratio. Waters C_{18} Sep-Pak cartridges were used for reversed phase purification.

Nuclear magnetic resonance (NMR) spectra were acquired on a Bruker AVIIIHD 400 MHz spectrometer, where proton (^{1}H) and carbon (^{13}C) spectra were obtained at 400 MHz and 100 MHz respectively. Proton and carbon assignments were also made using NMR spectroscopic techniques of DEPT and HSQC. Variable temperature ^{1}H NMR experiments were performed on a Bruker AVIIIHD 500 MHz spectrometer with spectra collected at 298 K, 303 K, 308 K, 313 K and 318 K. All NMR samples were prepared in either $CDCl_3$, CD_3CN, D_2O, DMSO-d_6 or D_2O with 10% NaOH depending on the solubility of the compounds. Chemical shifts (δ) were measured in parts per million (ppm) with reference to the respective solvent peak. The chemical shift (δ) of the solvent peaks were based on values obtained from Fulmer *et al.*[91] Carbon experiments performed in D_2O were additionally spiked with 1,4-dioxane (δ 67.19 ppm)[91] to allow for chemical shift referencing. Multiplicities are reported as singlet (s), doublet (d), triplet (t), doublet of triplets (dt), doublet of doublets (dd), doublet of doublet of doublets (ddd), multiplet (m) and broad (br).

Gas chromatography-mass spectrometry (GCMS) was performed using a Shimadzu GC-2010 system equipped with a Shimadzu GCMS-QP2010 gas chromatograph mass spectrometer with an electron

ionisation (EI) source. Low resolution electrospray ionisation mass spectrometry (LRESI-MS) was performed using direct injection on an Agilent 1200 Infinity HPLC system equipped with an Agilent 6130 quadrupole mass spectrometer with an electrospray ionisation source (ESI). Data were recorded in both positive and negative modes. Liquid chromatography-mass spectrometry (LC-MS), for metabolic studies, was performed on the same HPLC system used for LRESI-MS, with samples injected onto an Agilent Poroshell 120 SB-C18 (2.1 x 100 mm, 2.7 µm) analytical column.

5.2 Synthesis of Compounds

5.2.1 3-Amino-3-(4-fluorophenyl)propanoic Acid (55)

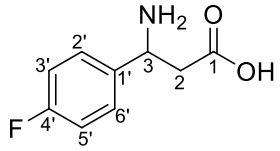

To a solution of 4-fluorobenzaldehyde (**53**, 0.500 g, 430 µL, 4.03 mmol) in ethanol (1.5 mL) were added ammonium acetate (0.684 g, 8.87 mmol) and malonic acid (**54**, 0.460 g, 4.43 mmol). The colourless solution was stirred and heated to reflux. After 6 h the white suspension was cooled to room temperature and the solid was collected by vacuum filtration and washed with ethanol (6.0 mL) and diethyl ether (3 x 6.0 mL). The white solid was then triturated using a 75:25 ethanol and water mixture and dried under high vacuum to afford 3-amino-3-(4-fluorophenyl)propanoic acid (0.289 g, 39%) as a fine white powder. **M.P.:** 216–217°C, Literature 216–217°C.[63] **FTIR**: ν_{max} (neat, cm^{-1}) 2742 (OH, br), 1604 (C=O), 1580 (NH_2), 1511, 1226 (C-O), 829 (disubstituted, *p*-Ar). **^{1}H NMR:** (D_2O, NaOH) δ: 7.39 (2H, dd, *J* = 8.7 Hz, 5.5 Hz, Ar-H-2'and Ar-H-6'), 7.13 (2H, dd, *J* = 8.7 Hz, 8.7 Hz, Ar-H-3'and Ar-H-5'), 4.26 (1H, dd, *J* = 7.6 Hz, 7.6 Hz, CH-3), 2.61 (dd, 1H, *J* = 14.4 Hz, 7.6 Hz, CH-2) 2.54 (dd, 1H, *J* = 14.4 Hz, 7.6 Hz, CH-2). **^{13}C NMR:** (D_2O, NaOH, Dioxane) δ: 180.6 (C-1), 163.3 (d, $^1J_{CF}$ = 241 Hz, C-4'), 140.9 (d, $^4J_{CF}$ = 3 Hz, C-1'), 128.7 (d, $^3J_{CF}$ = 8 Hz, C-2' and C-6'), 115.8 (d, $^2J_{CF}$ = 21 Hz, C-3' and C-5'), 53.0 (C-3), 47.7 (C-2). **LRESI-MS:** $[M+H]^+$ 184.1. The ^{1}H and ^{13}C NMR were in agreement with the literature of Tan *et al.*[63]

5.2.2 *(E)*-3-(4-Fluorophenyl)acrylic Acid (58)

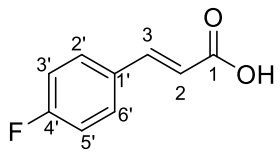

To a solution of 4-fluorobenzaldehyde (**53**, 0.500 g, 432 µL, 4.03 mmol) in pyridine (5 mL) were added malonic acid (**54**, 0.628 g, 6.04 mmol) and piperidine (0.103 g, 119 µL, 1.21 mmol). The resulting solution was stirred and heated to reflux for 2 h before being allowed to cool to room temperature. The colourless solution was acidified to pH 2-3 with 2 M HCl and extracted with ethyl acetate (3 x 15 mL). The organic phases were combined, washed with water (15 mL) then saturated aqueous brine (15 mL),

dried over anhydrous magnesium sulfate and evaporated to dryness under reduced pressure. The pale yellow solid was recrystallised from a 50:50 ethanol water mixture to afford *(E)*-3-(4-fluorophenyl)acrylic acid (0.428 g, 64%) as white crystals. **M.P.:** 206–208°C, Literature 205–207°C.[75] **FTIR:** ν_{max} (neat, cm^{-1}) 2974 (OH, br), 2605, 1679 (C=O), 1625 (C=C), 1226 (C-O), 1156, 980, 824 (disubstituted, *p*-Ar). **^{1}H NMR:** (DMSO-d_6) δ: 7.76 (2H, dd, *J* = 8.5 Hz, 5.2 Hz, Ar-H-2' and Ar-H-6'), 7.58 (1H, d, *J* = 16 Hz, CH-3), 7.25 (2H, dd, *J* = 8.5 Hz, 8.5 Hz, Ar-H-3' and Ar-H-5'), 6.50 (1H, d, *J* = 16 Hz, CH-2). **^{13}C NMR:** (DMSO-d_6) δ: 167.6 (C-1), 163.2 (d, $^1J_{CF}$ = 247 Hz, C-4'), 142.7 (C-3), 130.9 (C-1'), 131.0 (d,$^3J_{CF}$ = 9 Hz, C-2' and C-6'), 119.2 (C-2), 115.9 (d, $^2J_{CF}$ = 21 Hz, C-3' and C-5'). **LRESI-MS:** $[M-H]^-$ 165.1. The ^{1}H and ^{13}C NMR were in agreement with the literature of Fukuyama *et al.*[75]

5.2.3 3-((*tert*-Butoxycarbonyl)amino)-3-(4-fluorophenyl)propanoic Acid (56)

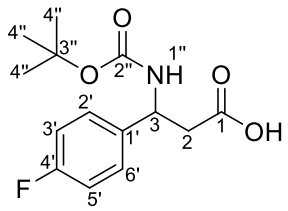

To a solution of 3-amino-3-(4-fluorophenyl)propionic acid (**55**, 0.250 g, 1.36 mmol) in saturated aqueous sodium hydrogen carbonate (10 mL) were added 1,4-dioxane (4 mL) and di-*tert*-butyl dicarbonate (0.447 g, 2.04 mmol). After stirring the solution at room temperature overnight (12 h), the solution was washed with *n*-hexane (2 x 10 mL) and the remaining aqueous layer was acidified to pH 1-2 using 2 M HCl and extracted with ethyl acetate (3 x 10 mL). The organic phases were combined, washed with water (30 mL) then saturated aqueous brine (30 mL), dried over anhydrous magnesium sulfate and evaporated to dryness under reduced pressure to afford the 3-((*tert*-butoxycarbonyl)amino)-3-(4-fluorophenyl)propanoic acid (0.210 g, 54%) as a white powder. **M.P.:** 149–150°C. **FTIR**: ν_{max} (neat, cm^{-1}) 3327 (NH), 2978 (OH, br), 1706 (C=O, acid), 1681 (C=O, carbamate), 1158, 835 (disubstituted, *p*-Ar). **^{1}H NMR:** (DMSO-d_6, at 313K) δ: 7.34-7.33 (3H, m, Ar-H-2' and Ar-H-6' and NH-1''), 7.13 (2H, dd, *J* = 8.8 Hz, 8.8 Hz, Ar-H-3' and Ar-H-5'), 4.86 (1H, d, *J* = 7.2 Hz, CH-3), 2.68–2.53 (m, 2H, CH_2-2), 1.34 (s, 9H, 3 X CH_3-4''). **^{13}C NMR** (DMSO-d_6) δ: 171.7 (C-1), 161.1 (d, $^1J_{CF}$ = 240 Hz, C-4'*),* 154.7 (C-2''), 139.4 (C-1'), 128.4 (d, $^3J_{CF}$ = 10 Hz, C-2' and C-6'), 114.9 (d, $^2J_{CF}$ = 20 Hz, C-3' and C-5'), 77.9 (C-3''), 50.5 (C-3), 41.2 (C-2), 28.2 (C-4''). **LRESI-MS:** $[M-H]^-$ 282.1. The ^{1}H NMR was in agreement with the literature of Axten et *al.*[76]

5.2.4 2-((*tert*-Butoxycarbonyl)amino)-3-(4-fluorophenyl)propanoic acid (45)

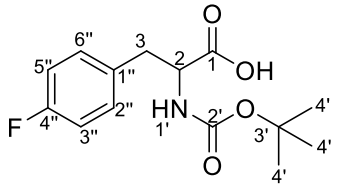

To a solution of 2-amino-3-(4-fluorophenyl)propionic acid (**44**, 0.250 g, 1.36 mmol) in saturated aqueous sodium hydrogen carbonate (15 mL) were added 1,4-dioxane (4 mL) and di-*tert*-butyl dicarbonate (0.447 g, 2.05 mmol). After stirring the solution at room temperature overnight (12 h), the solution was washed with *n*-hexane (2 x 10 mL) and the remaining aqueous layer was acidified to pH 1-2 using 2 M HCl and extracted with ethyl acetate (3 x 10 mL). The organic phases were combined, washed with water (30 mL) then saturated aqueous brine (30 mL), dried over anhydrous magnesium sulfate and evaporated to dryness under reduced pressure to afford 2-((*tert*-butoxycarbonyl)amino)-3-(4-fluorophenyl)propanoic acid (0.210 g, 54%) as a white powder. **M.P.:** 129–130°C, Literature 131°C.[77] **FTIR**: ν_{max} (neat, cm^{-1}) 3360 (NH), 2916 (OH, br), 1704 (C=O, acid), 1687 (C=O, carbamate), 1524, 1217, 1160, 825 (disubstituted, *p*-Ar). **^{1}H NMR:** (DMSO-d_6, at 313K) δ: 7.28–7.25 (2H, m, Ar-H-2'' and Ar-H-6''), 7.12–7.07 (3H, m, Ar-H-3'' and Ar-H-5''), 6.96 (1H, m, NH-1'), 4.09–4.02 (1H, m, CH-2), 3.03–2.79 (2H, m, CH_2-3) 1.31 (9H, s, 3 x CH_3-4'). **^{13}C NMR** (DMSO-d_6) δ: 173.5 (C-1), 161.0 (d, $^1J_{CF}$ = 240 Hz, C-4''), 155.4 (C-2'), 134.2 (C-1''), 131.0 (d, $^3J_{CF}$ = 10 Hz, C-2'' and C-6''), 114.8 (d, $^2J_{CF}$ = 20 Hz, C-3'' and C-5''), 78.1 (C-3'), 55.2 (C-3), 35.6 (C-2), 28.2 (C-4'). **LRESI-MS:** $[M-H]^-$ 282.2. The ^{1}H and ^{13}C NMR were in agreement with the literature of Tomooka *et al.*[77]

5.2.5 *(tert*-Butoxycarbonyl)-L-alanine (48)

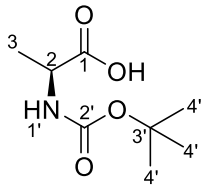

To a solution of *(S)*-2-aminopropanoic acid (L-alanine) (**47**, 0.250 g, 2.81mmol) in 2 M sodium hydroxide (2 mL) were added 1,4-dioxane (2 mL) and di-*tert*-butyl dicarbonate (0.734 g, 3.37 mmol) at 0 °C. The solution was then allowed to warm to room temperature and stirred overnight (12 h). The resulting solution was washed with *n*-hexane (2 x 5 mL) and the remaining aqueous layer was acidified to pH 1-2 using 2 M HCl and extracted with ethyl acetate (3 x 10 mL). The organic phases were combined, washed with water (15 mL) then saturated aqueous brine (15 mL), dried over anhydrous magnesium sulfate and evaporated to dryness under reduced pressure to afford *(tert*-butoxycarbonyl)-L-alanine (0.394 g, 74%) as a white powder. **M.P.:** 70–72°C, Literature 80–83°C.[92] **FTIR**: ν_{max} (neat, cm^{-1}) 3396 (NH), 2927 (OH, br), 1732 (C=O, acid), 1686 (C=O, carbamate), 1508 (NH), 1199. **^{1}H NMR:** (DMSO-d_6) δ: 7.09 (1H, d, *J* = 7.6 Hz, NH-1'), 3.91 (1H, m, CH-2), 1.37 (9H, s, 3 x CH_3-4'), 1.21 (3H, d, *J* = 7.6 Hz,

CH_3-3), **^{13}C NMR** (DMSO-d_6) δ: 174.7 (C-1), 155.3 (C-2'*),* 77.9 (C-3'), 48.8 (C-*2*), 28.2 (C-4'), 17.1 (C-3). **LRESI-MS:** $[M-H]^-$ 188.1.

5.2.6 3-((*tert*-Butoxycarbonyl)amino)propanoic Acid (51)

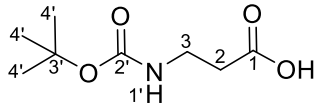

To a solution of 3-aminopropanoic acid (**50**, 0.125 g, 1.41 mmol) in 2 mL of 2 M sodium hydroxide were added 1,4-dioxane (2 mL) and di-*tert*-butyl dicarbonate (0.367 g, 1.685 mmol) at 0°C. The solution was then allowed to warm to room temperature and stirred overnight (12 h). The resulting solution was washed with *n*-hexane (2 x 10 mL) and the remaining aqueous layer was acidified to pH 1-2 with 2 M HCl and extracted with ethyl acetate (3 x 10 mL). The organic phases were combined, washed with water (30 mL) then saturated aqueous brine (30 mL), dried over magnesium sulfate and evaporated to dryness under reduced pressure to afford 3-((*tert*-butoxycarbonyl)amino)propanoic acid (0.1566 g, 59%) as a white powder. **M.P.:** 72–74°C, Literature 75–76°C.[79] **FTIR**: ν_{max} (neat, cm^{-1}) 3438 (NH), 2966, 2911(OH, br), 1697 (C=O), 1509 (NH), 1235 (C-O) 1158. **^{1}H NMR:** (DMSO-d_6) δ: 6.79 (1H, m, NH-1'), 3.12 (2H, dt, *J* = 7.2 Hz, 7.2 Hz, CH_2-3), 2.34 (3H, t, *J* = 7.2 Hz, CH_2-2), 1.37 (9H, s, 3 x CH_3-4'). **^{13}C NMR** (DMSO-d_6) δ: 172.8 (C-1), 155.4 (C-2'), 77.6 (C-3'), 36.1 (C-3), 34.2 (C-2), 28.2 (C-4'). **LRESI-MS:** $[M-H]^-$ 188.1. The ^{1}H and ^{13}C NMR were in agreement with the literature of Zhang *et al.*[79]

5.2.7 3-(4-Fluorophenyl)propanoic Acid (59)

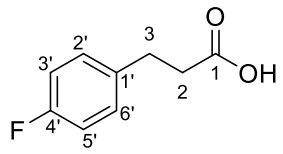

To a solution of *(E)*-3-(4-fluorophenyl)acrylic acid (**58**, 0.125 g, 0.745 mmol) in ethanol (8 mL) was added a catalytic amount of 10% palladium on carbon (0.013 g). The reaction flask was then evacuated, before being charged with hydrogen gas. The resulting mixture was stirred under a hydrogen atmosphere (1 atm) at room temperature for 5 h. The resulting mixture was vacuum filtered to remove the catalyst and the catalyst was washed with ethanol (5 mL). The resulting filtrate was evaporated to dryness under reduced pressure to afford 3-(4-fluorophenyl)propanoic acid (0.116 g, 91%) as a white powder. **M.P.:** 91–94 °C, Literature 95°C.[93] **FTIR**: ν_{max} (neat, cm^{-1}) 3043 (OH, br), 2956, 1698 (C=O), 1504, 1212 (C-O), 822 (disubstituted, *p*-Ar). **^{1}H NMR:** ($CDCl_3$) δ: 7.17 (2H, dd, *J* = 8.7 Hz, 5.4 Hz, Ar-H-2' and Ar-H-6'), 6.98 (2H, dd, *J* = 8.7 Hz, 8.7 Hz, Ar-H-3' and Ar-H-5'), 2.93 (2H, t, *J* = 7.6 Hz, CH_2-3), 2.66 (2H, t, *J* = 7.6 Hz, CH_2-2). **^{13}C NMR** ($CDCl_3$) δ: 178.9 (C-1), 161.7 (d, $^1J_{CF}$ = 243 Hz, C-4'), 135.9 (d, $^4J_{CF}$ = 3 Hz, C-1'), 129.9 (d, $^3J_{CF}$ = 8 Hz, C-2' and C-6'), 115.5 (d, $^2J_{CF}$ = 21 Hz, C-3' and C-5'), 35.8 (C-2), 29.9 (C-3). **LRESI-MS:** $[M-H]^-$ 167.1.

5.2.8 Ethyl (3-((*tert*-butoxycarbonyl)amino)propanoyl)glycinate (52)

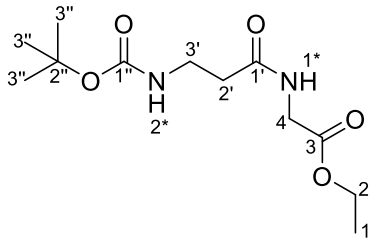

To a solution of 3-((*tert*-butoxycarbonyl)amino)propanoic acid (**51**, 0.100 g, 0.529 mmol) and glycine ethyl ester hydrochloride (**64**, 0.074 g, 0.53 mmol) in dichloromethane (8 mL), were added triethylamine (0.134 g, 184 µL, 1.32 mmol) and EDCI (0.122 g, 0.634 mmol). The solution was then stirred overnight (24 h) at room temperature. After 24 h, the solution was acidified to pH 2-3 with 2 M HCl and extracted with dichloromethane (3 x 10 mL). The organic phases were combined, washed with water (30 mL) and saturated aqueous brine (30 mL), dried over anhydrous magnesium sulfate and evaporated to dryness under reduced pressure. The impure residue was purified using column chromatography (normal phase silica) with a mobile phase of 3:1 ethyl acetate:*n*-hexane to give ethyl (3-((*tert*-butoxycarbonyl)amino)propanoyl)glycinate (0.116 g, 91%) as a white powder. **M.P.:** 69–70 °C. **FTIR**: ν_{max} (neat, cm^{-1}) 3348 (NH), 3325 (NH), 2916, 2848, 1751 (C=O, ester), 1682 (C=O carbamate), 1647 (C=O amide), 1523 (NH), 1192 (C-O), 1163 (C-O). **^{1}H NMR:** (DMSO-d_6) δ: 8.31 (1H, t, *J* = 7.2 Hz, NH-1*), 6.71 (1H, t, *J* = 7.2 Hz, NH-2*), 4.09 (2H, q, *J* = 7.1 Hz, CH_2-2), 3.80 (2H, d, *J* = 5.9 Hz, CH_2-4), 3.12 (2H, dt, *J* = 7.6 Hz, 7.6 Hz CH_2-3'), 2.29 (2H, t, *J* = 7.6 Hz, CH_2-2'), 1.37 (9H, s, 3 x CH_3-3''), 1.19 (2H, t, *J* = 7.1 Hz, CH_2-1). **^{13}C NMR** (DMSO-d_6) δ: 170.9 (C-3), 169.9 (C-1'), 155.4 (C-1''), 77.6 (C-2''), 60.4 (C-2), 40.6 (C-4), 36.6 (C-3'), 35.4 (C-2'), 28.2 (C-3''), 14.1 (C-1). **LRESI-MS:** $[M+H]^+$ 275.2.

5.2.9 Ethyl (*tert*-butoxycarbonyl)-L-alanylglycinate (49)

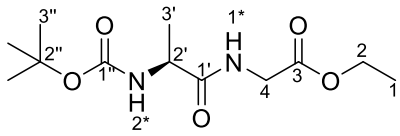

To a solution of *(tert*-butoxycarbonyl)-L-alanine (**48**, 0.100 g, 0.529 mmol) and glycine ethyl ester hydrochloride (**64**, 0.074 g, 0.53 mmol) in dichloromethane (8 mL) were added triethylamine (0.134 g, 184 µL, 1.32 mmol) and EDCI (0.122 g, 0.634 mmol). The solution was then stirred overnight (24 h) at room temperature. After 24 h the solution was acidified to pH 2-3 with 2 M HCl and extracted with dichloromethane (3 x 10 mL). The organic phases were combined, washed with water (30 mL) then saturated aqueous brine (30 mL), dried over anhydrous magnesium sulfate and evaporated to dryness under reduced pressure. The impure residue was purified using column chromatography (normal phase silica) with a mobile phase of 3:1 ethyl acetate:*n*-hexane to give ethyl (*tert*-butoxycarbonyl)-L-alanylglycinate (0.063 g, 46%) as a white powder. **M.P.:** 55–57 °C. **FTIR**: ν_{max} (neat, cm^{-1}): 3412 (NH), 3270 (NH), 2979, 2939, 1751 (C=O, ester), 1703 (C=O, carbamate), 1646 (C=O,

amide), 1518 (NH), 1187 (C-O), 1160 (C-O). **^{1}H NMR:** (DMSO-d_6) δ: 8.16 (1H, t, *J* = 7.2 Hz, NH-1*), 6.92 (1H, d, *J* = 7.6 Hz, NH-2*), 4.08 (2H, q, *J* = 7.1 Hz, CH_2-2), 4.00 (1H, m, CH-2'), 3.81 (2H, m, CH_2-4), 1.37 (9H, s, 3 x CH_3-3''), 1.20 – 1.16 (6H, m, CH_3-1 and CH_3-H3''). **^{13}C NMR** (DMSO-d_6) δ: 173.3 (C-1'), 169.7 (C-3), 155.0 (C-1''), 78.0 (C-2''), 60.3 (C-2), 49.4 (C-2'), 40.7 (C-4), 28.2 (C-3''), 18.2 (C-3'), 14.0 (C-1). **LRESI-MS:** $[M+Na]^+$ 297.2.

5.2.10 Ethyl (3-((*tert*-butoxycarbonyl)amino)-3-(4-fluorophenyl)propanoyl)glycinate (57)

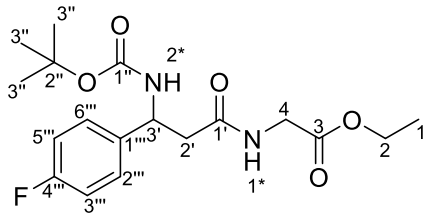

To a solution of 3-((*tert*-butoxycarbonyl)amino)-3-(4-fluorophenyl)propanoic acid (**56**, 0.100 g, 0.353 mmol) and glycine ethyl ester hydrochloride (**64**, 0.049 g, 0.35 mmol) in dichloromethane (10 mL) were added triethylamine (0.089 g, 117 µL, 0.88 mmol) and EDCI (0.081 g, 0.42 mmol). The solution was then stirred overnight (24 h) at room temperature. After 24 h the solution was acidified to pH 2-3 with 2 M HCl and extracted with dichloromethane (3 x 10 mL). The organic phases were combined, washed with water (30 mL) and saturated aqueous brine (30 mL), dried over anhydrous magnesium sulfate and evaporated to dryness under reduced pressure. The impure residue was purified using column chromatography (normal phase silica) with a mobile phase of 3:1 ethyl acetate:*n*-hexane to give ethyl (3-((*tert*-butoxycarbonyl)amino)-3-(4-fluorophenyl)propanoyl)glycinate (0.0972 g, 74%) as a white powder. **M.P.:** 122–124 °C. **FTIR**: ν_{max} (neat, cm^{-1}): 3360 (NH), 2978, 2923, 1739 (C=O, ester), 1673 (C=O, carbamate), 1651 (C=O, amide), 1511 (NH), 1210 (C-O), 1162 (C-O), 838 (disubstituted, *p*-Ar). **^{1}H NMR:** (CD_3CN) δ: 7.32 (2H, dd, *J* = 8.7 Hz, 5.5 Hz, Ar-H-2''' and Ar-H-6'''), 7.06 (2H, dd, *J* = 8.7 Hz, 8.7 Hz, Ar-H-3''' and Ar-H-5'''), 6.69 (1H, S, br, NH-1*), 6.17 (1H, S, br, NH-2*), 4.93 (1H, d, *J* = 6.4 Hz, CH-3'), 4.11 (2H, q, *J* = 7.1 Hz, CH_2-2), 3.80 (2H, d, *J* = 5.8 Hz, CH_2-4), 2.62 (2H, d, *J* = 6.7 Hz, CH_2-2'), 1.36 (9H, s, 3 x CH_3-3''), 1.21 (3H, t, *J* = 7.1 Hz, CH_3-1). **^{13}C NMR** (CD_3CN) δ: 171.3 (C-1'), 170.6 (C-3), 162.7 (d, $^{1}J_{CF}$ = 241 Hz, C-4'''), 156.0 (C-1''), 140.0 (C-1'''), 129.2 (d, $^{3}J_{CF}$ = 8 Hz, C-2''' and C-6'''), 115.9 (d, $^{2}J_{CF}$ = 21 Hz, C-3''' and C-5'''), 79.6 (C-2''), 61.8 (C-2), 52.2 (C-3'), 42.7 (C-2'), 41.8 (C-4), 28.5 (C-3''), 14.5 (C-1). **LRESI-MS:** $[M+H]^+$ 369.2.

5.2.11 Ethyl (2-((*tert*-butoxycarbonyl)amino)-3-(4-fluorophenyl)propanoyl)glycinate (46)

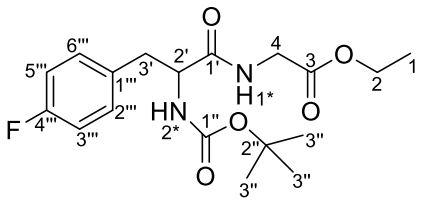

To a solution of 2-((*tert*-butoxycarbonyl)amino)-3-(4-fluorophenyl)propanoic acid (**45**, 0.100 g, 0.353 mmol) and glycine ethyl ester hydrochloride (**64**, 0.049 g, 0.35 mmol) in dichloromethane (10 mL) were added triethylamine (0.089 g, 117 µL, 0.88 mmol) and EDCI (0.081 g, 0.42 mmol). The solution was then stirred overnight (24 h) at room temperature. After 24 h the solution was acidified to pH 2-3 using 2 M HCl and extracted with dichloromethane (3 x 10 mL). The organic phases were combined, washed with water (30 mL) then saturated aqueous brine (30 mL), dried over anhydrous magnesium sulfate and evaporated to dryness under reduced pressure. The impure residue was purified using column chromatography (normal phase silica) with a mobile phase of 3:1 ethyl acetate:*n*-hexane to give ethyl (2-((*tert*-butoxycarbonyl)amino)-3-(4-fluorophenyl)propanoyl)glycinate (0.070 g, 53%) as a white powder. **M.P.:** 140–142 °C. **FTIR**: ν_{max} (neat, cm^{-1}) 3315 (NH), 2916, 1744 (C=O, ester), 1675 (C=O, carbamate), 1652 (C=O, amide), 1525 (NH), 1210 (C-O), 1165 (C-O), 827 (disubstituted, *p*-Ar). **^{1}H NMR:** (DMSO-d_6) δ: 8.38 (1H, t, *J* = 5.7 Hz, NH-1*), 7.31 (2H, dd, *J* = 8.6 Hz, 5.8 Hz, Ar-H-2’’’ and Ar-H-6’’’), 7.08 (2H, dd, *J* = 8.6 Hz, 8.6 Hz, Ar-H-3’’’ and Ar-H-5’’’), 6.95 (1H, d, *J* = 8.8 Hz, NH-2*), 4.93 (1H, d, *J* = 6.4 Hz, NH-2*), 4.18 (1H, ddd, *J* 17.5 Hz, 5.8 Hz , 5.8 Hz, 3.9 Hz, CH-2’), 4.10 (2H, q, *J* = 7.1 Hz, CH_2-2), 3.89 (1H, dd, *J* = 17.5 Hz, 5.8 Hz, CH_2-4), 3.81 (1H, dd, *J* = 17.5 Hz, 5.8 Hz, CH_2-4) 2.97 (1H, dd, *J* = 13.8 Hz, 3.7 Hz, CH_2-3’), 2.71 (1H, dd, *J* = 13.8 Hz, 3.7 Hz, CH_2-3’), 1.36 (9H, s, 3 x CH_3-3’’), 1.20 (3H, t, *J* = 7.1 Hz, CH_3-1). **^{13}C NMR** (DMSO-d_6) δ: 172.2 (C-1’), 169.7 (C-3), 160.9 (d, $^1J_{CF}$ = 240 Hz, C-4’’’), 155.2 (C-1’’), 268.7 (d, $^4J_{CF}$ = 3 Hz, C-1’’’), 131.0 (d, $^3J_{CF}$ = 8 Hz, C-2’’’ and C-6’’’), 114.6 (d, $^2J_{CF}$ = 21 Hz, C-3’’’ and C-5’’’), 78.0 (C-2’’), 60.1 (C-2), 55.5 (C-2’), 40.7 (C-4), 36.6 (C-3’), 28.1 (C-3’’), 14.0 (C-1). **LRESI-MS:** $[M+Na]^+$ 391.1, $[M+H]^+$ 369.2

5.2.12 Ethyl (3-(4-fluorophenyl)propanoyl)glycinate (42)

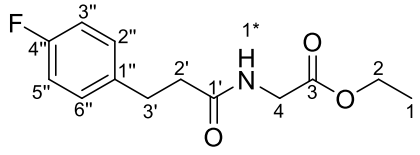

To a solution of 3-(4-fluorophenyl)propanoic acid (**59**, 0.100 g, 0.595 mmol) and glycine ethyl ester hydrochloride (**64**, 0.082 g, 0.60 mmol) in dichloromethane (10 mL) were added triethylamine (0.150 g, 207 µL, 1.49 mmol) and EDCI (0.137 g, 0.714mmol). The solution was then stirred overnight (24 h) at room temperature. After 24 h the solution was acidified to pH 2-3 using 2 M HCl and extracted with dichloromethane (3 x 10 mL). The organic phases were combined,

washed with water (30 mL) and brine (30 mL), dried over anhydrous magnesium sulfate and evaporated to dryness under reduced pressure. The impure white powder was purified using column chromatography (normal phase silica) with a mobile phase of 3:1 ethyl acetate:*n*-hexane to give ethyl (3-(4-fluorophenyl)propanoyl)glycinate (0.102 g, 68%) as a white powder. **M.P.:** 58–60 °C. **FTIR**: ν_{max} (neat, cm^{-1}) 3325 (NH), 2916, 1738 (C=O, amide), 1640 (C=O, ester), 1509 (NH), 1208 (C-O), 1163 (C-O), 830 (disubstituted, *p*-Ar). **^{1}H NMR:** ($CDCl_3$) δ: 7.15 (2H, dd, *J* = 8.7 Hz, 5.4 Hz, Ar-H-2'' and Ar-H-6''), 6.97 (2H, dd, *J* = 8.7 Hz, 8.7 Hz, Ar-H-3'' and Ar-H-5''), 5.88 (1H, S, br, NH-1*), 4.21 (2H, q, *J* = 7.2 Hz, CH_2-2), 4.01 (2H, d, *J* = 5.0 Hz, CH_2-4), 2.95 (2H, t, *J* = 5.8 Hz, CH_2-3'), 2.52 (2H, t, *J* = 6.7 Hz, CH_2-2'), 1.28 (3H, t, *J* = 7.2 Hz, CH_3-1). **^{13}C NMR** ($CDCl_3$) δ: 172.0 (C-1'), 170.1 (C-3), 161.6 (d, $^1J_{CF}$ = 244 Hz, C-4''), 136.5 (d, $^4J_{CF}$ = 3 Hz, C-1''), 129.9 (d, $^3J_{CF}$ = 8 Hz, C-2'' and C-6''), 115.4 (d, $^2J_{CF}$ = 21 Hz, C-3''and C-5''), 61.7 (C-2), 41.5 (C-4), 38.2 (C-3'), 30.7 (C-2'), 14.2 (C-1). **LRESI-MS:** $[M+H]^+$ 254.2.

5.2.13 Ethyl (4-fluorobenzoyl)glycinate (43)

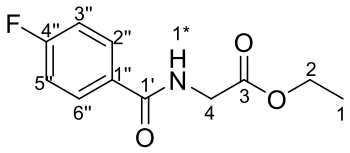

To a solution of 4-fluorobenzoic acid (**60**, 0.100 g, 0.714 mmol) and glycine ethyl ester hydrochloride (**64**, 0.099 g, 0.714 mmol) in dichloromethane (10 mL) were added triethylamine (0.181 g, 249 µL, 1.78 mmol) and EDCI (0.164 g, 0.856 mmol). The solution was then stirred overnight (24 h) at room temperature. After 24 h the solution was acidified to pH 2-3 with 2 M HCl and extracted using dichloromethane (3 x 10 mL). The organic phases were combined, washed with water (30 mL) then saturated aqueous brine (30 mL), dried over anhydrous magnesium sulfate and evaporated to dryness under reduced pressure to afford ethyl (4-fluorobenzoyl)glycinate (0.1080 g, 67%) as a white powder. **M.P.:** 99–101°C. **FTIR**: ν_{max} (neat, cm^{-1}): 3269 (N-H), 2980, 1744 (C=O, ester), 1643 (C=O, amide), 1556 (N-H), 1168 (C-O), 849 (disubstituted, *p*-Ar). **^{1}H NMR:** ($CDCl_3$) δ: 7.83 (2H, dd, *J* = 8.8 Hz, 5.3 Hz, Ar-H-2'' and Ar-H-6''), 7.13 (2H, dd, *J* = 8.8 Hz, 8.8 Hz, Ar-H-3'' and Ar-H-5''), 6.58 (1H, S, br, NH-1*),4.27 (2H, q, *J* = 7.2 Hz, CH_2-2), 4.23 (2H, d, *J* = 5.0 Hz, CH_2-4), 1.32 (2H, t, *J* = 7.1 Hz, CH_3-1). **^{13}C NMR** ($CDCl_3$) δ: 170.1 (C-1'), 166.5 (C-3), 165.1 (d, $^1J_{CF}$ = 250 Hz, C-4''), 130.1 (d, $^4J_{CF}$ = 3 Hz, C-1''), 129.6 (d, $^3J_{CF}$ = 9 Hz, C-2'' and C-6''), 115.8 (d, $^2J_{CF}$ = 22 Hz, C-3''and C-5''), 61.9 (C-2), 42.0 (C-4), 14.3 (C-1). **LRESI-MS:** $[M+H]^+$ 226.1.

5.2.14 Ethyl (3-aminopropanoyl)glycinate (39)

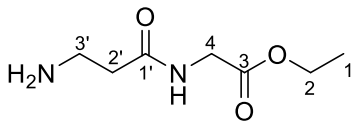

Ethyl (3-((*tert*-butoxycarbonyl)amino)propanoyl)glycinate (**52**, 0.050 g, 0.18 mmol) was dissolved in a solution of 4 M HCl in dioxane (1.00 mL). The resulting solution was stirred at room temperature for 1 h, before being diluted with 1,4-dioxane (4 mL). The solvent was then evaporated under reduced pressure to afford a waxy oil, which was lyophilised to remove the remaining water. This afforded ethyl (3-aminopropanoyl)glycinate.HCl (0.0162 g, 51%) as a brown waxy solid. **FTIR**: ν_{max} (neat, cm^{-1}) 3290 (N-H), 2989, 2906, 1723 (C=O, ester), 1641 (C=O, amide), 1549 (N-H), 1212 (C-O). **^{1}H NMR:** (D_2O) δ: 4.15 (2H, q, *J* = 7.1 Hz, CH_2-2), 3.94 (2H, s, CH_2-4), 3.21 (2H, t, *J* = 6.6 Hz, CH_2-2'), 2.69 (2H, t, *J* = 6.7 Hz, CH2-3'), 1.19 (3H, t, *J* = 7.1 Hz, CH_3-1). **^{13}C NMR** (D_2O, Dioxane) δ: 173.4 (C-3), 172.4 (C-1'), 63.2 (C-2), 41.9 (C-4), 36.2 (C-3'), 32.3 (C-2'), 13.9 (C-1). **LRESI-MS:** $[M+H]^+$ 175.2.

5.2.15 Ethyl L-alanylglycinate (41)

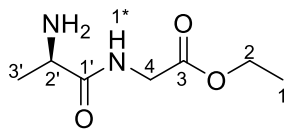

Ethyl (*tert*-butoxycarbonyl)-L-alanylglycinate (**49**, 0.050 g, 0.18 mmol) was dissolved in a solution of 4 M HCl in dioxane (1.00 mL). The resulting solution was stirred at room temperature for 1 h, before being diluted with 1,4-dioxane (4 mL). The solvent was then reduced under pressure to afford a waxy crude oil, which was lyophilised to remove the remaining water. This afforded ethyl L-alanylglycinate.HCl (0.0205 g, 65%) as a waxy oil. **FTIR**: ν_{max} (neat, cm^{-1}) 3215 (N-H), 2981, 1737 (C=O, ester), 1677 (C=O, amide), 1555 (NH), 1201(C-O). **^{1}H NMR:** (D_2O) δ: 4.24 (2H, q, *J* = 7.1 Hz, CH_2-2), 4.13 (1H, m, CH-2'), 4.07 (2H, d, *J* = 5.8 Hz, CH_2-4), 3.66 (1H, s, NH-1*), 1.59 (3H, d, *J* = 7.2 Hz, CH_3-3'), 1.28 (3H, t, *J* = 7.1 Hz, CH_3-1). **^{13}C NMR** (D_2O, 1,4-dioxane) δ: 171.9 (C-3 and C-1', overlapping), 63.2 (C-2), 49.5 (C-2'), 41.9 (C-4), 16.9 (C-3'), 13.8 (C-1). **LRESI-MS:** $[M+H]^+$ 175.1.

5.2.16 Ethyl (3-amino-3-(4-fluorophenyl)propanoyl)glycinate (38)

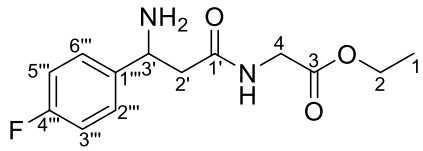

Ethyl (3-((*tert*-butoxycarbonyl)amino)-3-(4-fluorophenyl)propanoyl)glycinate (**57**, 0.050 g, 0.14 mmol) was dissolved in a solution of 4 M HCl in dioxane (1.00 mL). The resulting solution was stirred at room temperature for 1.5 h, before being diluted with 1,4-dioxane (4 mL). The solvent was then reduced under a stream of nitrogen to afford an impure white solid, which was dissolved in water (10 mL) and purified *via* a C_{18} reversed phase SEP-Pak and lyophilised,

to afford ethyl (3-amino-3-(4-fluorophenyl)propanoyl)glycinate.HCl (0.0275g, 65%) as a white powder. **M.P.:** 145–146 °C. **FTIR**: ν_{max} (neat, cm^{-1}) 3329 (N-H), 2907, 1744 (C=O, ester), 1655 (C=O, amide), 1515 (N-H), 1227 (C-O), 1190 (C-O), 836 (disubstituted, *p*-Ar). **^{1}H NMR:** (D_2O) δ: 7.49 (2H, dd, *J* = 8.8 Hz, 5.2 Hz, Ar-H-2'' and Ar-H-6''), 7.23 (2H, dd, *J* = 8.8 Hz, 8.8 Hz, Ar-H-3'' and Ar-H-5''), 4.73 (1H, dd, *J* = 8.0 Hz, 6.9 Hz, CH, H-3'), 4.16 (2H, q, *J* = 7.2 Hz, CH_2-2), 3.90 (2H, s, CH_2-4), 3.13 (1H, dd, *J* = 15.4 Hz, 6.9 Hz, CH-2'), 3.06 (1H, dd, *J* = 15.4 Hz, 8.0 Hz, CH-2'), 1.21 (3H, t, *J* = 7.2 Hz, CH_3-1). **^{13}C NMR:** (D_2O, 1,4-dioxane) δ: 172.1 (C-1' and C-3, overlapping), 163.7 (d, $^1J_{CF}$ = 245 Hz, C-4''), 131.5 (d, $^4J_{CF}$ = 3 Hz, C-1''), 129.7 (d, $^3J_{CF}$ = 9 Hz, C-2'' and C-6''), 116.8 (d, $^2J_{CF}$ = 22 Hz, C-3'' and C-5''), 63.1 (C-2), 52.1 (C-3'), 41.8 (C-2'), 39.3 (C-4), 13.8 (C-1). **LRESI-MS:** $[M+H]^+$ 269.2.

5.2.17 Ethyl (2-amino-3-(4-fluorophenyl)propanoyl)glycinate (40)

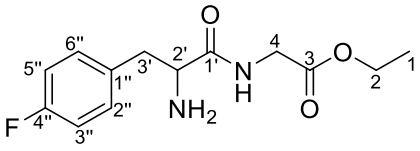

Ethyl (2-((*tert*-butoxycarbonyl)amino)-3-(4-fluorophenyl)propanoyl)glycinate (**46**, 0.050 g, 0.14 mmol) was dissolved in a solution of 4 M HCl in dioxane (1.00 mL). The resulting solution was stirred at room temperature for 1.5 h, before being diluted with 1,4-dioxane (4 mL). The solvent was then reduced under a stream of nitrogen to afford an impure white solid, which was dissolved in water (10 mL), purified *via* a C_{18} reversed phase SEP-Pak and lyophilised to afford ethyl (2-amino-3-(4-fluorophenyl)propanoyl)glycinate.HCl (0.0327g, 77%) as a white powder. **M.P.:** 183 – 184 °C. **FTIR**: ν_{max} (neat, cm^{-1}) 3339 (N-H), 2860, 1738 (C=O, ester), 1673 (C=O, amide), 1510 (N-H), 1216 (C-O), 1162 (C-O), 835 (disubstituted, *p*-Ar) . **^{1}H NMR:** (D_2O) δ: 7.33 (2H, dd, *J* = 8.9 Hz, 5.4 Hz, Ar-H-2'' and Ar-H-6''), 7.16 (2H, dd, *J* = 8.9 Hz, 8.9 Hz, Ar-H-3'' and Ar-H-5''), 4.30 (1H, dd, *J* = 7.2 Hz, 7.2 Hz, CH-2'), 4.23 (2H, q, *J* = 7.2 Hz, CH_2-2), 4.00 (2H, s, CH_2, H-4), 3.31 (1H, dd, *J* = 14.4 Hz, 7.2 Hz, CH-3'), 3.21 (1H, dd, *J* = 14.4 Hz, 7.2 Hz, CH-3'), 1.27 (3H, t, *J* = 7.2 Hz, CH_3-1). **^{13}C NMR:** (D_2O, Dioxane) δ: 171.7 (C-1'), 170.2 (C-2), 162.9 (d, $^1J_{CF}$ = 242 Hz, C-4''), 131.9 (d, $^3J_{CF}$ = 9 Hz, C-2'' and C-6''), 130.2 (d, $^4J_{CF}$ = 3 Hz, C-1''), 116.4 (d, $^2J_{CF}$ = 21 Hz, C-3'' and C-5''), 63.3 (C-2), 55.0 (C-2'), 41.9 (C-4), 36.6 (C-3'), 13.8 (C-1). **LRESI-MS:** $[M+H]^+$ 269.2.

5.3 Metabolic Stability Studies

5.3.1 Activity of Porcine Liver Esterase

To confirm the activity of the porcine liver esterase (PLE) (Sigma Aldrich), the spectrophotometric (Uv-Vis) method of Landowski *et al*.[87] was employed. Varying concentrations **(Table 5.1)** of *p*-nitrophenyl butyrate (*p*-NPB) were incubated at 37°C with PLE in a phosphate buffer medium. The formation of *p*-nitrophenol was monitored over a 5 min interval at 405 nm.

Table 5.1 *p*-Nitrophenyl butyrate concentrations for spectrophotometric assay

Final [*p*-NPB] (mM)	Volume of 10 mM[a] or 100 mM[b] stock of *p*-NPB DMSO (µL)	Volume of DMSO (µL)	Volume of 10 mM potassium phosphate pH 7.4 buffer (µL)	Volume of PLE solution [28 µg/mL] (µL)	Total volume (µL)
0.025*	5[a]	95	1800	100	2000
0.05*	10[a]	90	1800	100	2000
0.1*	20[a]	80	1800	100	2000
0.2	4[b]	96	1800	100	2000
0.4	8[b]	92	1800	100	2000
0.8	16[b]	84	1800	100	2000
1	20[b]	80	1800	100	2000

To determine the initial rate of the conversion of *p*-nitrophenyl butyrate to *p*-nitrophenol, linear regression was performed on the plot of absorbance *vs* time **(Figure 3.1A)** for each of the concentrations in Table 5.1. Linearity of the plot was determined when R^2 value was approximately 0.99. A Michaelis-Menten Plot **(Figure 3.1B)** was then generated to determine the Michaelis constant for the enzyme.

5.3.2 Metabolic Stability Assay

To determine the metabolic stability of the glycine ethyl ester conjugates **(38**-**43)**, assay samples were prepared according to concentrations listed in Table 5.2. Control assays of the glycine ethyl ester conjugates **(38**-**43)** and predicted amide cleavage products, the carboxylic acid compounds **(44**, **47**, **50**, **55**, **59** and **60)** and glycine ethyl ester **(64)** were also prepared, without PLE present.

The assays were started by adding freshly prepared PLE solution **(Table 5.2)** to the prepared compound **(38-43)** solutions, both pre-warmed to 37 °C. The resulting assay solutions were then shaken and incubated at 37 °C for 4 h. Aliquots (10 µL) were withdrawn at 1 h intervals, up to the

final time interval of 4 h. In addition, a 10 µL aliquot was taken initially after the addition of the enzyme solution at time point 0 min. Each aliquot was then quenched with an acetonitrile solution with 2% (*v/v*) of trifluoroacetic acid (10 µL). Following the quenching of samples, analysis was performed *via* TLC and mass spectrometry.

Table 5.2 Metabolic Stability Assays Concentrations

Final concentration of compound (mM)	Volume of 100 mM stock of compound in DMSO (µL)	Volume of DMSO (µL)	Volume of 10 mM potassium phosphate pH 7.4 buffer (µL)	Volume of PLE [28 µg/mL] (µL)	Total volume (µL)
10	10	4	36	50	100

5.3.2.1 Analysis *via* Thin Layer Chromatography.

Aliquots were analysed using either cellulose or reversed phase TLC plates. Mobile phases for the plates were as follows; cellulose 12:3:5 *n*-butanol:acetic acid:water, reversed phase 1:1:0.0001 acetonitrile:water:trifluoroacetic acid. Following the development of the plates in their respective mobile phases, plates were visualised using both long (365 nm) and short (254 nm) UV light and stained with ninhydrin. Control assays of the glycine ethyl ester conjugates **(38-43)** and predicted amide cleavage products, the carboxylic acid compounds **(44**, **47**, **50**, **55**, **59** and **60)** and glycine ethyl ester **(64)** were also analysed for comparison.

5.3.2.2 Analysis *via* Mass Spectrometry Methods.

Aliquots were lyophilised to remove excess water before being dissolved in acetonitrile. Samples were then analysed using a direct injection method *via* LRESI-MS. If no positive or negative molecular ion was observed, samples were further analysed via LC-MS methods. Data were recorded in both positive and negative electrospray ionisation modes. Control assay aliquots, without PLE present, were also analysed using the same procedures.

Chapter 6: References

1. Chen, K.; Conti, P. S., Target-specific delivery of peptide-based probes for PET imaging. *Advanced Drug Delivery Reviews* **2010**, *62* (11), 1005-1022.
2. Li, Z.; Conti, P. S., Radiopharmaceutical chemistry for positron emission tomography. *Advanced Drug Delivery Reviews* **2010**, *62* (11), 1031-1051.
3. Wadsak, W.; Mitterhauser, M., Basics and principles of radiopharmaceuticals for PET/CT. *European Journal of Radiology* **2010**, *73* (3), 461-469.
4. Paterson, B. M.; Roselt, P.; Denoyer, D.; Cullinane, C.; Binns, D.; Noonan, W.; Jeffery, C. M.; Price, R. I.; White, J. M.; Hicks, R. J., PET imaging of tumours with a 64 Cu labeled macrobicyclic cage amine ligand tethered to Tyr 3-octreotate. *Dalton Transactions* **2014**, *43* (3), 1386-1396.
5. Charron, C.; Hickey, J.; Nsiama, T.; Cruickshank, D.; Turnbull, W.; Luyt, L., Molecular imaging probes derived from natural peptides. *Natural Product Reports* **2016**, *33* (6), 761-800.
6. Fani, M.; Maecke, H. R.; Okarvi, S. M., Radiolabeled Peptides: Valuable Tools for the Detection and Treatment of Cancer. *Theranostics* **2012**, *2* (5), 481-501.
7. Bacher, L.; Fischer, G.; Litau, S.; Schirrmacher, R.; Wängler, B.; Baller, M.; Wängler, C., Improving the stability of peptidic radiotracers by the introduction of artificial scaffolds: which structure element is most useful? *Journal of Labelled Compounds and Radiopharmaceuticals* **2015**, *58* (10), 395-402.
8. Ramogida, C. F.; Orvig, C., Tumour targeting with radiometals for diagnosis and therapy. *Chemical Communications* **2013**, *49* (42), 4720-4739.
9. Pimlott, S. L.; Sutherland, A., Molecular tracers for the PET and SPECT imaging of disease. *Chemical Society Reviews* **2011**, *40* (1), 149-162.
10. Matesic, L.; Wyatt, N. A.; Fraser, B. H.; Roberts, M. P.; Pham, T. Q.; Greguric, I., Ascertaining the suitability of aryl sulfonyl fluorides for [18F]radiochemistry applications: A systematic investigation using microfluidics. *The Journal of Organic Chemistry* **2013**, *78* (22), 11262-11270.
11. Vallabhajosula, S.; Solnes, L.; Vallabhajosula, B. In *A broad overview of positron emission tomography radiopharmaceuticals and clinical applications: what is new?*, Seminars in nuclear medicine, Elsevier: 2011; pp 246-264.
12. Ametamey, S. M.; Honer, M.; Schubiger, P. A., Molecular imaging with PET. *Chemical reviews* **2008**, *108* (5), 1501-1516.
13. Ell, P. J.; Kayani, I.; Groves, A. M., 18F-Fluorodeoxyglucose PET/CT in cancer imaging. *Clinical Medicine* **2006**, *6* (3), 240-244.
14. Charron, C. L.; Farnsworth, A. L.; Roselt, P. D.; Hicks, R. J.; Hutton, C. A., Recent developments in radiolabelled peptides for PET imaging of cancer. *Tetrahedron Letters* **2016**, *57* (37), 4119-4127.
15. Laverman, P.; Sosabowski, J. K.; Boerman, O. C.; Oyen, W. J., Radiolabelled peptides for oncological diagnosis. *European Journal of Nuclear Medicine and Molecular Imaging* **2012**, *39* (1), 78-92.
16. Fani, M.; Maecke, H., Radiopharmaceutical development of radiolabelled peptides. *European Journal of Nuclear Medicine and Molecular Imaging* **2012**, *39* (Supplement 1), 11-30.
17. Richter, S.; Wuest, F., 18F-Labeled peptides: The future is bright. *Molecules* **2014**, *19* (12), 20536.

18. Lee, S.; Xie, J.; Chen, X., Peptides and peptide hormones for molecular imaging and disease diagnosis. *Chemical Reviews* **2010**, *110* (5), 3087-3111.
19. Blok, D.; Feitsma, R. I. J.; Vermeij, P.; Pauwels, E. J. K., Peptide radiopharmaceuticals in nuclear medicine. *European Journal of Nuclear Medicine* **1999**, *26* (11), 1511-1519.
20. Okarvi, S., Recent progress in fluorine-18 labelled peptide radiopharmaceuticals. *European Journal of Nuclear Medicine* **2001**, *28* (7), 929-938.
21. Jackson, I. M.; Scott, P. J. H.; Thompson, S., Clinical applications of radiolabeled peptides for PET. *Seminars in Nuclear Medicine* **2017**, *47* (5), 493-523.
22. Price, E. W.; Orvig, C., Matching chelators to radiometals for radiopharmaceuticals. *Chemical Society Reviews* **2014**, *43* (1), 260-290.
23. Smith, S. V., Molecular imaging with copper-64. *Journal of Inorganic Biochemistry* **2004**, *98* (11), 1874-1901.
24. Liu, S., The role of coordination chemistry in the development of target-specific radiopharmaceuticals. *Chemical Society Reviews* **2004**, *33* (7), 445-461.
25. Jacobson, O.; Kiesewetter, D. O.; Chen, X., Fluorine-18 radiochemistry, labeling strategies and synthetic routes. *Bioconjugate Chemistry* **2015**, *26* (1), 1-18.
26. Carberry, P.; Carpenter, A. P.; Kung, H. F., Fluoride-18 radiolabeling of peptides bearing an aminooxy functional group to a prosthetic ligand via an oxime bond. *Bioorganic & Medicinal Chemistry Letters* **2011**, *21* (23), 6992-6995.
27. Wuest, F.; Köhler, L.; Berndt, M.; Pietzsch, J., Systematic comparison of two novel, thiol-reactive prosthetic groups for 18F labeling of peptides and proteins with the acylation agent succinimidyl-4-[18F]fluorobenzoate ([18F]SFB). *The Forum for Amino Acid, Peptide and Protein Research* **2009**, *36* (2), 283-295.
28. Roberts, M. P.; Pham, T. Q.; Doan, J.; Jiang, C. D.; Hambley, T. W.; Greguric, I.; Fraser, B. H., Radiosynthesis and 'click'conjugation of ethynyl-4-[18F] fluorobenzene—an improved [18F] synthon for indirect radiolabeling. *Journal of Labelled Compounds and Radiopharmaceuticals* **2015**, *58* (13-14), 473-478.
29. Sugiura, G.; Kühn, H.; Sauter, M.; Haberkorn, U.; Mier, W., Radiolabeling strategies for tumor-targeting proteinaceous drugs. *Molecules* **2014**, *19*, 2135-2165.
30. Hou, S.; Phung, D. L.; Lin, W.-Y.; Wang, M.-w.; Liu, K.; Shen, C. K.-F., Microwave-assisted one-pot synthesis of *N*-succinimidyl-4-[(18)F]fluorobenzoate ([(18)F]SFB). *Journal of Visualized Experiments : JoVE* **2011**, (52), 2755.
31. Poethko, T.; Schottelius, M.; Thumshirn, G.; Hersel, U., Two-step methodology for high-yield routine radiohalogenation of peptides: 18F-labeled RGD and octreotide analogs. *The Journal of Nuclear Medicine* **2004**, *45* (5), 892-902.
32. Jacobson, O.; Chen, X., PET designated flouride-18 production and chemistry. *Current Topics in Medicinal Chemistry* **2010**, *10* (11), 1048-1059.
33. Becaud, J.; Mu, L.; Karramkam, M.; Schubiger, P. A.; Ametamey, S. M.; Graham, K.; Stellfeld, T.; Lehmann, L.; Borkowski, S.; Berndorff, D.; Dinkelborg, L.; Srinivasan, A.; Smits, R.; Koksch, B., Direct one-step 18F-labeling of peptides via nucleophilic aromatic substitution. *Bioconjugate Chemistry* **2009**, *20* (12), 2254-2261.
34. Jacobson, O.; Zhu, L.; Ma, Y.; Weiss, I. D.; Sun, X.; Niu, G.; Kiesewetter, D. O.; Chen, X., Rapid and simple one-step F-18 labeling of peptides. *Bioconjugate Chemistry* **2011**, *22* (3), 422-428.
35. Mu, L.; Honer, M.; Becaud, J.; Martic, M.; Schubiger, P. A.; Ametamey, S. M.; Stellfeld, T.; Graham, K.; Borkowski, S.; Lehmann, L.; Dinkelborg, L.; Srinivasan, A., *In vitro* and *in vivo* characterization of novel 18F-labeled bombesin analogues for targeting GRPR-positive tumors. *Bioconjugate Chemistry* **2010**, *21* (10), 1864-1871.

36. McBride, W. J.; Sharkey, R. M.; Karacay, H.; D'Souza, C. A.; Rossi, E. A.; Laverman, P.; Chang, C.-H.; Boerman, O. C.; Goldenberg, D. M., A novel method of 18F radiolabeling for PET. *Journal of Nuclear Medicine* **2009**, *50* (6), 991.
37. McBride, W. J.; Sharkey, R. M.; Goldenberg, D. M., Radiofluorination using aluminum-fluoride (Al18F). *EJNMMI Research* **2013**, *3* (1), 36.
38. Cleeren, F.; Lecina, J.; Ahamed, M.; Raes, G.; Devoogdt, N.; Caveliers, V.; McQuade, P.; Rubins, D. J.; Li, W.; Verbruggen, A., Al18F-labeling of heat-sensitive biomolecules for positron emission tomography imaging. *Theranostics* **2017**, *7* (11), 2924.
39. Hofman, M. S.; Kong, G.; Neels, O. C.; Eu, P.; Hong, E.; Hicks, R. J., High management impact of Ga-68 DOTATATE (GaTate) PET/CT for imaging neuroendocrine and other somatostatin expressing tumours. *Journal of Medical Imaging and Radiation Oncology* **2012**, *56* (1), 40-47.
40. Nock, B. A.; Maina, T.; Krenning, E. P.; de Jong, M., "To serve and protect": enzyme inhibitors as radiopeptide escorts promote tumor targeting. *Journal of Nuclear Medicine* **2014**, *55* (1), 121-127.
41. Ocak, M.; Helbok, A.; Rangger, C.; Peitl, P. K.; Nock, B. A.; Morelli, G.; Eek, A.; Sosabowski, J. K.; Breeman, W. A.; Reubi, J. C.; Decristoforo, C., Comparison of biological stability and metabolism of CCK2 receptor targeting peptides, a collaborative project under COST BM0607. *European Journal of Nuclear Medicine and Molecular Imaging* **2011**, *38*, 1426-1435.
42. Gentilucci, L.; De Marco, R.; Cerisoli, L., Chemical modifications designed to improve peptide stability: incorporation of non-natural amino acids, pseudo-peptide bonds, and cyclization. *Current Pharmaceutical Design* **2010**, *16* (28), 3185-3203.
43. Jamous, M.; Tamma, M. L.; Gourni, E.; Waser, B.; Reubi, J. C.; Maecke, H. R.; Mansi, R., PEG spacers of different length influence the biological profile of bombesin-based radiolabeled antagonists. *Nuclear Medicine and Biology* **2014**, *41* (6), 464-470.
44. Smith, C. J.; Gali, H.; Sieckman, G. L.; Higginbotham, C.; Volkert, W. A.; Hoffman, T. J., Radiochemical investigations of 99mTc−N3S-X-BBN[7−14]NH2: *an in vitro/in vivo* structure−activity relationship study where X = 0-, 3-, 5-, 8-, and 11-carbon tethering moieties. *Bioconjugate Chemistry* **2003**, *14* (1), 93-102.
45. Popp, I.; Del Pozzo, L.; Waser, B.; Reubi, J. C.; Meyer, P. T.; Maecke, H. R.; Gourni, E., Approaches to improve metabolic stability of a statine-based GRP receptor antagonist. *Nuclear Medicine and Biology* **2017**, *45*, 22-29.
46. Werle, M.; Bernkop-Schnürch, A., Strategies to improve plasma half life time of peptide and protein drugs. *Amino Acids* **2006**, *30* (4), 351-367.
47. Aumailley, M.; Gurrath, M.; Müller, G.; Calvete, J.; Timpl, R.; Kessler, H., Arg-Gly-Asp constrained within cyclic pentapoptides strong and selective inhibitors of cell adhesion to vitronectin and laminin fragment P1. *FEBS Letters* **1991**, *291* (1), 50-54.
48. Haubner, R.; Finsinger, D.; Kessler, H., Stereoisomeric peptide libraries and peptidomimetics for designing selective inhibitors of the αvβ3 integrin for a new cancer therapy. *Angewandte Chemie International Edition* **1997**, *36* (13-14), 1374-1389.
49. Shi, J.; Wang, F.; Liu, S., Radiolabeled cyclic RGD peptides as radiotracers for tumor imaging. *Biophysics Reports* **2016**, *2* (1), 1-20.
50. Däpp, S.; Garayoa, E. G.; Maes, V.; Brans, L.; Tourwé, D. A.; Müller, C.; Schibli, R., PEGylation of 99mTc-labeled bombesin analogues improves their pharmacokinetic properties. *Nuclear Medicine and Biology* **2011**, *38* (7), 997-1009.
51. Zhang, H.; Schuhmacher, J.; Waser, B.; Wild, D.; Eisenhut, M.; Reubi, J. C.; Maecke, H. R., DOTA-PESIN, a DOTA-conjugated bombesin derivative designed for the imaging and targeted

radionuclide treatment of bombesin receptor-positive tumours. *European Journal of Nuclear Medicine and Molecular Imaging* **2007**, *34* (8), 1198-1208.

52. Däpp, S.; Müller, C.; Garayoa, E. G.; Bläuenstein, P.; Maes, V.; Brans, L.; Tourwé, D. A.; Schibli, R., PEGylation, increasing specific activity and multiple dosing as strategies to improve the risk-benefit profile of targeted radionuclide therapy with 177 Lu-DOTA-bombesin analogues. *EJNMMI Research* **2012**, *2* (1), 24.
53. Kolenc-Peitl, P.; Mansi, R.; Tamma, M.; Gmeiner-Stopar, T.; Sollner-Dolenc, M.; Waser, B.; Baum, R. P.; Reubi, J. C.; Maecke, H. R., Highly improved metabolic stability and pharmacokinetics of indium-111-DOTA-gastrin conjugates for targeting of the gastrin receptor. *Journal of Medicinal Chemistry* **2011**, *54* (8), 2602-2609.
54. Valverde, I. E.; Vomstein, S.; Mindt, T. L., Toward the optimization of bombesin-based radiotracers for tumor targeting. *Journal of Medicinal Chemistry* **2016**, *59* (8), 3867-3877.
55. Valverde, I. E.; Bauman, A.; Kluba, C. A.; Vomstein, S.; Walter, M. A.; Mindt, T. L., 1, 2, 3-Triazoles as amide bond mimics: triazole scan yields protease-resistant peptidomimetics for tumor targeting. *Angewandte Chemie International Edition* **2013**, *52* (34), 8957-8960.
56. Valverde, I. E.; Vomstein, S.; Fischer, C. A.; Mascarin, A.; Mindt, T. L., Probing the backbone function of tumor targeting peptides by an amide-to-triazole substitution strategy. *Journal of Medicinal Chemistry* **2015**, *58* (18), 7475-7484.
57. Correia, J. D.; Paulo, A.; Raposinho, P. D.; Santos, I., Radiometallated peptides for molecular imaging and targeted therapy. *Dalton Transactions* **2011**, *40* (23), 6144-6167.
58. Paganelli, G.; Bodei, L.; Handkiewicz Junak, D.; Rocca, P.; Papi, S.; Lopera Sierra, M.; Gatti, M.; Chinol, M.; Bartolomei, M.; Fiorenza, M., 90Y–DOTA–D-Phe1–Try3–octreotide in therapy of neuroendocrine malignancies. *Peptide Science* **2002**, *66* (6), 393-398.
59. Bauer, W.; Briner, U.; Doepfner, W.; Haller, R.; Huguenin, R.; Marbach, P.; Petcher, T. J.; Pless, J., SMS 201–995: a very potent and selective octapeptide analogue of somatostatin with prolonged action. *Life Sciences* **1982**, *31* (11), 1133-1140.
60. Harris, A. G., Somatostatin and somatostatin analogues: pharmacokinetics and pharmacodynamic effects. *Gut* **1994**, *35* (3 Suppl), S1-S4.
61. Kaloudi, A.; Nock, B. A.; Lymperis, E.; Krenning, E. P.; De Jong, M.; Maina, T., Improving the *In vivo* profile of minigastrin radiotracers: a comparative study involving the neutral endopeptidase inhibitor phosphoramidon. *Cancer Biotherapy and Radiopharmaceuticals* **2016**, *31* (1), 20-28.
62. Juaristi, E.; Soloshonok, V. A., *Enantioselective Synthesis of Beta-Amino Acids*. Wiley: 2005.
63. Tan, C. Y. K.; Weaver, D. F., A one-pot synthesis of 3-amino-3-arylpropionic acids. *Tetrahedron* **2002**, *58* (37), 7449-7461.
64. Frackenpohl, J.; Arvidsson, P. I.; Schreiber, J. V.; Seebach, D., The outstanding biological stability of β- and γ-peptides toward proteolytic enzymes: an *in vitro* investigation with fifteen peptidases. *ChemBioChem* **2001**, *2* (6), 445-455.
65. Hansen, T.; Moe, M. K.; Anderssen, T.; Strøm, M. B., Metabolism of small antimicrobial β 2, 2-amino acid derivatives by murine liver microsomes. *European Journal of Drug Metabolism and Pharmacokinetics* **2012**, *37* (3), 191-201.
66. Tørfoss, V.; Ausbacher, D.; Cavalcanti-Jacobsen, C. d. A.; Hansen, T.; Brandsdal, B. O.; Havelkova, M.; Strøm, M. B., Synthesis of anticancer heptapeptides containing a unique lipophilic β2, 2-amino acid building block. *Journal of Peptide Science* **2012**, *18* (3), 170-176.
67. Ali, S.; Hoemann, M.; Aube, J.; Mitscher, L.; Georg, G. I.; McCall, R.; Jayasinghe, L., Novel cytotoxic 3'-(tert-butyl) 3'-dephenyl analogs of paclitaxel and docetaxel. *Journal of Medicinal Chemistry* **1995**, *38* (19), 3821-3828.

68. Garayoa, E. G.; Rüegg, D.; Bläuenstein, P.; Zwimpfer, M.; Khan, I. U.; Maes, V.; Blanc, A.; Beck-Sickinger, A. G.; Tourwé, D. A.; Schubiger, P. A., Chemical and biological characterization of new Re (CO) 3/[99mTc](CO) 3 bombesin analogues. *Nuclear Medicine and Biology* **2007**, *34* (1), 17-28.
69. García Garayoa, E.; Schweinsberg, C.; Maes, V.; Brans, L.; Bläuenstein, P.; Tourwé, D. A.; Schibli, R.; Schubiger, P. A., Influence of the molecular charge on the biodistribution of bombesin analogues labeled with the [99mTc (CO) 3]-core. *Bioconjugate Chemistry* **2008**, *19* (12), 2409-2416.
70. Schjoeth-Eskesen, C.; Hansen, P. R.; Kjaer, A.; Gillings, N., Efficient regioselective ring opening of activated aziridine-2-carboxylates with [18F]fluoride. *ChemistryOpen* **2015**, *4* (1), 65-71.
71. Martin, K. S.; Soldi, C.; Candee, K. N.; Wettersten, H. I.; Weiss, R. H.; Shaw, J. T., From bead to flask: synthesis of a complex β-amido-amide for probe-development studies. *Beilstein Journal of Organic Chemistry* **2013**, *9*, 260.
72. Clayden, J.; Greeves, N.; Warren, S., *Organic Chemistry*. Oxford University Press: Oxford, United Kingdom, 2012.
73. Wade, L. G., *Organic chemistry*. Pearson Prentice Hall: 2006.
74. Li, F.-N.; Kim, N.-J.; Paek, S.-M.; Kwon, D.-Y.; Min, K. H.; Jeong, Y.-S.; Kim, S.-Y.; Park, Y.-H.; Kim, H.-D.; Park, H.-G., Design, synthesis, and biological evaluation of novel diarylalkyl amides as TRPV1 antagonists. *Bioorganic & Medicinal Chemistry* **2009**, *17* (10), 3557-3567.
75. Fukuyama, T.; Arai, M.; Matsubara, H.; Ryu, I., Mizoroki− Heck Arylation of α, β-unsaturated acids with a hybrid fluorous ether, F-626: facile filtrative separation of products and efficient recycling of a reaction medium containing a catalyst. *The Journal of Organic Chemistry* **2004**, *69* (23), 8105-8107.
76. Axten, J., Michael; Faucher, N., Eric; Daugan, A., Claude-Marie; Kethiri, R., Raghava; Kristam, Rajendra; Venkateshappa, Chandregowda. 1-Phenylpyrolidin-2-one Derivatives as Perk Inhibitors. WO2017046737A1, 23rd March 2017.
77. Tomooka, K.; Iso, C.; Uehara, K.; Suzuki, M.; Nishikawa-Shimono, R.; Igawa, K., Planar-chiral [7] orthocyclophanes. *Angewandte Chemie* **2012**, *124* (41), 10501-10504.
78. Ghosh, A. K.; Brindisi, M., Organic carbamates in drug design and medicinal chemistry. *Journal of Medicinal Chemistry* **2015**, *58* (7), 2895-2940.
79. Zhang, W.; He, J.; Wu, J.; Schmuck, C., *In vivo* detoxification of lipopolysaccharide by antimicrobial peptides. *Bioconjugate Chemistry* **2016**, *28* (2), 319-324.
80. McManus, I.; Daly, H.; Thompson, J.; Connor, E.; Hardacre, C.; Wilkinson, S.; Bonab, N. S.; Ten Dam, J.; Simmons, M.; Stitt, E., Effect of solvent on the hydrogenation of 4-phenyl-2-butanone over Pt based catalysts. *Journal of Catalysis* **2015**, *330*, 344-353.
81. Hata, R.; Nonaka, H.; Takakusagi, Y.; Ichikawa, K.; Sando, S., Design of a hyperpolarized molecular probe for detection of aminopeptidase N activity. *Angewandte Chemie* **2016**, *128* (5), 1797-1800.
82. El-Faham, A.; Albericio, F., Peptide coupling reagents, more than a letter soup. *Chemical Reviews* **2011**, *111* (11), 6557-6602.
83. Duan, J.; Sun, Y.; Chen, H.; Qiu, G.; Zhou, H.; Tang, T.; Deng, Z.; Hong, X., HMDO-promoted peptide and protein synthesis in ionic liquids. *The Journal of Organic Chemistry* **2013**, *78* (14), 7013-7022.
84. Löser, R.; Fischer, S.; Hiller, A.; Köckerling, M.; Funke, U.; Maisonial, A.; Brust, P.; Steinbach, J., Use of 3-[18F] fluoropropanesulfonyl chloride as a prosthetic agent for the radiolabelling of amines: Investigation of precursor molecules, labelling conditions and enzymatic stability of the corresponding sulfonamides. *Beilstein Journal of Organic Chemistry* **2013**, *9*, 1002.

85. Franz, W.; Krisch, K., Carboxylesterase aus schweinenierenmikrosomen, I. Isolierung, eigenschaften und substratspezifität. In *Hoppe-Seyler´s Zeitschrift für physiologische Chemie*, 1968; Vol. 349, p 575.
86. Fukami, T.; Yokoi, T., The emerging role of human esterases. *Drug Metabolism and Pharmacokinetics* **2012**, *27* (5), 466-477.
87. Landowski, C. P.; Lorenzi, P. L.; Song, X.; Amidon, G. L., Nucleoside ester prodrug substrate specificity of liver carboxylesterase. *Journal of Pharmacology and Experimental Therapeutics* **2006**, *316* (2), 572-580.
88. Sterling, H. J.; Batchelor, J. D.; Wemmer, D. E.; Williams, E. R., Effects of buffer loading for electrospray ionization mass spectrometry of a noncovalent protein complex that requires high concentrations of essential salts. *Journal of the American Society for Mass Spectrometry* **2010**, *21* (6), 1045-1049.
89. Cartwright, A. J.; Jones, P.; Wolff, J. C.; Evans, E. H., Derivatisation of carboxylic acid groups in pharmaceuticals for enhanced detection using liquid chromatography with electrospray ionisation tandem mass spectrometry. *Rapid Communications in Mass Spectrometry: An International Journal Devoted to the Rapid Dissemination of Up-to-the-Minute Research in Mass Spectrometry* **2005**, *19* (8), 1058-1062.
90. Nassar, A.-E. F.; Kamel, A. M.; Clarimont, C., Improving the decision-making process in the structural modification of drug candidates: enhancing metabolic stability. *Drug Discovery Today* **2004**, *9* (23), 1020-1028.
91. Fulmer, G. R.; Miller, A. J.; Sherden, N. H.; Gottlieb, H. E.; Nudelman, A.; Stoltz, B. M.; Bercaw, J. E.; Goldberg, K. I., NMR chemical shifts of trace impurities: common laboratory solvents, organics, and gases in deuterated solvents relevant to the organometallic chemist. *Organometallics* **2010**, *29* (9), 2176-2179.
92. Ling, Y.; Ye, X.; Ji, H.; Zhang, Y.; Lai, Y.; Peng, S.; Tian, J., Synthesis and evaluation of nitric oxide-releasing derivatives of farnesylthiosalicylic acid as anti-tumor agents. *Bioorganic & Medicinal Chemistry* **2010**, *18* (10), 3448-3456.
93. Walter, M.; Besendorf, H.; Schnider, O., Syntheses in the isoquinoline series. 1,2-substituted octahydroisoquinolines. *Helvetica Chimica Acta* **1961**, *44*, 1546.

Chapter 7: Appendices

7.1 ^{1}H NMR of Target Glycine Ethyl Ester Conjugates

7.1.1 Ethyl (3-amino-3-(4-fluorophenyl)propanoyl)glycinate (38)

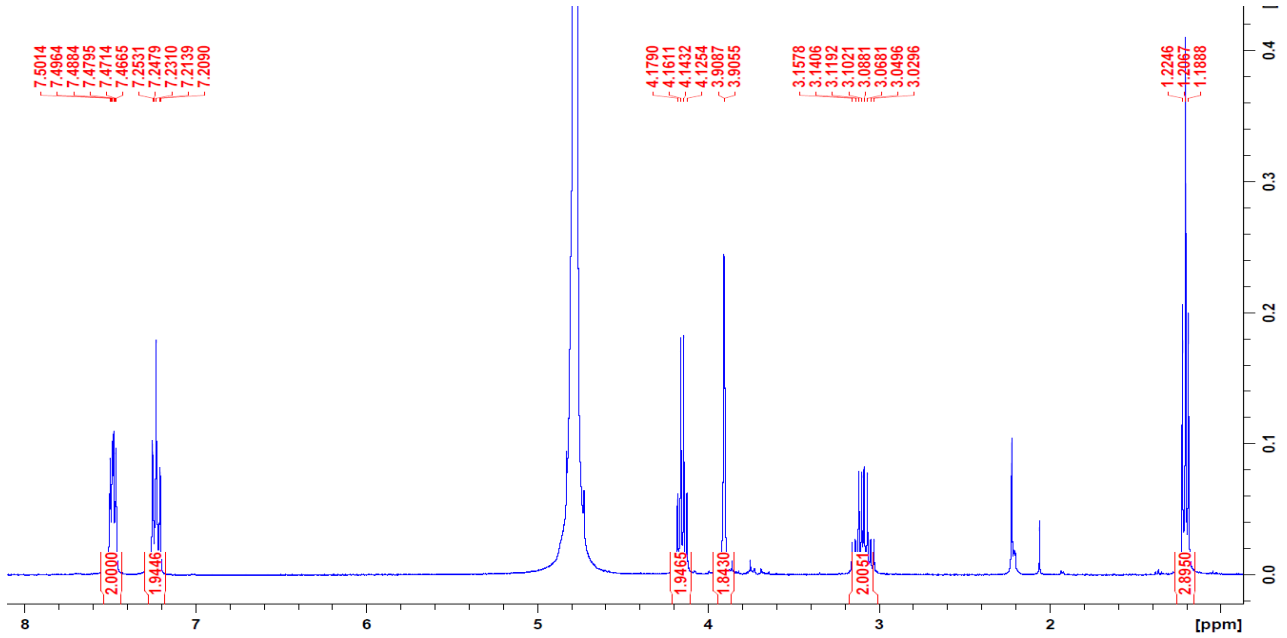

Figure 7.1 Ethyl (3-amino-3-(4-fluorophenyl)propanoyl)glycinate **(38)**, D_2O solvent seen

7.1.2 Ethyl (3-aminopropanoyl)glycinate (39)

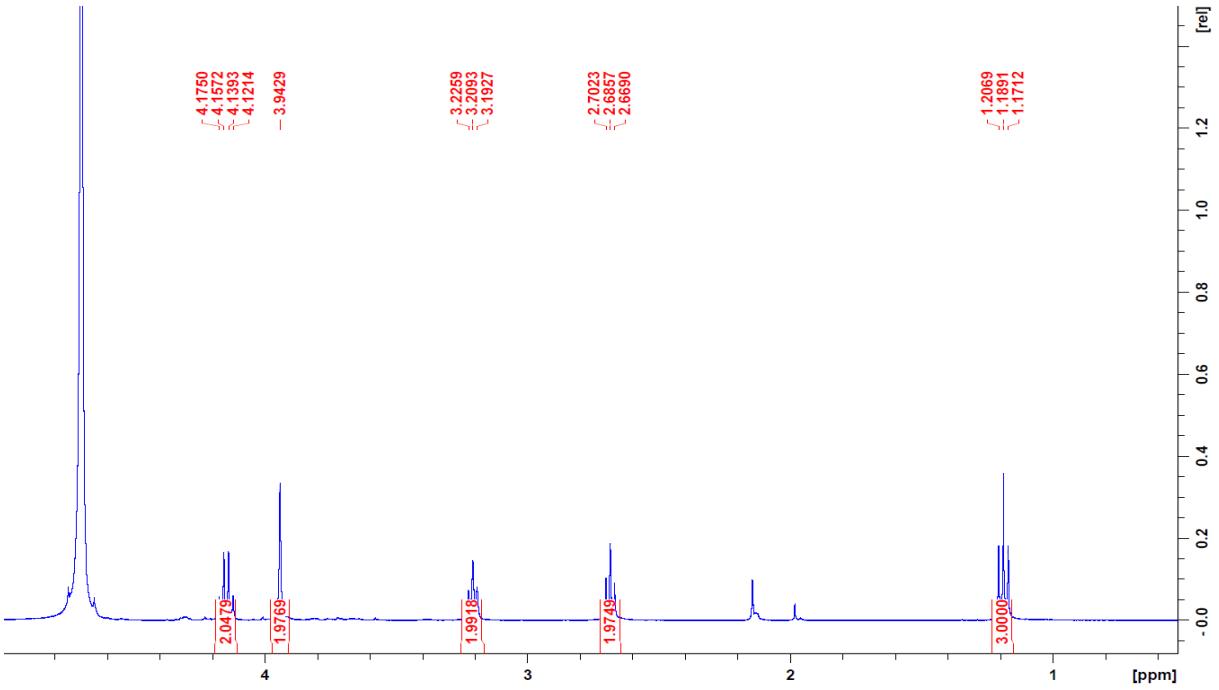

Figure 7.2 Ethyl (3-aminopropanoyl)glycinate **(39)**, D_2O solvent seen

7.1.3 Ethyl (2-amino-3-(4-fluorophenyl)propanoyl)glycinate (40)

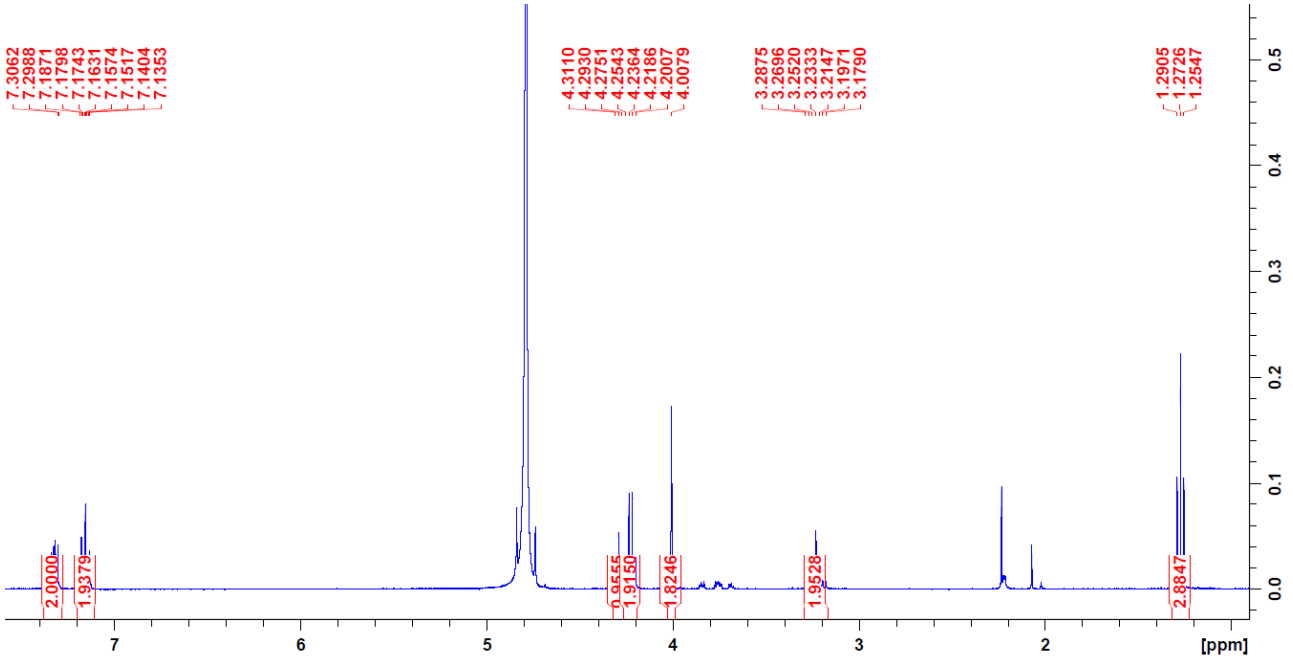

Figure 7.3 Ethyl (2-amino-3-(4-fluorophenyl)propanoyl)glycinate **(40)**, D_2O solvent seen

7.1.4 Ethyl L-alanylglycinate (41)

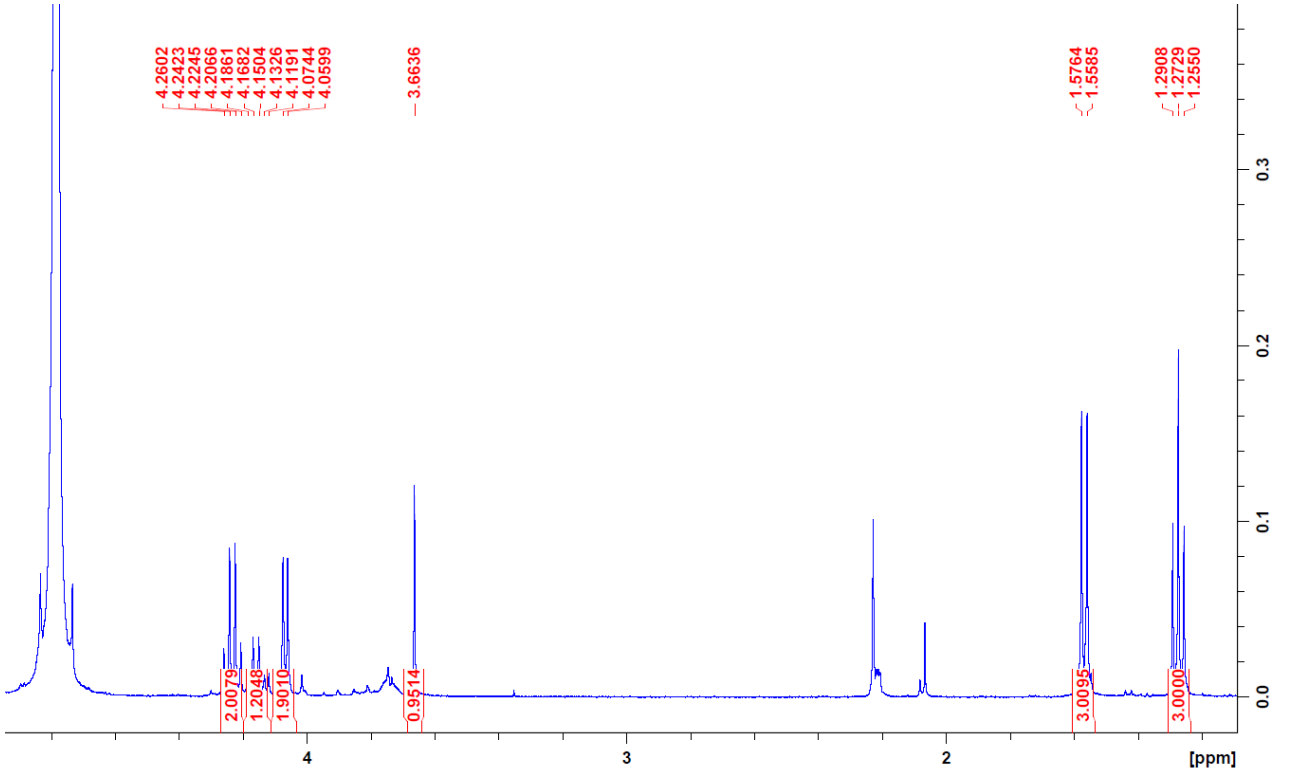

Figure 7.4 Ethyl L-alanylglycinate **(41)**, D_2O solvent seen

7.1.5 Ethyl (3-(4-fluorophenyl)propanoyl)glycinate (42)

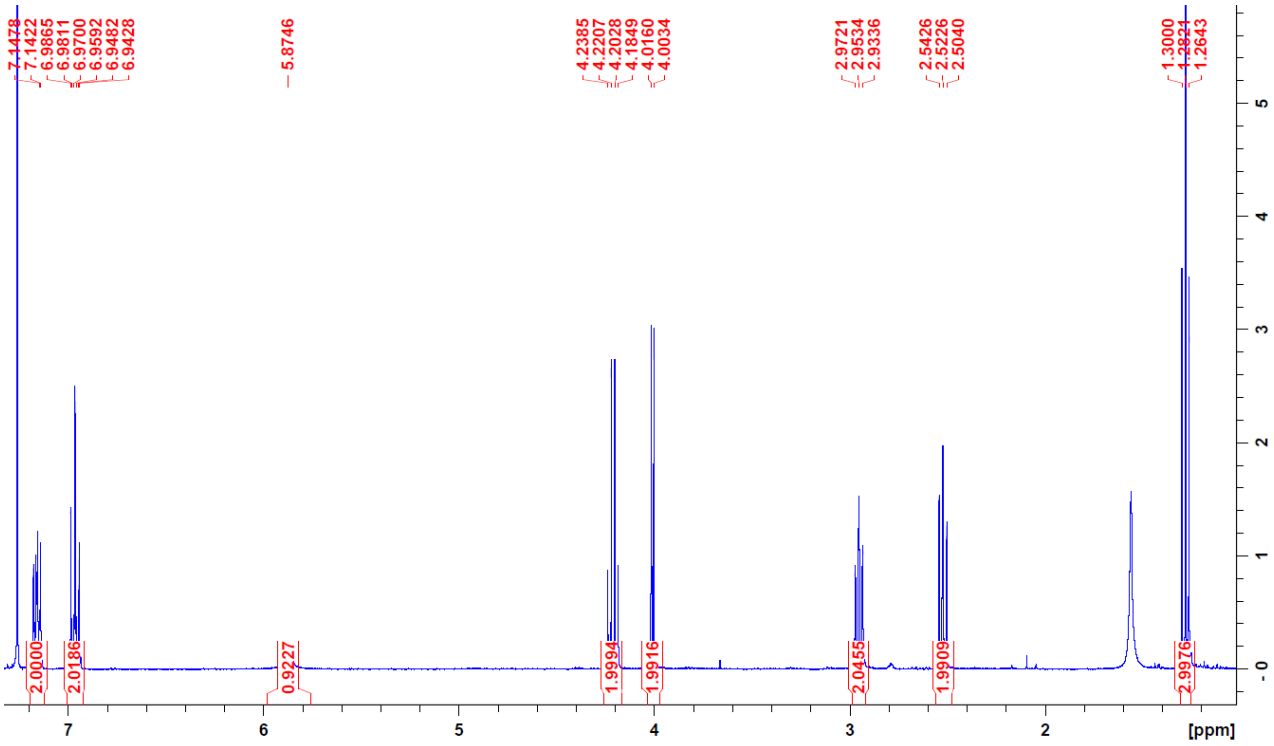

Figure 7.5 Ethyl (3-(4-fluorophenyl)propanoyl)glycinate **(42)**, $CDCl_3$ solvent and H_2O in $CDCl_3$ seen

7.1.6 Ethyl (4-fluorobenzoyl)glycinate (43)

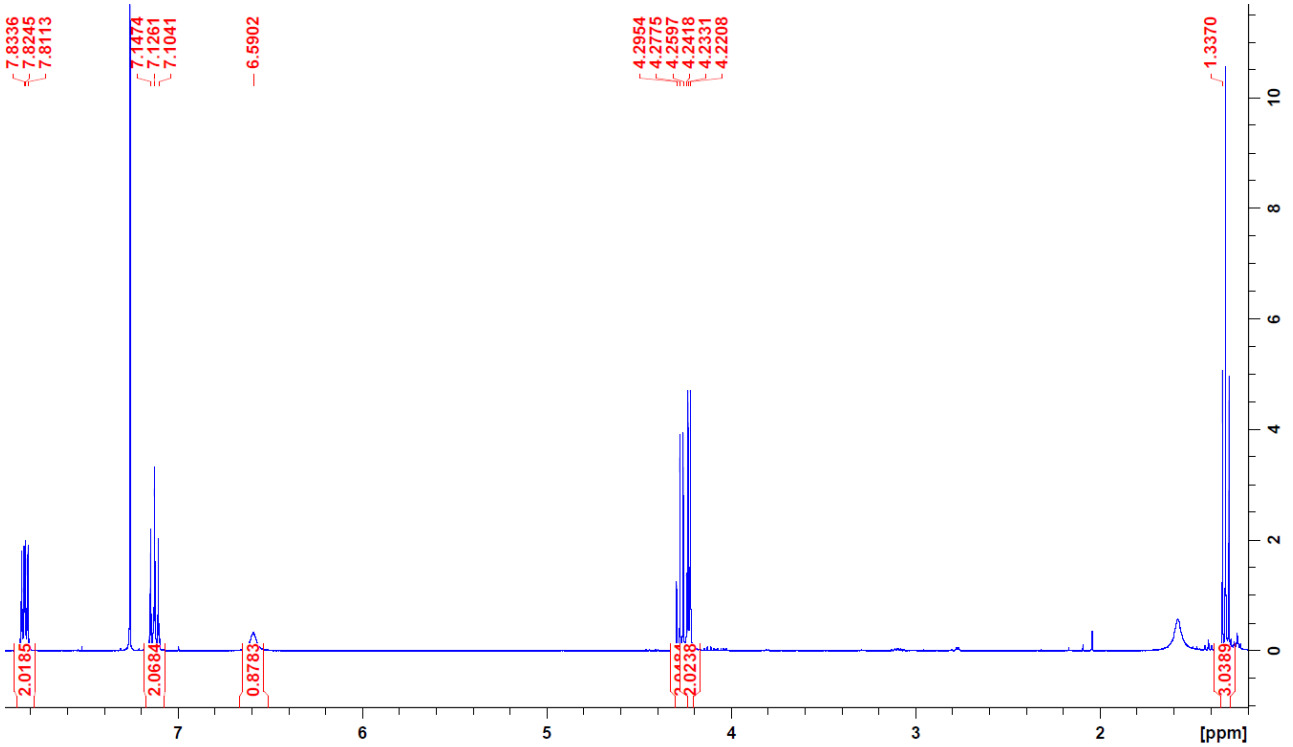

Figure 7.6 Ethyl (4-fluorobenzoyl)glycinate **(43)**, $CDCl_3$ solvent and H_2O in $CDCl_3$ seen

7.2 Metabolic Stability Data

7.2.1 Thin Layer Chromatography Analysis

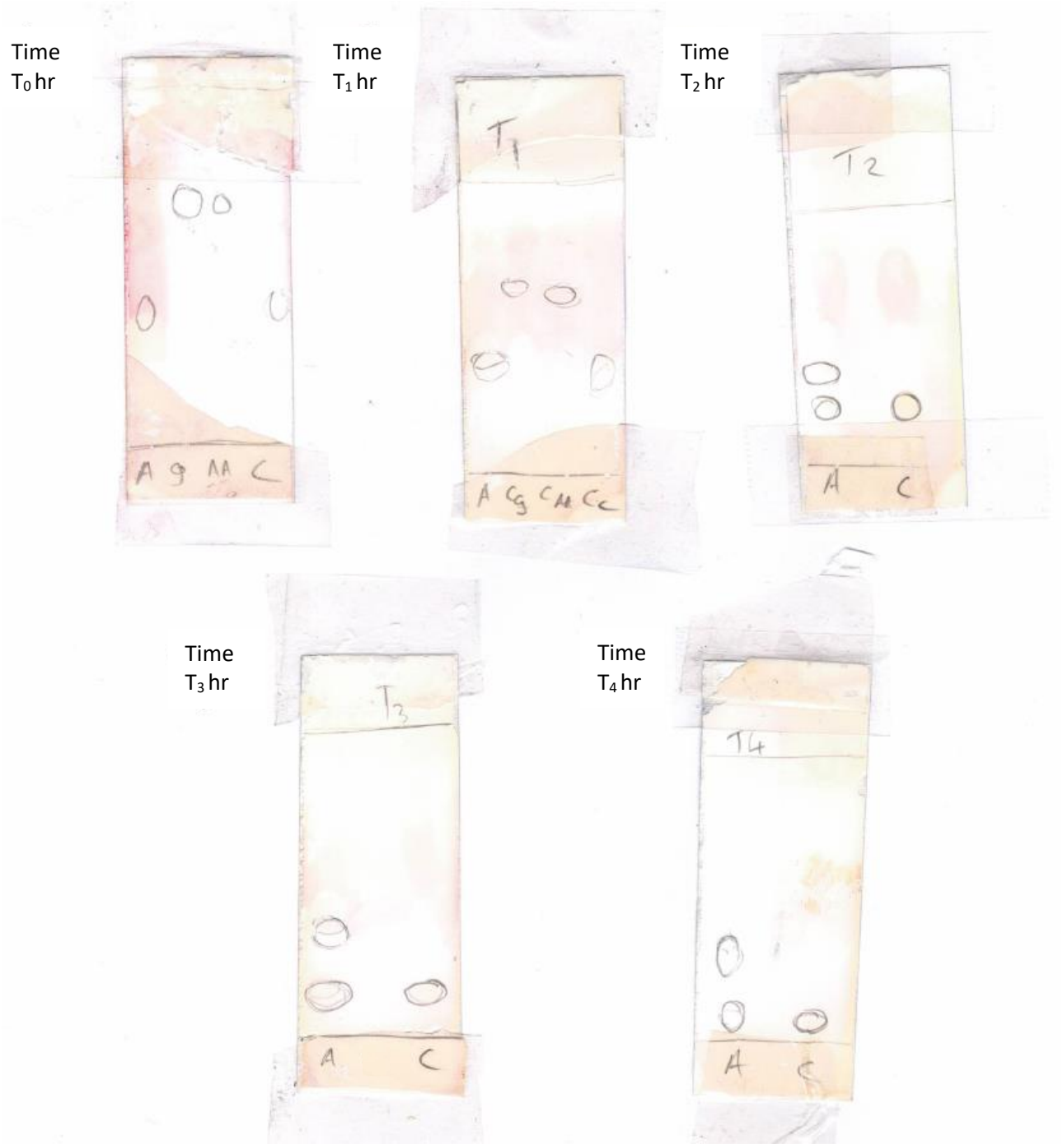

Figure 7.7 Exemplar reverse phase TLC plates for metabolic stability studies of ethyl (2-amino-3-(4-fluorophenyl)propanoyl)glycinate **(40)** at time points 0, 1, 2, 3, 4 hours. Legend: A – assay, g – glycine ethyl ester, AA – amino acid cleavage product **(44)**, C - control without PLE

7.2.2 Low Resolution Electrospray Ionisation Mass Spectrometry (LRESI-MS) Analysis

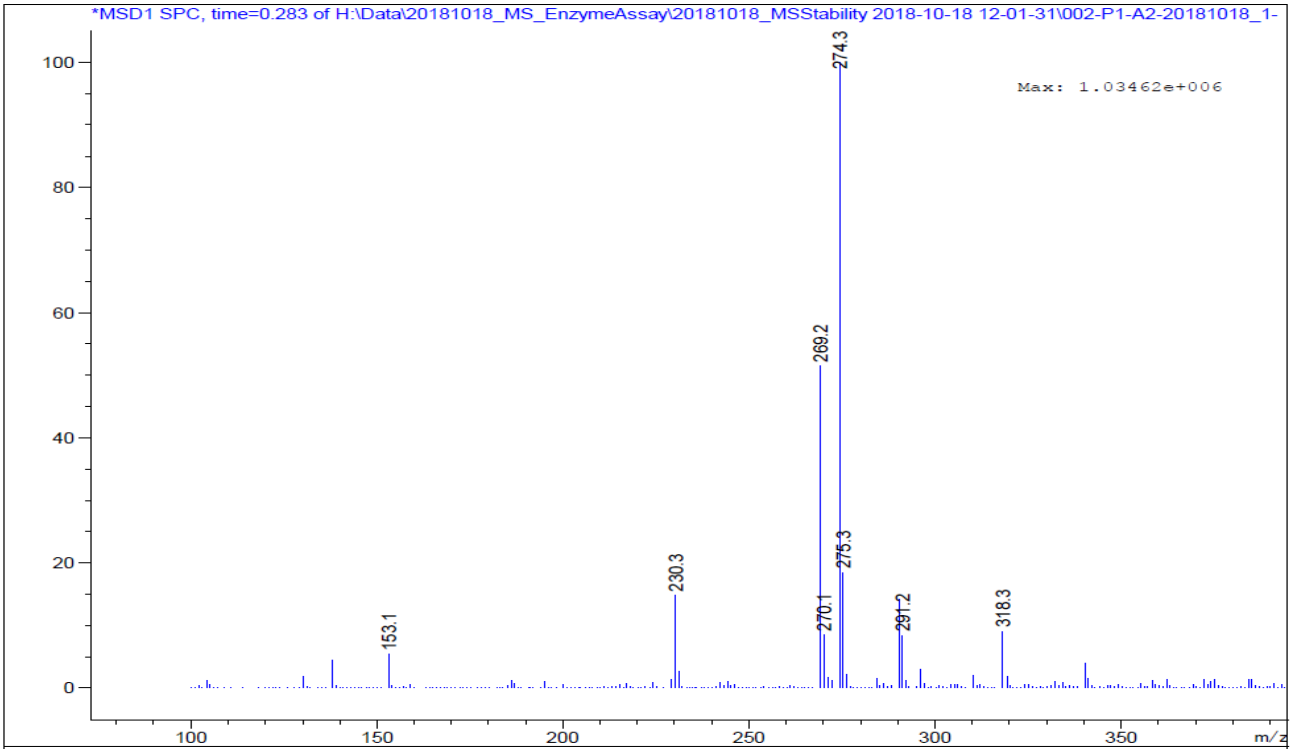

Figure 7.8 Exemplar LRESI-MS for metabolic stability studies assay of ethyl (2-amino-3-(4-fluorophenyl)propanoyl)glycinate **(40)** at time point 2 hours
M/Z 247.3 is from contamination of HPLC system

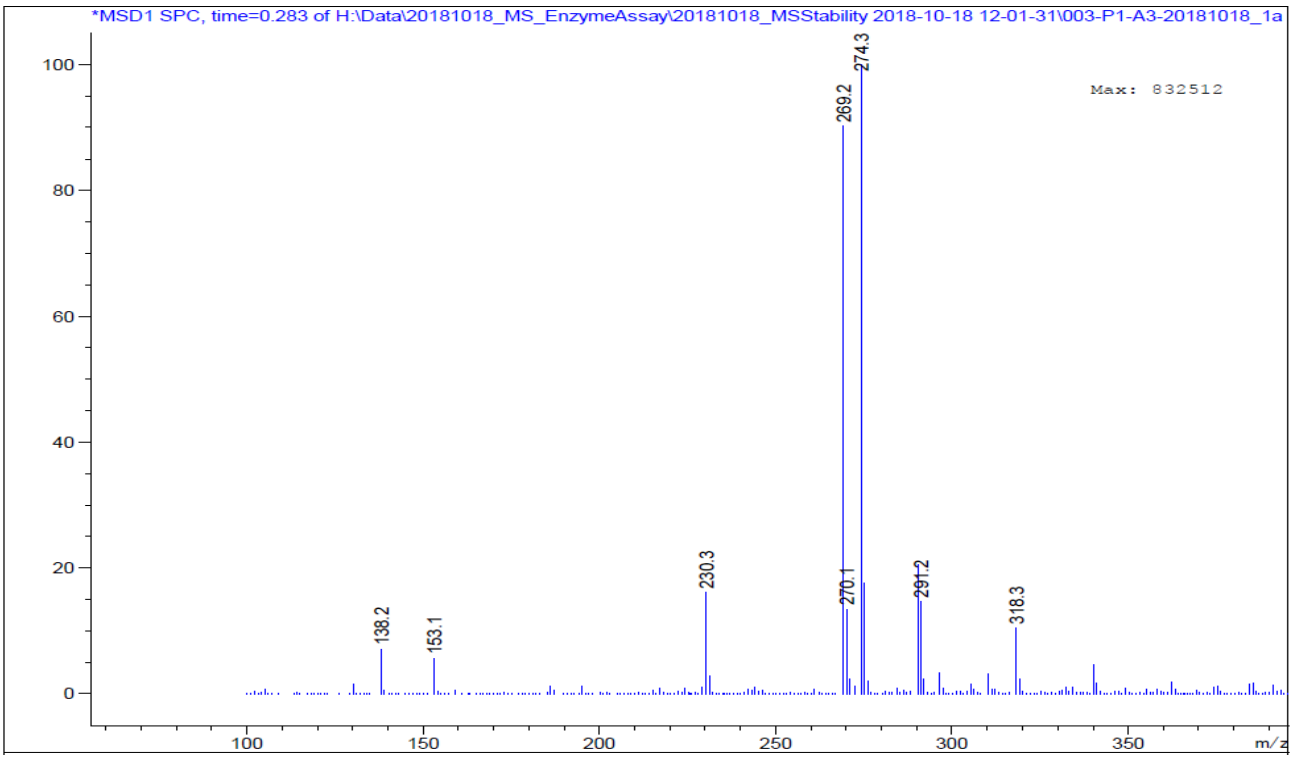

Figure 7.9 Exemplar LRESI-MS for metabolic stability studies control assay (without PLE) of ethyl (2-amino-3-(4-fluorophenyl)propanoyl)glycinate **(40)** at time point 2 hours
M/Z 247.3 is from contamination of HPLC system

7.2.3 Liquid Chromatography Mass Spectrometry (LC-MS) Analysis

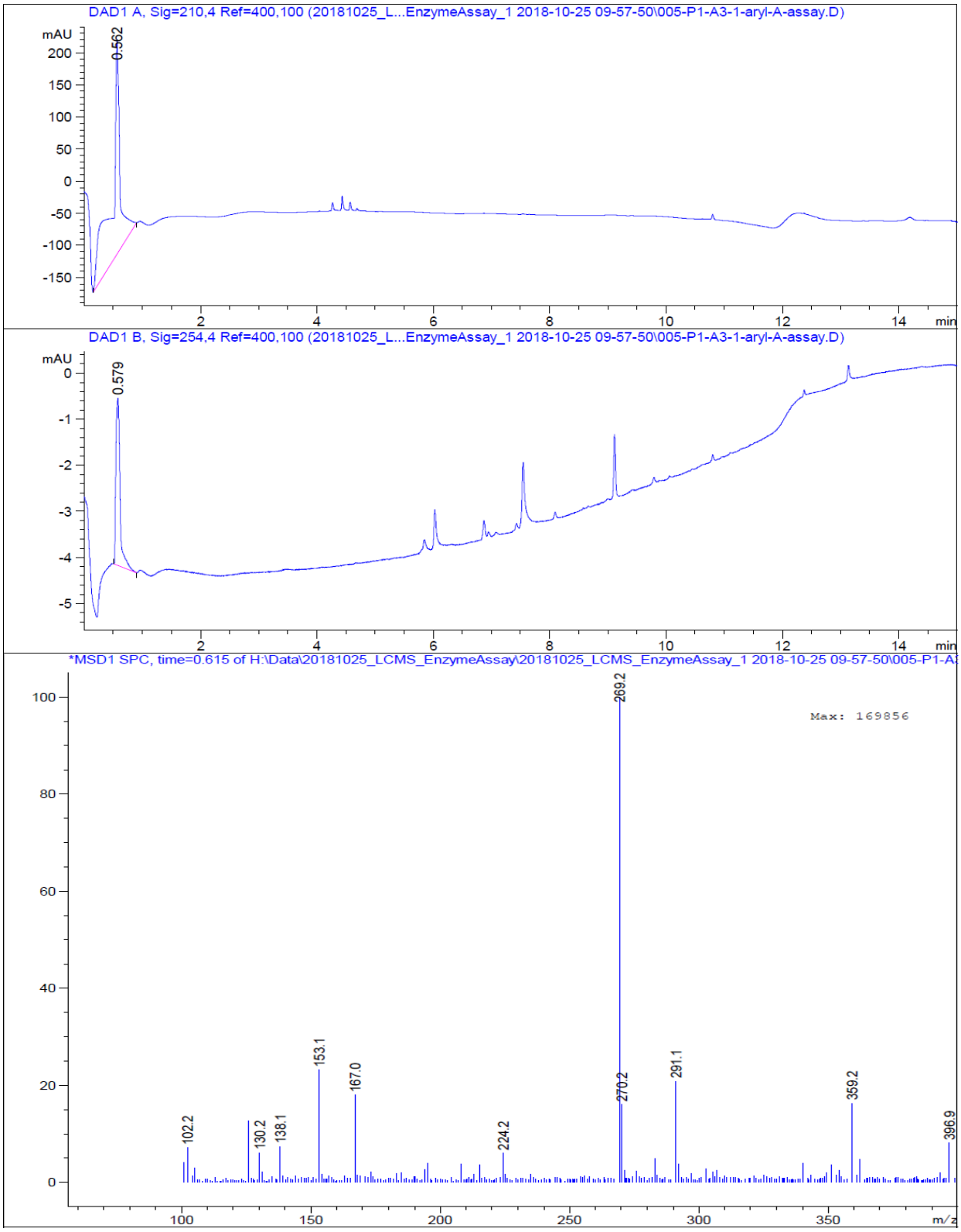

Figure 7.10 Exemplar LC-MS for metabolic stability studies assay of ethyl (2-amino-3-(4-fluorophenyl)propanoyl)glycinate **(40)** at time point 2 hours

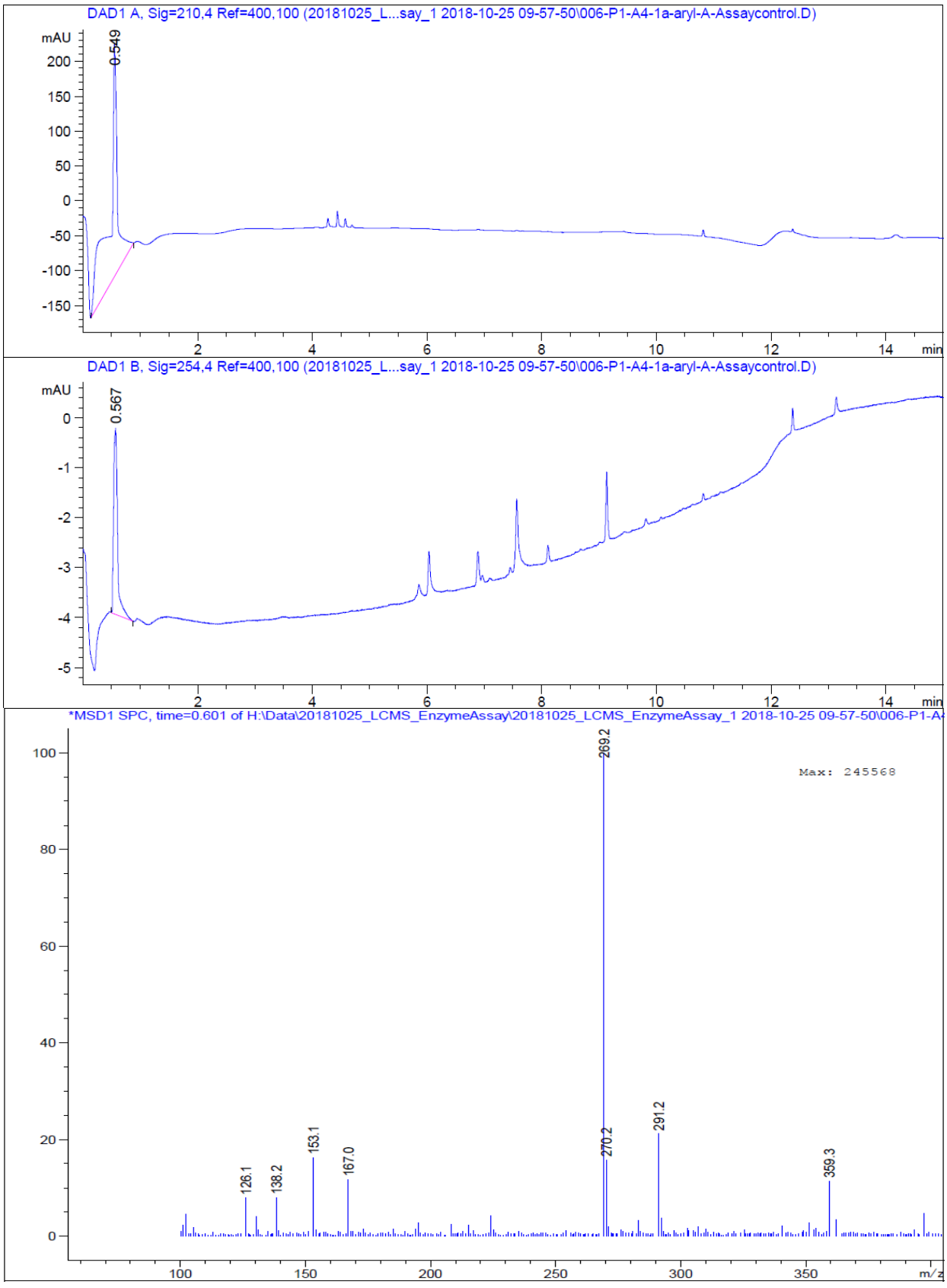

Figure 7.11 Exemplar LC-MS for metabolic stability studies control assay (without PLE) of ethyl (2-amino-3-(4-fluorophenyl)propanoyl)glycinate **(40)** at time point 2 hours